T H E U N I V E R S I T Y O F M I C H I G A N

COLLEGE OF ENGINEERING
Department of Naval Architecture and Marine Engineering

Final Report

MODEL TESTS OF PROJECT MOHOLE DRILLING PLATFORM

F. C. Michelsen
N. Rabe

ORA Project 06333

under contract with:

BROWN AND ROOT, INC.
HOUSTON, TEXAS

administered through:

OFFICE OF RESEARCH ADMINISTRATION ANN ARBOR

August 1964

TABLE OF CONTENTS

LIST OF FIGURES

1. INTRODUCTION

This report presents the results of resistance and self-propulsion tests performed with a model of the Mohole Drilling Platform. The general arrangement of the prototype is shown in Figure 1.1 (Brown and Root Drawing 1-T-10002). Size of model was selected on the basis of propeller diameter. To avoid significant scale effect in propeller performance, the propeller diameter was made equal to 7 in. (16'-0" full size) which led to a model scale ratio of approximately 27.5. Under these conditions the size of the model was such that a blockage effect existed when towing the model in the model basin. On the basis of past experience with conventional ships this blockage effect was estimated to increase the resistance by about 3%.

In addition to testing the platform, the performance of the steering propulsion unit was also investigated as part of this test program. The arrangement of the steering unit prototype is shown in Figure 1.2. The model was built to a scale ratio of 7.5 which made the propeller diameter 9.2 in. (5'-9" full size).

In outline the total test program conducted is as follows:

1.1 Measurements of steady state resistance, side force yaw, trim and heel moments under the following conditions:

1.1.1 28' draft (transit condition) at headings of 0°, 10°, 20°, 90°, and 180°, and at speeds up to 12 knots for headings of 0°, 10°, and 20°, up to 4 knots for 90° heading and 8 knots for 180°.

1.1.2 70' draft (drilling condition) at headings of 0°, 10°, 20°, 45°, 90°, 135°, and 180°, and at speeds up to 8 knots for headings 0° and 180°, 6.5 knots for 10°,5.0 knots for 20°, and 4.0 knots for headings for 45°, 90°, and 135°.

1.2 Self-propulsion tests of the platform, in which propeller torque, thrust, and rpm of both propellers were measured in addition to quantities listed under 1.1, under the following conditions:

1.2.1 28' draft (transit condition) at headings of 0°, 20°, and 180°, and at speeds up to 12 knots for 0°, 9 knots for 20° and 180° with propellers operating astern and 6 knots for 180° with propellers operating ahead. Propellers run in incremental steps up to maximum power of 8,000 hp.

1.2.2 70' draft (drilling condition) at headings of 0°, 20°, 45°, 135°, 160°, and 180°, and at speeds up to 6.3 knots for 0° and 180°,

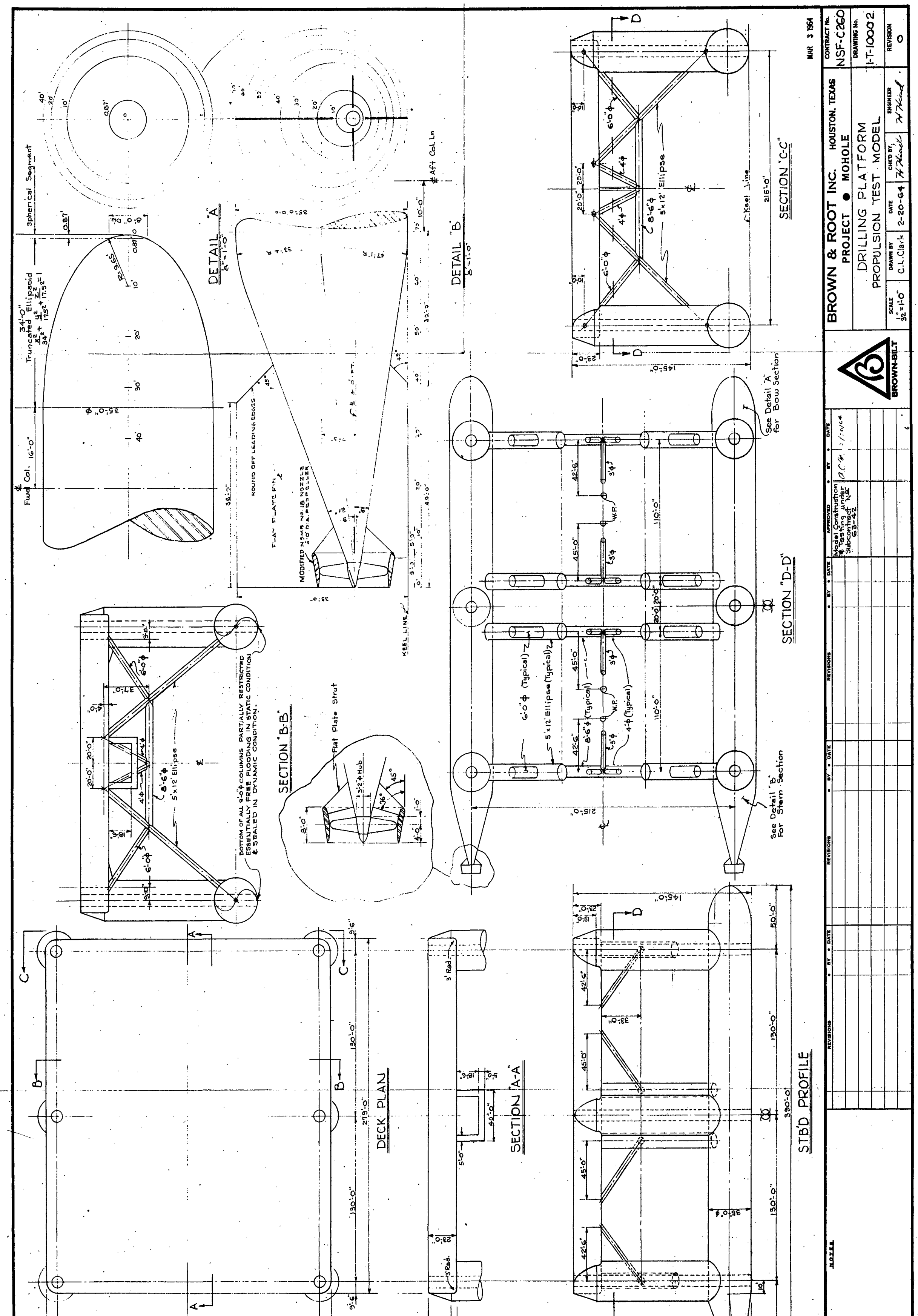
BROWN & ROOT INC. HOUSTON, TEXAS
PROJECT ● MOHOLE
DRILLING PLATFORM
PROPULSION TEST MODEL
CONTRACT No. NSF-C260
DRAWING No. I-T-10002
REVISION 0
SCALE 1/32"=1'-0"
DRAWN BY C.L.Clark
DATE 2-20-64
MAR 3 1964
DETAIL "A"
DETAIL "B"
SECTION "B-B"
SECTION "C-C"
SECTION "D-D"
SECTION "A-A"
DECK PLAN
STB'D PROFILE
BROWN-BILT

Fig. 1.1

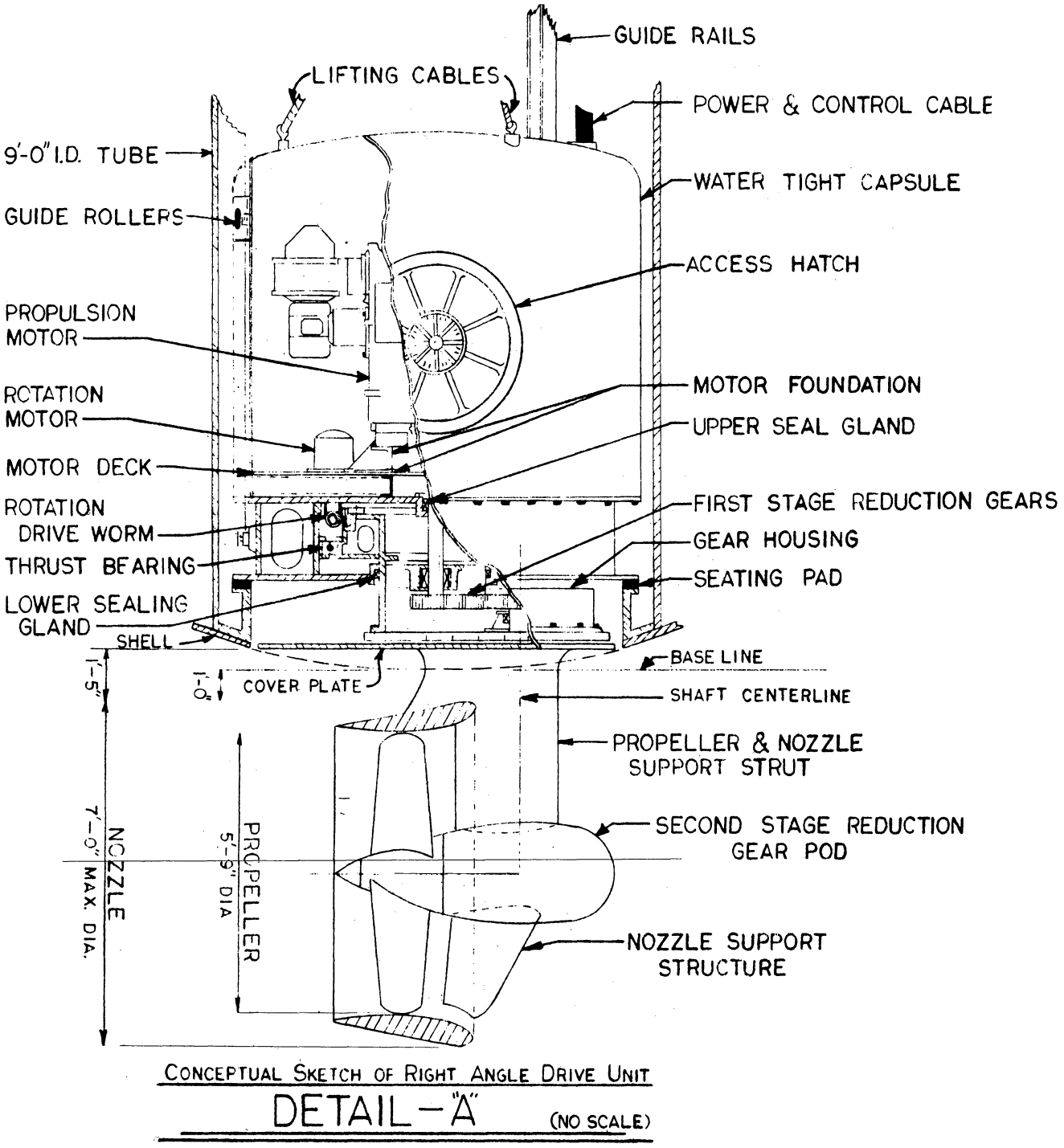

CONCEPTUAL SKETCH OF RIGHT ANGLE DRIVE UNIT

DETAIL – "A" (NO SCALE)

Fig. 1.2

4.75 knots for 20° and 160°, and 3.75 knots for 45° and 135°. Incremental power loading was done in a manner similar to the procedure used under 1.2.1. At angles above 90° the model was also tested with propellers operating astern.

1.2.3 "Bollard pull" in drilling and transit conditions at speeds of about one knot and over the range of angles covered under 1.2.1 and 1.2.2. Propeller was run at near maximum power.

1.3 Open water tests of steering propulsion units at headings of 0°, 30°, 60°, and 85°. The unit was tested over a complete speed range from bollard to free wheeling (no thrust) at constant rate of rotation. Both 600 and 800 rpm were used and it was verified that no noticeable Reynolds number effect existed.

The steering propulsion unit was also tested under bollard conditions when placed under a model simulating the platform hull. The axis of this model was always transverse to the towing tank whereas the steering unit was tested at all heading angles listed above. Furthermore, performance over a small range of advance coefficients was investigated.

1.4 Open water tests were performed with both main propulsion propellers. The propellers were tested operating in a nozzle of the same dimensions as the nozzles designed for the drilling platform except that the angle of attack of the nozzle foil section was reduced to make it equal to the value given by Van Manen for unobstructed inflow conditions. The force on the nozzle was not measured. The nozzles were considered an integral part of the drilling platform and were, therefore, built as fixed appendages. Both propellers were tested at straight inflow conditions and one propeller (left hand) was tested at an inflow angle to the propeller axis of approximately 10° and 20°. It was found that within this range of angles the propeller characteristics were not significantly altered. Free-wheeling propeller tests were also run to determine the velocity increase at the propeller disc produced by the nozzle, and also the change in average velocity due to a non-zero angle of inflow. Free wheeling propeller tests were also run with the propellers in their normal running position which allowed an independent evaluation of advance coefficients to be made, different from that normally made by comparison of propeller performance behind the hull and the open water propeller characteristics.

1.5 Deceleration tests were made at drilling platform headings of 0°, 90°, and 180° at 70 ft draft. It was initially intended to conduct acceleration tests. A careful consideration of all factors such as the number of readings, noise level of records and the fact that the towing carriage does not provide for positive acceleration control lead to the conclusion that the desired information could most easily be obtained by releasing the model from the carriage when moving at constant speed and subsequently the speed of the towing carriage be continuously adjusted to that of the deceler-

ating free moving drilling platform. This scheme was then used during 8 to 15 runs at each of the headings mentioned above. The large number of runs was necessary to develop a sufficiently coordinated testing pattern by the testing personnel.

2. MODELS AND INSTRUMENTATION

2.1 DRILLING PLATFORM AND MAIN PROPELLERS

The model was made almost entirely from aluminum. Cylinders were rolled from 1/8 in. aluminum plate. The vertical cylinders were made in such a way that their length could be adjusted to the draft of the model. This was necessary to allow the model to fit under the carriage during testing. The two longitudinal units each consisting of one longitudinal cylinder and three vertical cylinders were connected by three pairs of 4 in. aluminum channels, bolted together at the joints. The model is shown during testing in Figure 2.1.1.

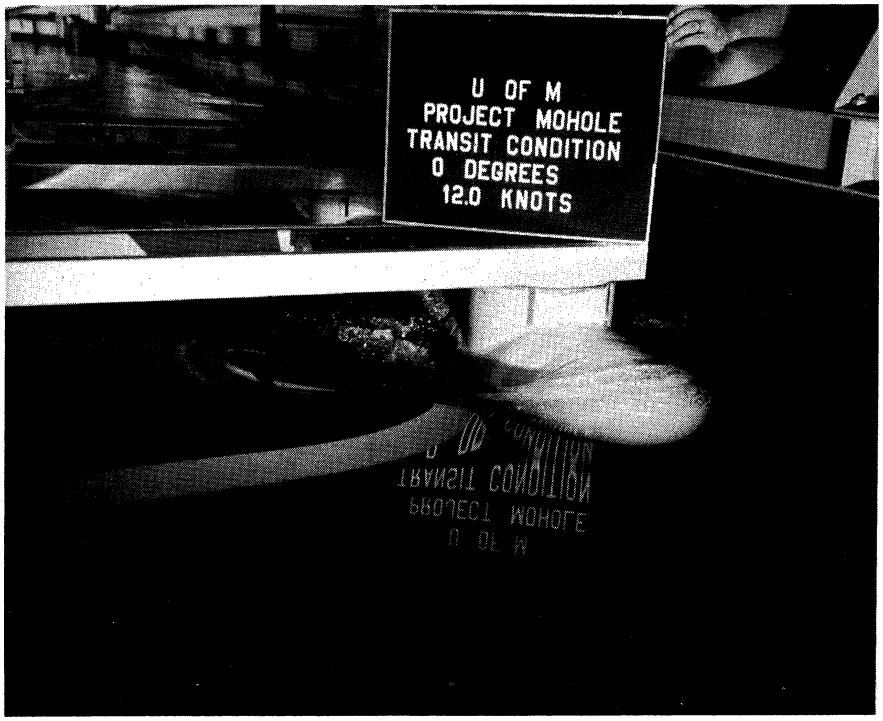

Figure 2.1.1

Nose and tail pieces were made from laminated mahogany and fastened to the aluminum cylinders with wood screws.

Propeller dynamometers and drive motors were mounted on a foundation attached to the tail pieces. Thus, it was possible to readily remove the whole tail assembly including propeller drives for installation and alignment. Fins were made of aluminum plates 1/8 in. thick. The nozzles were turned on a lathe from a block of Plexiglass. The profile of the nozzles is shown in Figure 2.1.2. After some difficulties experienced in obtaining aluminum cast-

MAIN PROPULSION FOR MODEL TESTS

NOZZLE

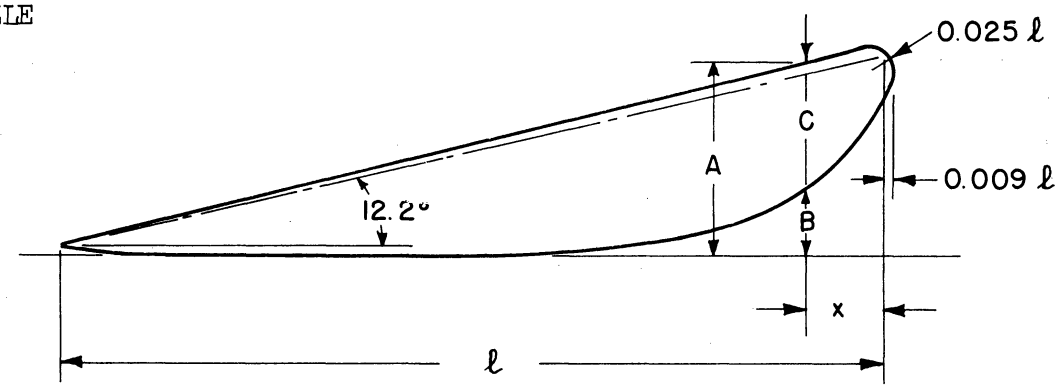

NOZZLE SECTION OFFSETS			
x/ℓ x 100	A/ℓ x 100	B/ℓ x 100	C/ℓ x 100
0	23.43	18.33	5.10
2.5	23.89	13.99	9.90
5.0	23.35	11.06	12.29
7.5	22.81	8.87	13.94
10.0	22.26	7.08	15.18
15.0	21.17	4.48	16.69
20.0	20.09	2.64	17.45
25.0	19.01	1.43	17.58
30.0	17.92	0.65	17.27
40.0	15.75	0.08	15.67
50.0	13.58	0	13.58
60.0	11.41	0	11.41
70.0	9.24	0.12	9.32
80.0	7.07	0.53	6.54
90.0	4.90	1.10	3.80
95.0	3.81	1.45	2.36
100.0	2.73	1.78	0.95

NOZZLE SECTION IS MODIFICATION OF VAN MANEN NO. 18

Sketch RT-117-01
27 December 1963

PROPELLER

4 Bladed Kaplan Type (K4-55)
Diameter 16'- 0"
Pitch 13'-11"

Figure 2.1.2

ings for the main propellers, it was decided to manufacture them entirely by hand from a block of magnesium. This proved in general to be a success, although a check of finished propellers revealed that the left hand propeller was about one half percent overpitched and the right hand propeller about 5-1/2% overpitched. The difference in pitch is thought to be mostly due to release of built-in stresses. The performance characteristics of the two propellers are completely compatible, however, in that one curve can be calculated with sufficient accuracy from the other simply by taking the pitch variations into account.

All dynamometers for measurement of the forces and moments acting on the platform were attached to a 4 in. x 4 in. wooden beam which was always oriented along the carriage centerline.

The drilling platform was attached to this wooden beam, and was rotated around a bolt located at the intersection of the longitudinal centerline of the platform and the transverse centerline of the middle vertical cylinders when tested at non-zero heading angles.

As a result, test data refers initially to the carriage coordinates. These correspond to what may be considered the flow coordinates and the force components measured in the horizontal plane are therefore designated Drag and Lift. Decomposed to the platform coordinates the forces are referred to as Resistance and Side Force. Figure 3.0.1 illustrates these coordinates.

Yaw moment is taken with respect to the bolt location referred to above. Other moments are those of trim and heel. During deep draft tests it is inevitable to introduce trim and heel moments because the tow bar and side force attachments are located about 15 in. above the water surface on the model. A system of loading and unloading weights at specified points was therefore desired so that the model would remain essentially horizontal during testing. The magnitude of the corrective moments when applied were recorded. In no cases were they found to be required under transit conditions and neither did the self-propelled test ever cause any significant trim and heel conditions, except under drilling conditions when propelled opposite to direction of motion. Even under these severe conditions the trim and heel moments were not excessive.

It is fairly safe to conclude that heel and trim due to hydrodynamic drag and lift together with propeller thrust should not be of much concern in the case of the full size platform.

2.2 POSITIONING UNIT

The overall model design is shown in Figure 2.2.1. Because this figure

includes both dynamometer parts in addition to the steering unit itself, a

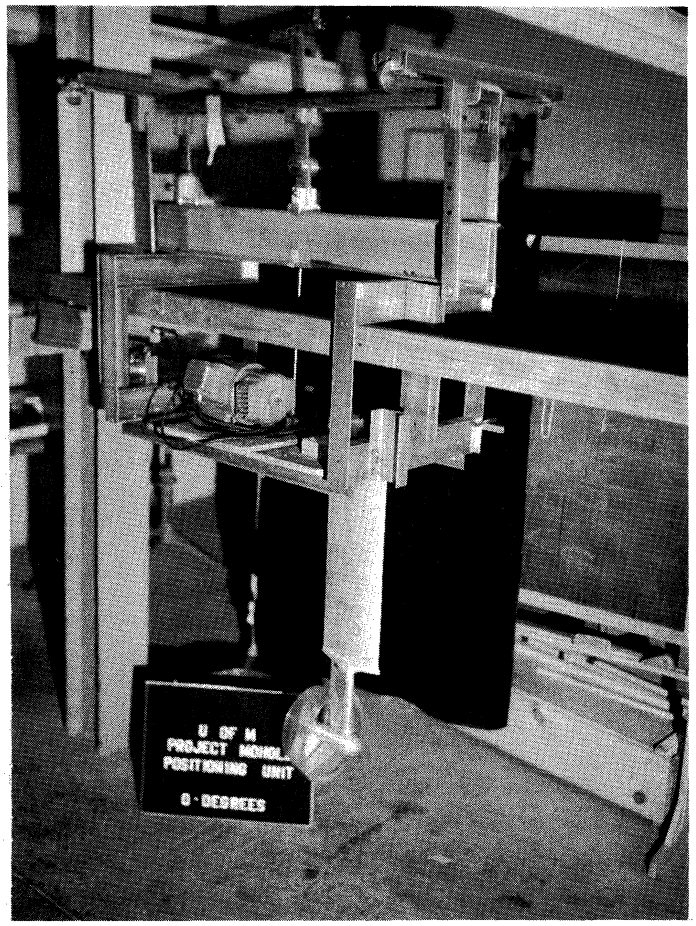

Figure 2.2.1

few words of description of the various parts are in order. The steering unit tests were designed to measure side forces at non-zero heading angles as well as the force developed in the direction of motion, all as a function of torque, propeller rpm, and carriage speed.

To accomplish this, a platform was suspended by four leaf springs, one at each corner, from two transverse channels fastened to a floating beam dynamometer which was already available. The leaf springs allowed a fairly free lateral motion relative to the longitudinal dynamometer beam. Load cells introduced to restrain this motion would therefore measure almost the entire lateral force, thus providing good resolution of data. The entire system is linear and the complete dynamometer was calibrated by applying known side forces statically to the platform. Because two load cells were used, one at each end of the platform, it was hoped that turning moments could be evaluated from the record. In this respect we were disappointed, however, when final calibration revealed that the separation of forces between the two load cells depended upon the moment of forces around a longitudinal axis.

The drive motor and torque transducer were located on the platform. The propeller was driven through two pairs of bevel gears (1:1 ratio). Since the propeller was to be tested at various heading angles, it was found necessary to make the vertical strut in two parts. The upper part was fixed, and all the data were corrected to compensate for the fixed portion of the strut.

The steering propulsion unit model is shown in greater detail in Figure 2.2.2.

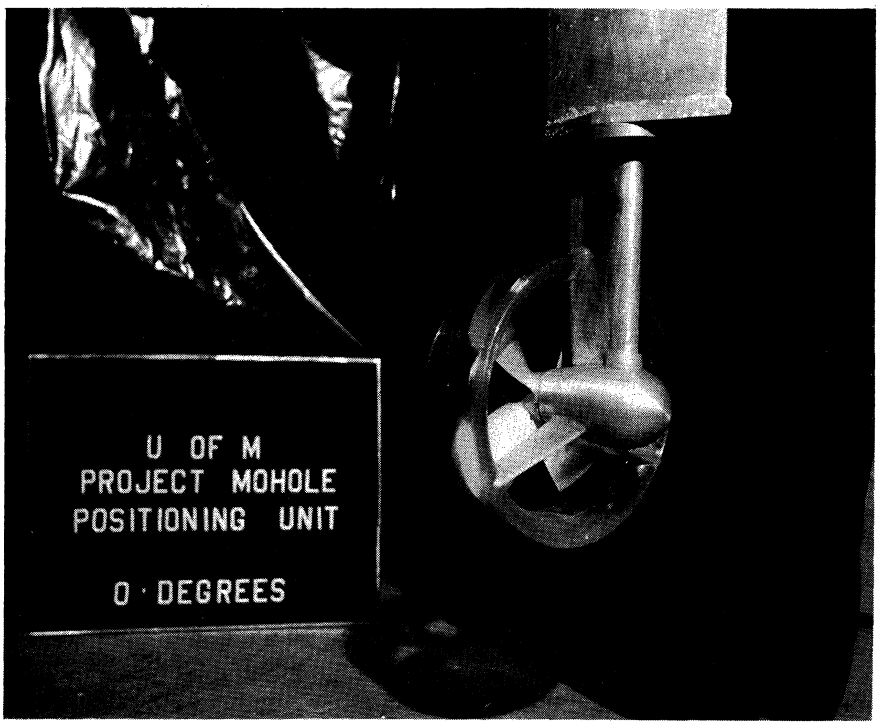

Figure 2.2.2

The diameter of the aluminum propeller was 9.2 in. and the Plexiglass nozzle was made in accordance with dimensions given in Figure 2.2.3 allowing a 1/32-in. clearance between propeller blades and nozzle. The principal prototype propeller dimensions are also given in Figure 2.2.3.

The propeller axis was located at a depth of about 17 in. below the free surface during testing. This depth was increased during the testing of the steering propulsion unit under the semi-cylindrical shell which simulated the drilling platform hull.

This semi-cylindrical shell consisted of a masonite sheet wrapped around a wooden frame made to dimensions given in Figure 2.2.4. The shell was attached directly to the carriage. No contact existed between steering propeller unit and shell.

It has already been mentioned that dynamometer forces were calibrated by applying forces directly to the dynamometer. To this should be added that

STFERING UNIT PROPULSION FOR MODEL TESTS

NOZZLE

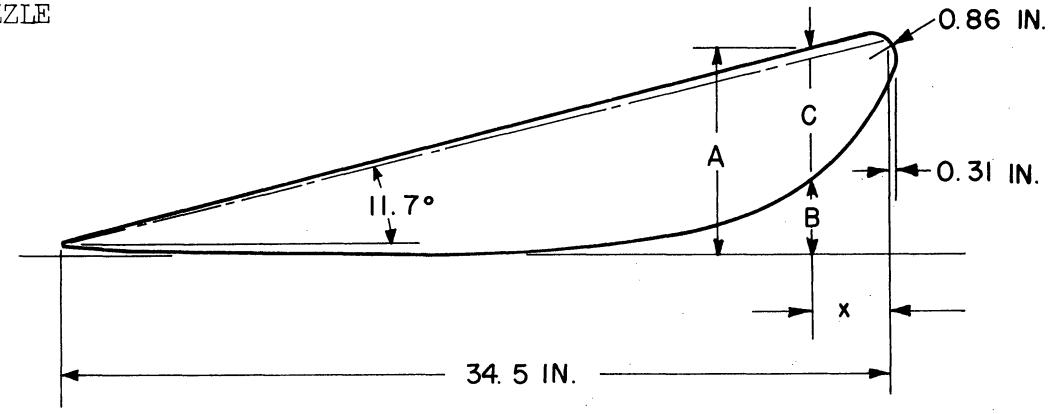

KORT NOZZLE FOR POSITIONING UNITS
MOHOLE DRILLING PLATFORM

NOZZLE SECTION OFFSETS			
x ~ in	A ~ in	B ~ in	C ~ in
0	7.90	6.14	1.76
.86	8.07	4.65	3.42
1.72	7/89	3.65	4.24
2.59	7.71	2.90	4.81
3.45	7.53	2.29	5.24
5.18	7.17	1.40	5.77
6.90	6.82	.78	6.04
8.62	6.46	.37	6.09
10.35	6.10	.17	5.93
13.80	5.39	0	5.39
17.25	4.67	0	4.67
20.70	3.96	0	3.96
24.15	3.25	.12	3.13
27.60	2.53	.28	2.25
31.05	1.82	.52	1.30
32.78	1.46	.65	.81
34.50	1.10	.81	.29

NOZZLE SECTION IS MODIFICATION OF VAN MANEN NO. 18

Sketch RT-117-04
20 March 1964

PROPELLER

4 Bladed Kaplan Type (K4-55)
Diameter 5'-9"
Pitch 5'-0"

Figure. 2.2.3

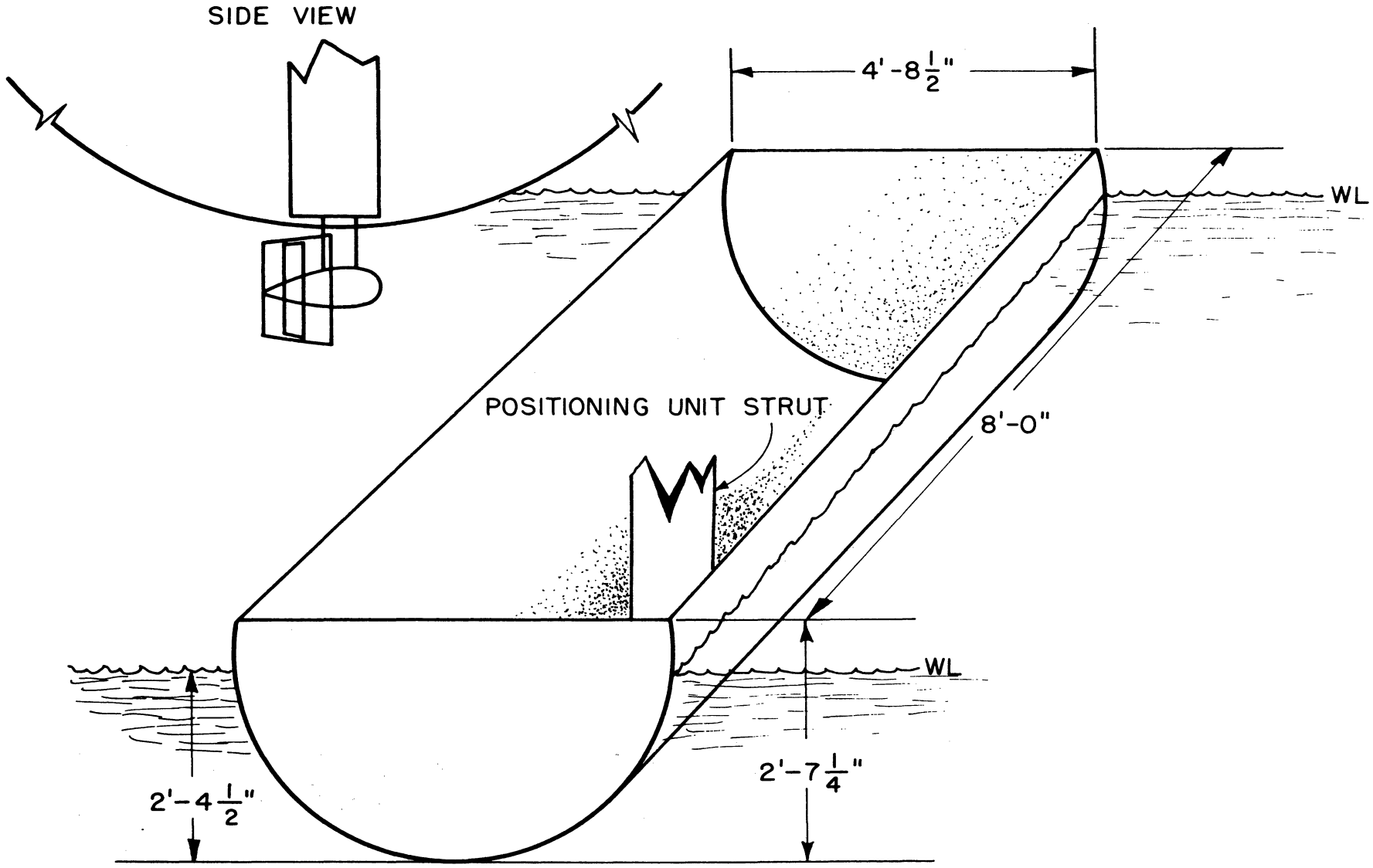

Fig. 2.2.4

the torque dynamometer was calibrated dynamically against a calibration generator. Since this generator was attached directly to the propeller shaft during calibration, it was possible also to evaluate the friction loss in the bevel gear drive as a function of load and rpm.

3. DATA AND FULL SCALE PERFORMANCE PREDICTIONS

Before referring to the detailed test results it may be advantageous to list here definitions of all symbols used in the figures. These are as follows:

Towing Tests

D Component of hydrodynamic force in pounds on the platform parallel to the direction of motion. Positive D is in direction opposite to V_k vector.

L Component of hydrodynamic force in pounds on the platform perpendicular to the direction of motion. L is positive if it is at an angle of + 90° to V_k.

M Yawing moment in foot-pounds acting on the platform measured about the intersection of the fore and aft centerline and the line connecting the centers of the middle vertical cylinders. Positive moments are counter-clockwise.

R Component of hydrodynamic force in pounds on the platform parallel to the longitudinal centerline. Positive R acts opposite to the direction of the component of the V_k vector parallel to R.

S Component of the hydrodynamic force in pounds acting on the platform perpendicular to the longitudinal centerline. Positive S acts at an angle of + 90° off the bow.

V_k Speed of platform in knots.

Θ Angle of model to flow in degrees. Positive Θ is measured clockwise.

Open Water Tests of Main Propulsion Propellers

d Diameter of propeller in feet.

n Revolutions per second.

T Propeller thrust in pounds.

Q Propeller torque in pounds.

V_a Velocity of advance in feet per second (carriage coordinates).

ρ Density of water in slugs per cubic foot.

J_a Advance coefficient, $\frac{V_a}{nd}$

K_t Thrust coefficient, $\frac{T}{\rho n^2 d^4}$

K_q Torque coefficient, $\frac{Q}{\rho n^2 d^5}$

η Propeller efficiency, $\frac{K_t J_a}{K_q 2\pi}$

V_m Velocity of model in feet per second (carriage coordinates).

Self-Propulsion Tests

D_p, L_p, M_p, R_p, S_p Hydrodynamic forces on the platform with the propellers running. They are defined exactly the same as the un-subscripted forces.

T_p Total propeller thrust in pounds along propeller axis.

t Propeller-hull interaction force in pounds. Positive t in the same direction as T_p.

SHP Total shaft horsepower.

Other symbols used in this section have been previously defined.

Positioning Unit

T Force component exerted by unit parallel to V_a vector. Positive T is in same direction as V_a.

F_s Force component exerted by unit perpendicular to V_a vector. Positive F_s acts at an angle of + 90° to V_a.

K_t Thrust coefficient, $\frac{T}{\rho n^2 d^4}$

K_s Side force coefficient, $\frac{F_s}{\rho n^2 d^4}$

D_n Drag of the nozzle and strut in pounds with the propeller freewheeling. Positive D_n is in direction opposite to V_a vector.

L_n Lift of the nozzle and strut in pounds with the propeller freewheeling. Positive L_n is in direction + 90° from V_a vector.

Other symbols used in this section have been defined previously.

Figure 3.0.1 illustrates clearly the definitions of the forces acting on the platform.

Although all tests are parts of the same overall program it soon became convenient to refer to individual sections almost as separate programs by themselves. This breakdown has been carried over into this report as follows.

3.1 TOWING TESTS (EHP TESTS)

It was stated in the introduction that size of towing tank (maximum width of 22 ft) imposed an upper limit on model size. This was much in evidence when testing at angles of around 45° yaw. Initially, it was thought that at these large angles the blockage would be quite significant. A careful look at the streamlines around the ends when testing under transit conditions revealed that the flow around the longitudinal cylindrical hulls had become, to a large extent, two dimensional, however, and the blockage effect was not judged to have been greatly changed due to large yaw angles.

A more serious question may be that concerned with Reynolds number effects. The strange behavior of circular cylinders as a function of Reynolds number is

FIGURE 3.0.1
DEFINITION OF
COORDINATE SYSTEMS

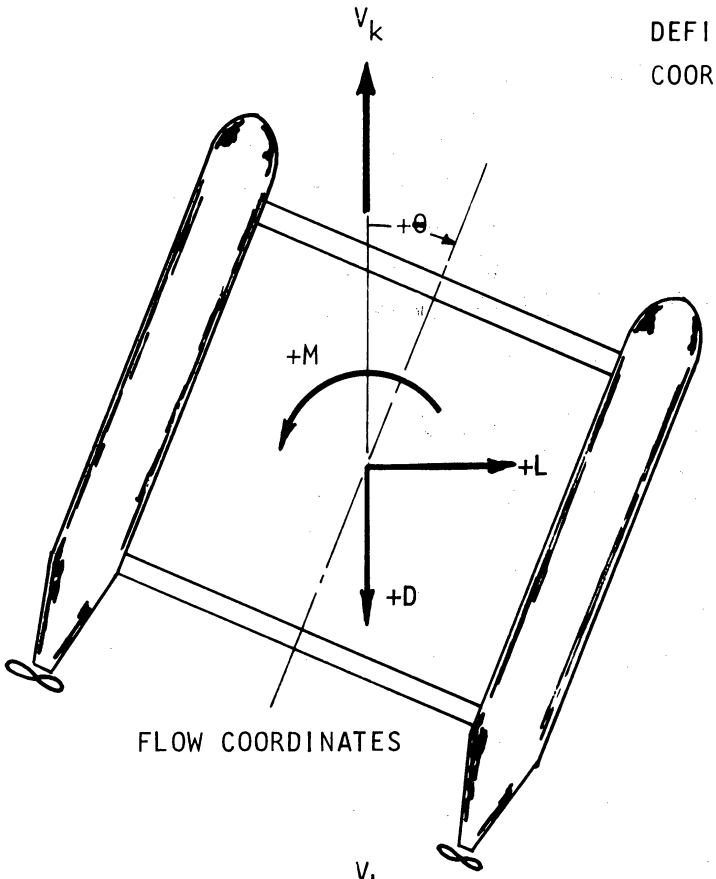

FLOW COORDINATES

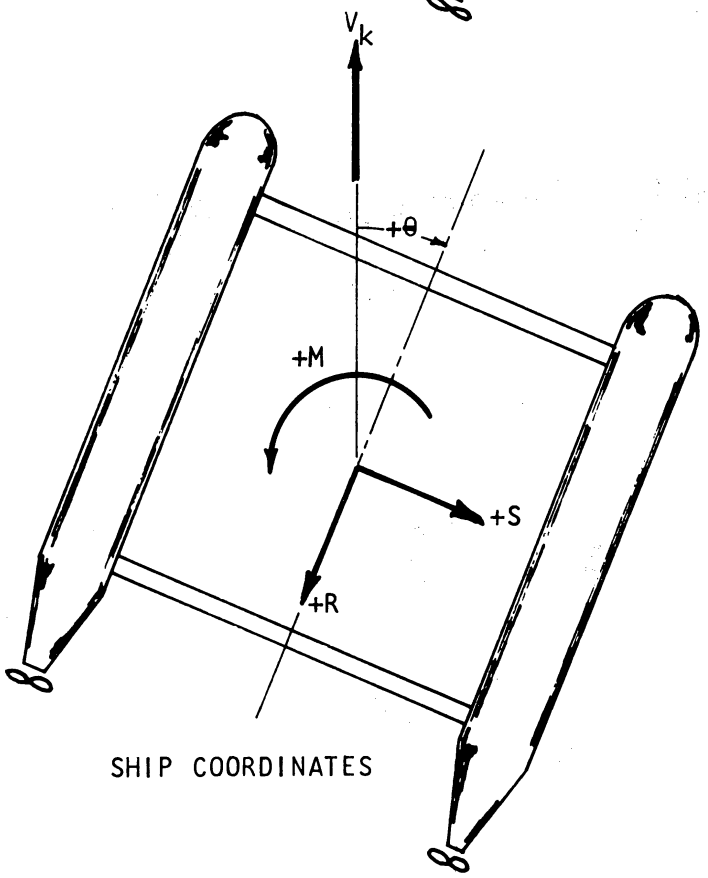

SHIP COORDINATES

well known as is the conclusion reached from it that it is imperative to make the boundary layer flow turbulent some distance ahead of maximum beam. To accomplish this, wide longitudinal strips of coarse sandpaper were glued to all cylinders every 45° of circumference. We are quite confident that these strips did perform satisfactorily. Previous tests with two models of an oil drilling platform made to different scale ratios indicate that the laminar-turbulent transition takes place at a model size considerably smaller than that of the Mohole drilling platform.

It is also of interest to note from Figure 3.1.21 that extrapolation of data by the usual ship method using the ATTC friction line gives results only a little below the simple λ^3 extrapolation. The nature of the flow is probably such that a λ^3 extrapolation (hydrodynamic forces proportional to the square of the velocity) is a better approximation than the ATTC method. In essence it implies that the resistance is independent of the Reynolds number. In this report the λ^3 extrapolation is used throughout. A 3% allowance has been made for the difference in density of salt and fresh water. A different flow separation problem of interest is that occurring at the transition between the longitudinal cylinders and the stern sections. This problem was studied to some extent both in the transit and drilling conditions. The separation under transit conditions and 0° yaw is shown in Figure 3.1.0 to be severe.

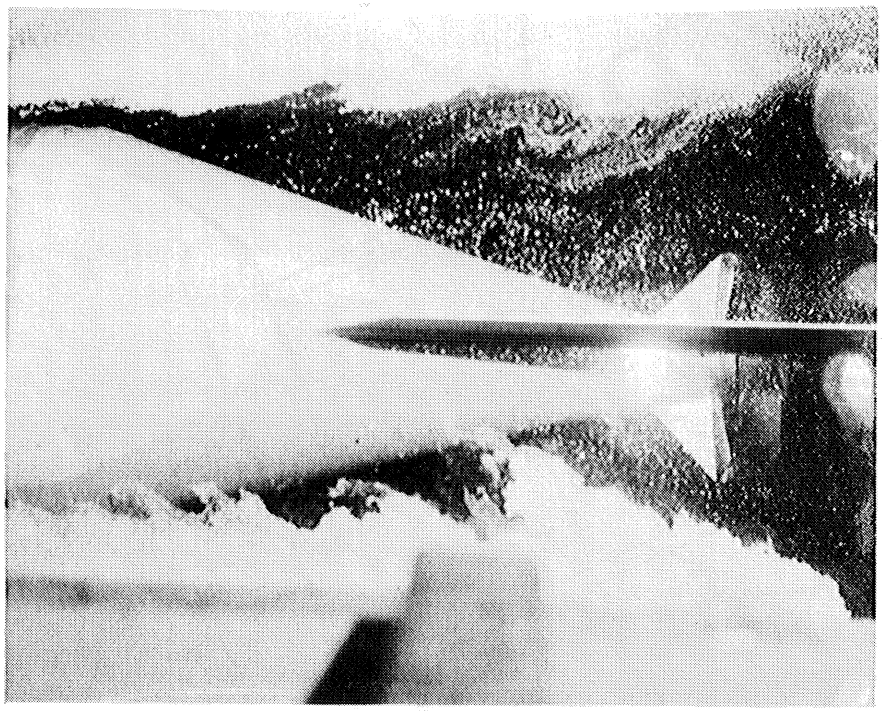

Figure 3.1.0

The picture was taken with aluminum powder on the surface and the dark area indicates the wake region behind the points of separation. A floating particle in this region would sometimes follow the model the whole length of a run.

The situation does not appear to be quite that serious under drilling conditions. Separation could here best be observed by injecting aluminum powder mixed with alcohol through a tube into the flow. Separation seemed to occur half way aft on the stern section, but with the propeller working the flow appeared to be stabilized.

Figures 3.1.1 through 3.1.10 show the performance of the platform during transit conditions (28 ft draft). Figures 3.1.11 through 3.1.20 cover the same for drilling conditions (70 ft draft). Figures 2.1.22 and 2.1.23 give the results of the deceleration tests (70 ft draft). These results are a little startling. A priori it was expected that the deceleration would be smaller than that obtained from Newton's law using the steady state drag as a force. The reason for this was based on the idea of the hydrodynamic mass. Results show, however, that at 0° heading and at speeds close to release speeds the deceleration measured is higher than expected. The platform was apparently adding to the fluid rather than recovering from it kinetic energy as it is slowing down. The behavior is as expected at the lower speeds and also for 90° heading. This phenomena may need further investigation.

3.2 OPEN WATER TESTS OF MAIN PROPELLERS

Propeller tests were made with the propeller boat in the usual manner except that a Plexiglass nozzle was attached to the propeller boat. Only forces acting on the propellers were measured.

The characteristics curves of the right hand propeller are shown in Figure 3.2.1. This propeller, being about 5-1/2% overpitched was tested only in axial flow. Figure 3.2.2 shows the same curves for the left handed propeller in addition to those obtained for 10° and 20° angle of flow relative to propeller axis. It is interesting to note that the propeller performance is for all practical purposes not influenced by inflow angles up to at least 20°, which was the maximum angle that could be investigated without modification of existing testing facilities. Free wheeling test results given in Figures 3.2.3 and 3.2.4 reveal that the nozzle serves as a very good flow deflector so that the average velocity of the flow at the propeller disc is fairly constant with respect to angle of inflow over the range of angles considered.

3.3 SELF-PROPULSION TESTS

The objective here was to study the change of dynamometer forces as a function of shaft horsepower output of the main propellers. The same quantities were therefore measured as under Section 3.1 and plotted versus SHP, with angle of heading as a parameter. SHP was obtained directly from the propeller dynamometers installed in the model. The dynamometer in the starboard

unit measured torque, thrust and rpm whereas a rented dynamometer in the port unit only measured torque and rpm. The speeds of rotation of the two propellers were adjusted to correct for the difference in pitch. As expected it was found that the propeller nozzles were developing a significant thrust force. Unfortunately, we were not instrumented to measure this force by itself, but it was possible to calculate by the use of the propeller curves a thrust interaction force which would include the nozzle thrust and the force normally referred to as thrust deduction. This interaction thrust can be either positive or negative and several non-dimensional ratios can be formed by dividing it with other forces acting on the platform. Because of this multiplicity of choice it was decided to plot only the measured dimensional force.

The extrapolation of the SHP data to the ship scale was carried out in the standard manner with one exception. Normally, in SHP tests, a small correction is made in extrapolation to account for Reynolds number effects. As previously stated, Reynolds number effects were found to be negligible with this model. Thus thrust is extrapolated according to λ^3 in the same way as in drag. Torque is proportional to λ^4 and rpm to $\lambda^{-0.5}$. Since SHP = constant x torque x rpm, shaft horsepower is proportional to $\lambda^{3.5}$.*

Self-propulsion tests were run at several headings under both transit and drilling conditions. Figures 3.3.1 through 3.3.13 cover the transit condition, whereas Figures 3.3.14 through 3.3.48 refer to tests performed at the drilling operation draft of 70 ft. Figure 3.3.49 shows the platform performance at bollard pull.

3.4 STEERING PROPULSION UNIT

The steering propulsion unit has already been described in some detail under Section 2.2. Nondimensional plots of propeller characteristics are shown in Figures 3.4.1 through 3.4.15 covering tests with and without simulated hull model in place.

In reducing the test data it was at first believed necessary to add to the thrust force in the flow direction the drag of the strut and the nozzle. Because it was thought that this drag, being primarily due to the boundary layer and eddies, would not behave as a potential flow. However, it was found that non-dimensional coefficients calculated from total measured forces obtained from runs at constant values of the advance coefficient but at two different rpm's (600 and 800) would plot on the same curves. It was, therefore, decided that it would be most suitable to use total measured forces. The force acting on the unit without the propeller in place is given in Figure 3.4.15.

---

*Principles of Naval Architecture, Rossell and Chapman, Vol. II, S.N.A.M.E., Chapter 3.

All variables are referred to the flow coordinates, i.e., the thrust coefficient is evaluated from the force measured in the direction of inflow (direction of motion in the stationary fluid). Performance characteristics can easily be transferred, however, to the coordinate system fixed in the positioning unit, or any other coordinate system in which magnitude of force components are needed, by the use of Figure 3.4.9. A line in this figure extending from origin to a point on a contour of constant θ represents the total force coefficient at a particular value of the advance coefficient. This force coefficient can then be decomposed into any two directions. In Figure 3.4.9 the vertical axis represents the thrust coefficient in the direction of flow and the horizontal axis represents the side-force coefficient. Contours of constant values of advance and torque coefficients have been added to the figure so that in reality it represents a complete performance chart of the steering propulsion unit.

ACKNOWLEDGMENTS

A test program as unique as the one described in this report will usually demand a great deal more from those taking part in it than will a more routine job. The final results depend, therefore, to a large extent upon how test personnel respond to this demand.

Without exception it has been the gratifying experience of the authors to witness efforts put forth by all concerned with the Mohole Project far beyond what would normally be expected. A majority of our staff members have at some time or another worked on this program and to mention everyone by name is perhaps not necessary. However, the authors wish to give special recognition to Mr. Phil Schnell who supervised the construction of the aluminum platform model and many more of the model details. Also Mr. Corning Townsend deserves to be mentioned for his effort in designing and building the steering propulsion unit. In addition he was responsible for much of the tesing of that unit. Last but not least, Mr. John Gebhardt and Mr. Bruce Nelson have contributed a great deal towards the completion of the testing program. Theirs has been the task of running many of the tests and the reduction of most of the data.

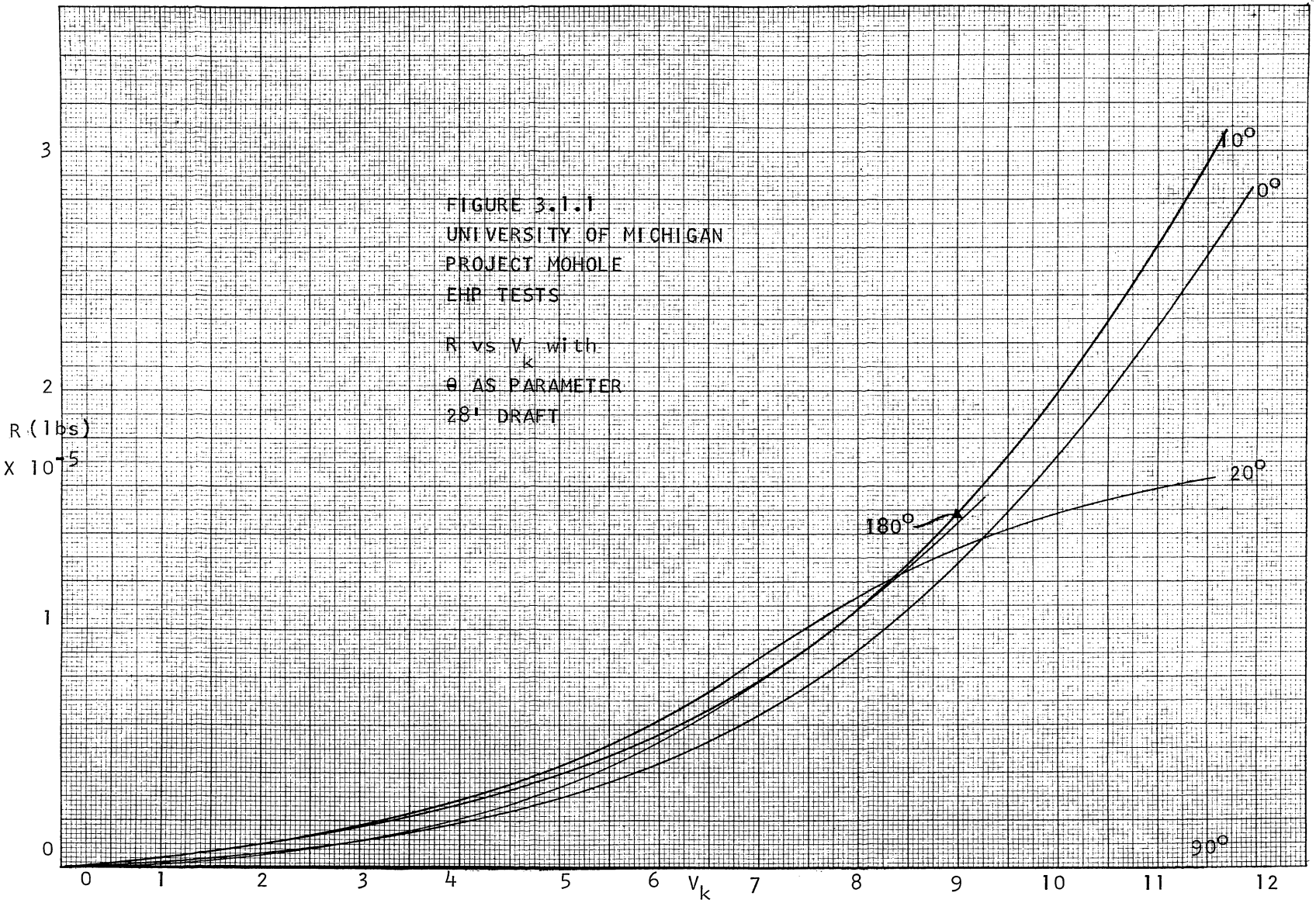
FIGURE 3.1.1
UNIVERSITY OF MICHIGAN
PROJECT MOHOLE
EHP TESTS
R vs V_k with
θ AS PARAMETER
28' DRAFT
R (lbs)
X 10^{-5}
3
2
1
0
0 1 2 3 4 5 6 V_k 7 8 9 10 11 12
10°
0°
20°
180°
90°

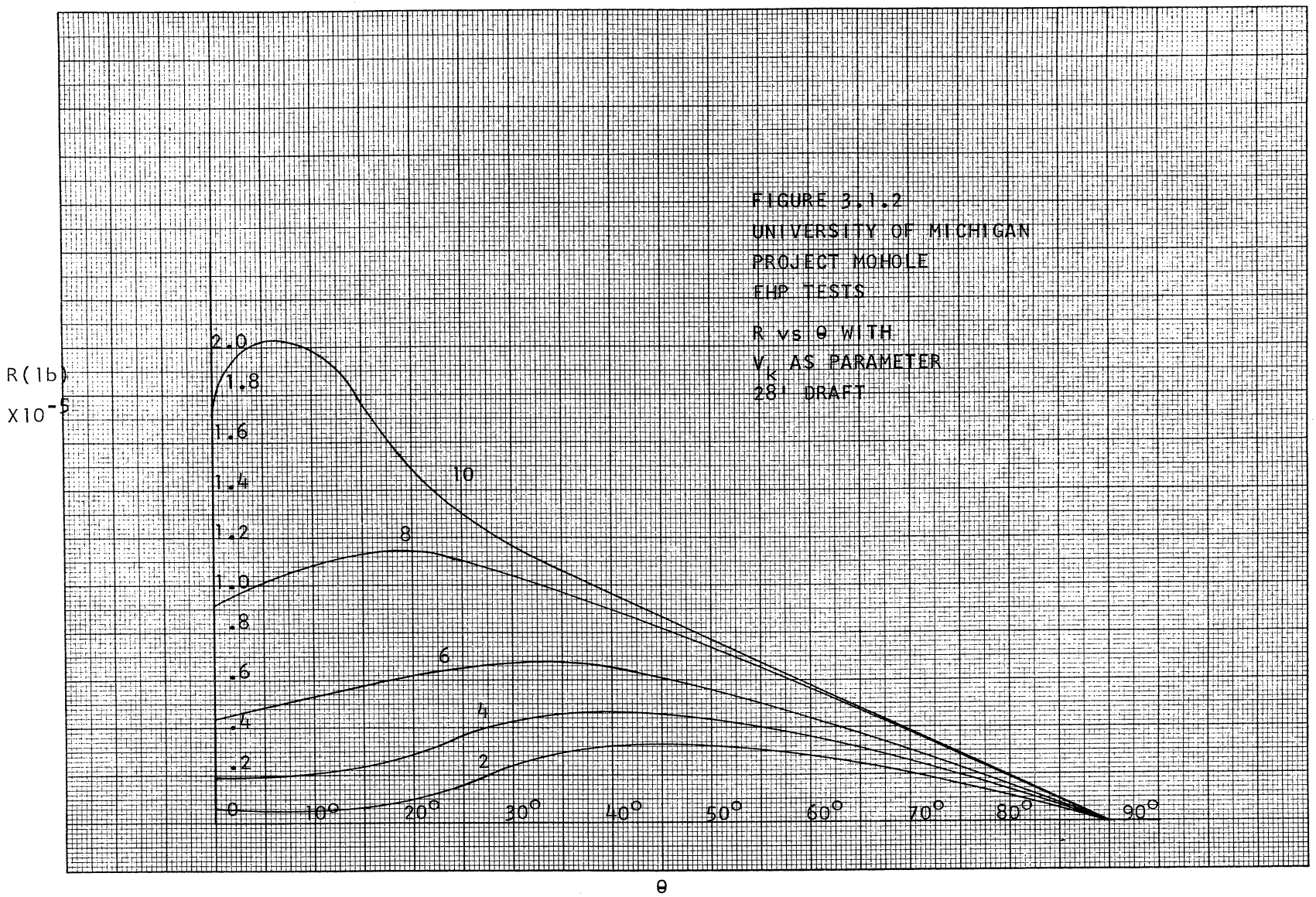
FIGURE 3.1.2
UNIVERSITY OF MICHIGAN
PROJECT MOHOLE
FHP TESTS
R vs θ WITH
V_K AS PARAMETER
28' DRAFT
R(lb)
X10⁻⁵
2.0
1.8
1.6
1.4
1.2
1.0
.8
.6
.4
.2
0
10
8
6
4
2
10°
20°
30°
40°
50°
60°
70°
80°
90°
θ

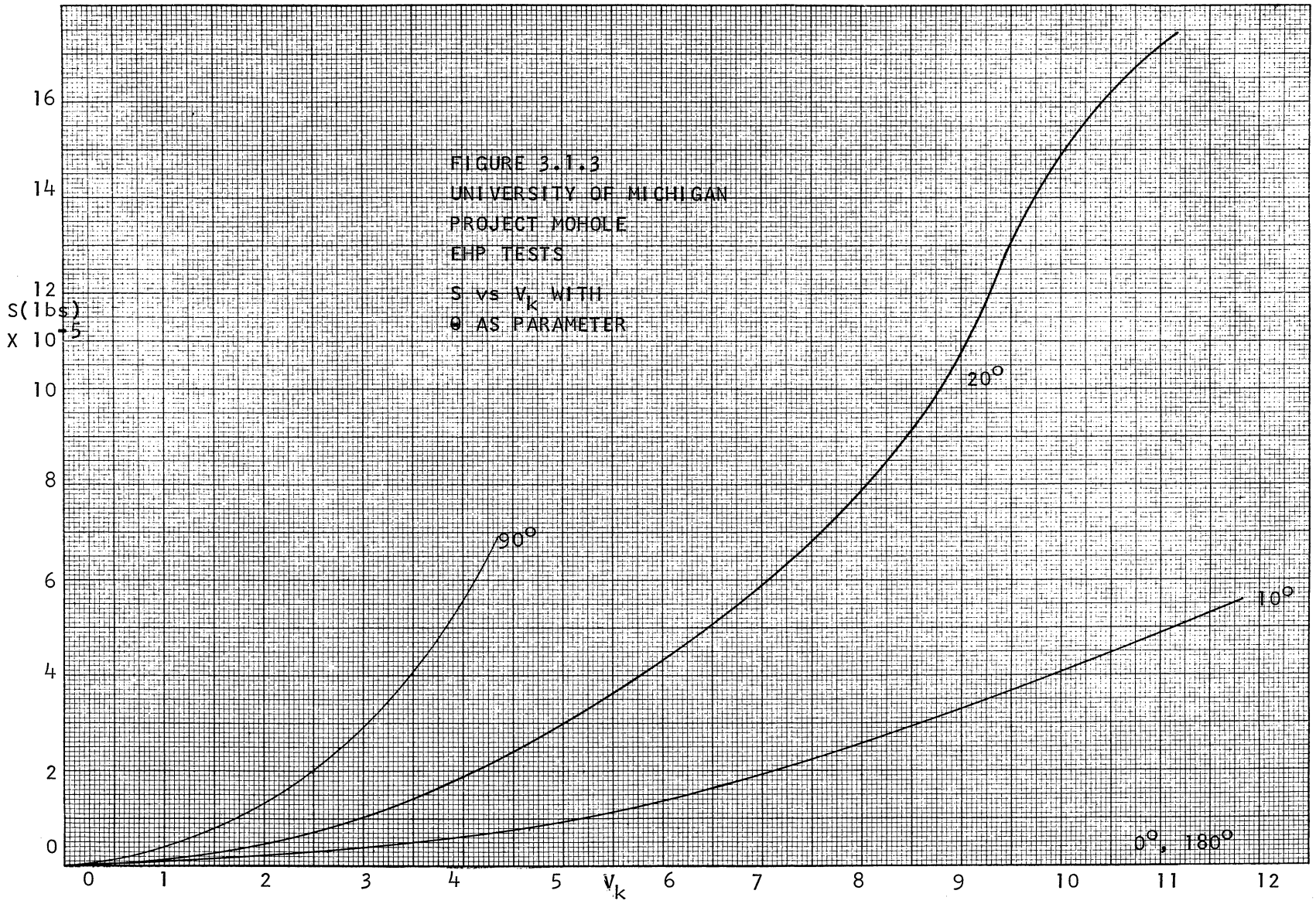
FIGURE 3.1.3
UNIVERSITY OF MICHIGAN
PROJECT MOHOLE
EHP TESTS
S vs V_k WITH
θ AS PARAMETER
S(lbs)
X 10^{-5}
V_k
90°
20°
10°
0°, 180°
0
1
2
3
4
5
6
7
8
9
10
11
12
0
2
4
6
8
10
12
14
16

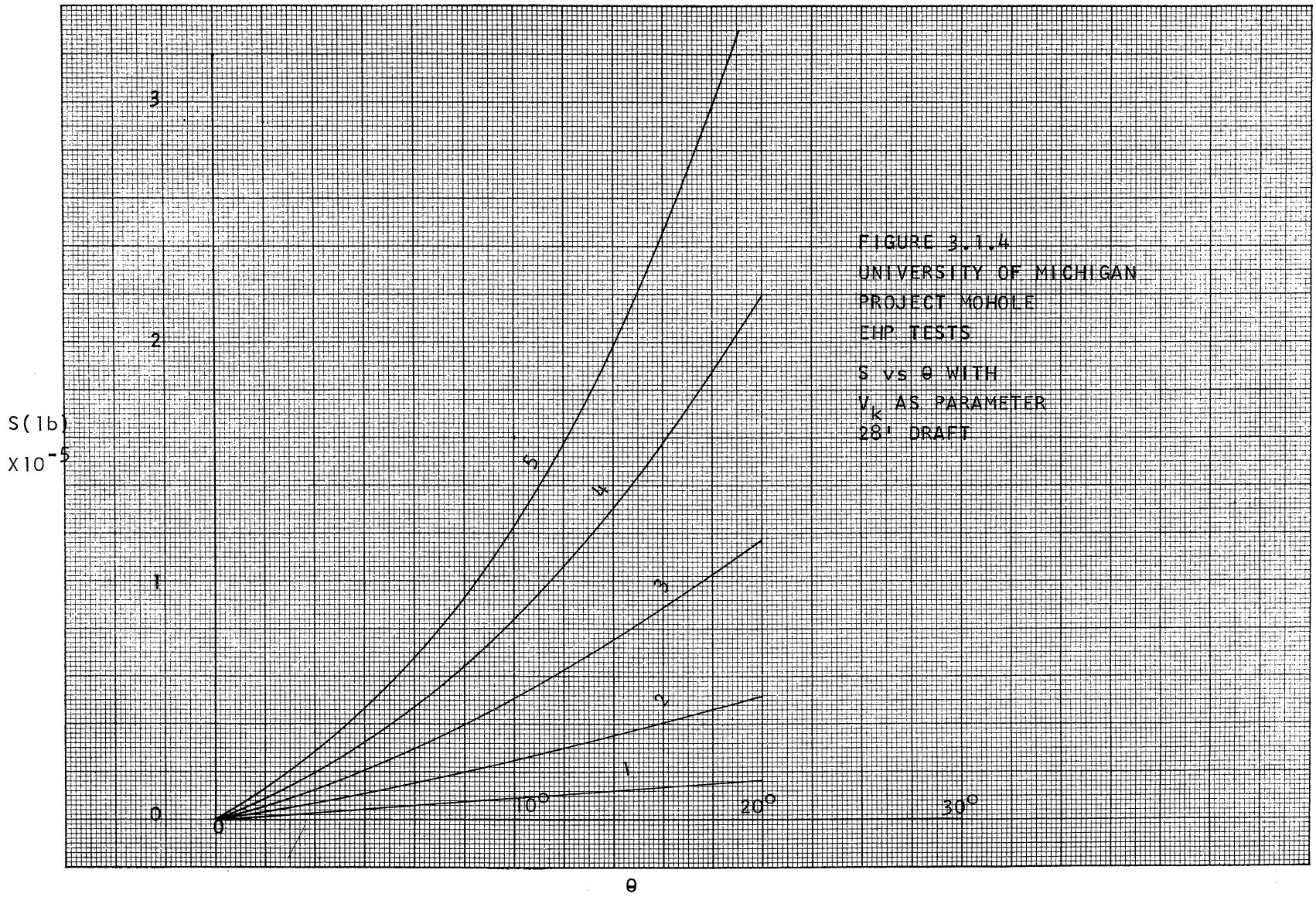

FIGURE 3.1.4
UNIVERSITY OF MICHIGAN
PROJECT MOHOLE
EHP TESTS
S vs θ WITH
V_k AS PARAMETER
28' DRAFT

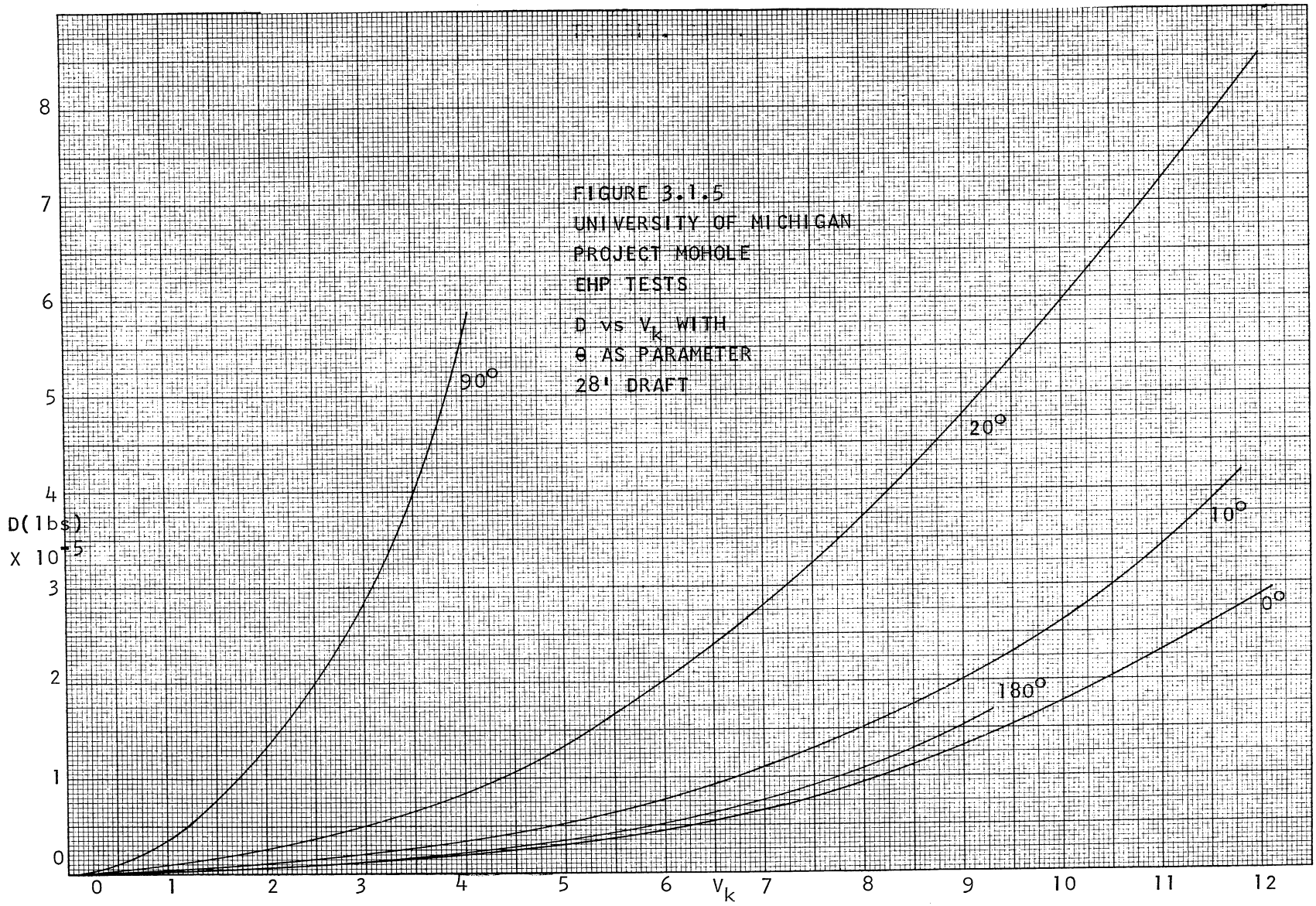
FIGURE 3.1.5
UNIVERSITY OF MICHIGAN
PROJECT MOHOLE
EHP TESTS
D vs V_k WITH
θ AS PARAMETER
28' DRAFT
D(lbs)
X 10^{-5}
V_k
90°
20°
10°
0°
180°
0
1
2
3
4
5
6
7
8
9
10
11
12

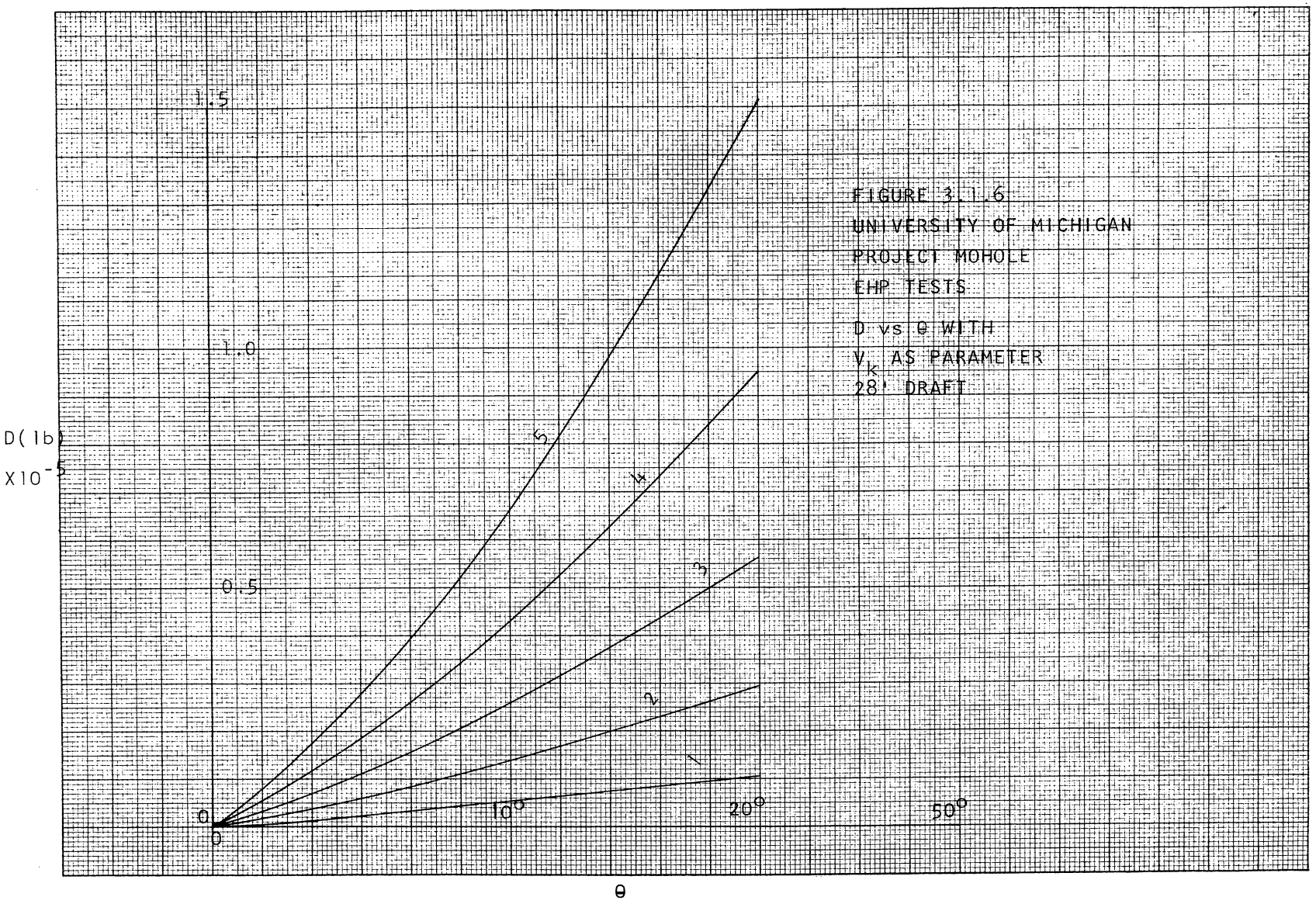

FIGURE 3.1.6
UNIVERSITY OF MICHIGAN
PROJECT MOHOLE
EHP TESTS
D vs θ WITH
V_k AS PARAMETER
28' DRAFT

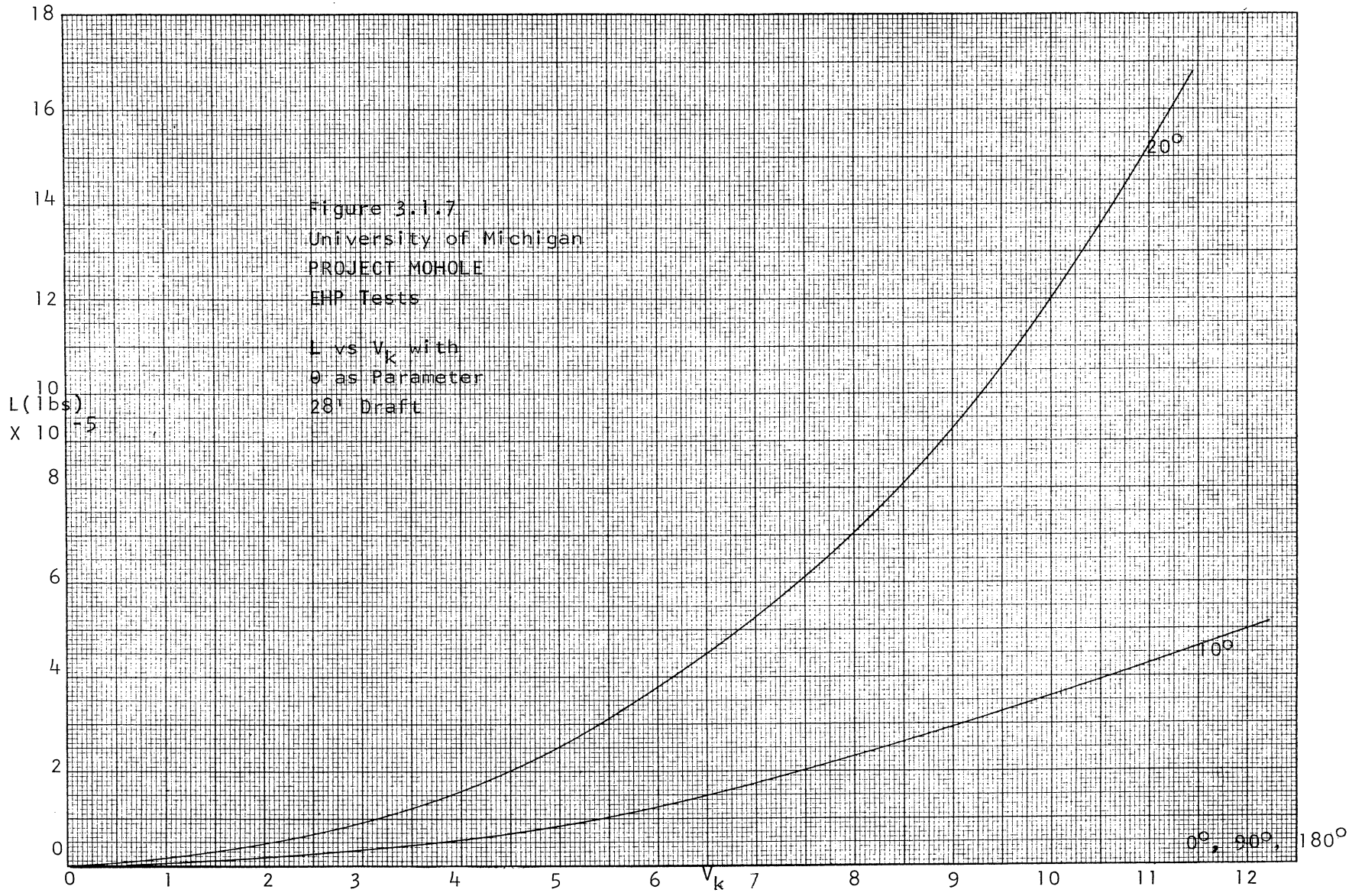
Figure 3.1.7
University of Michigan
PROJECT MOHOLE
EHP Tests
L vs V_k with
θ as Parameter
28' Draft
L(lbs)
X 10 -5
V_k
20°
10°
0°, 90°, 180°
0
2
4
6
8
10
12
14
16
18
0
1
2
3
4
5
6
7
8
9
10
11
12

FIGURE 3.1.8
UNIVERSITY OF MICHIGAN
PROJECT MOHOLE
EHP TESTS
L VS θ WITH
V_K AS PARAMETER
28' DRAFT
L (lbs)
X10⁻⁵
14
12
10
8
6
4
2
0
θ°
0°
10°
20°
30°
V_K

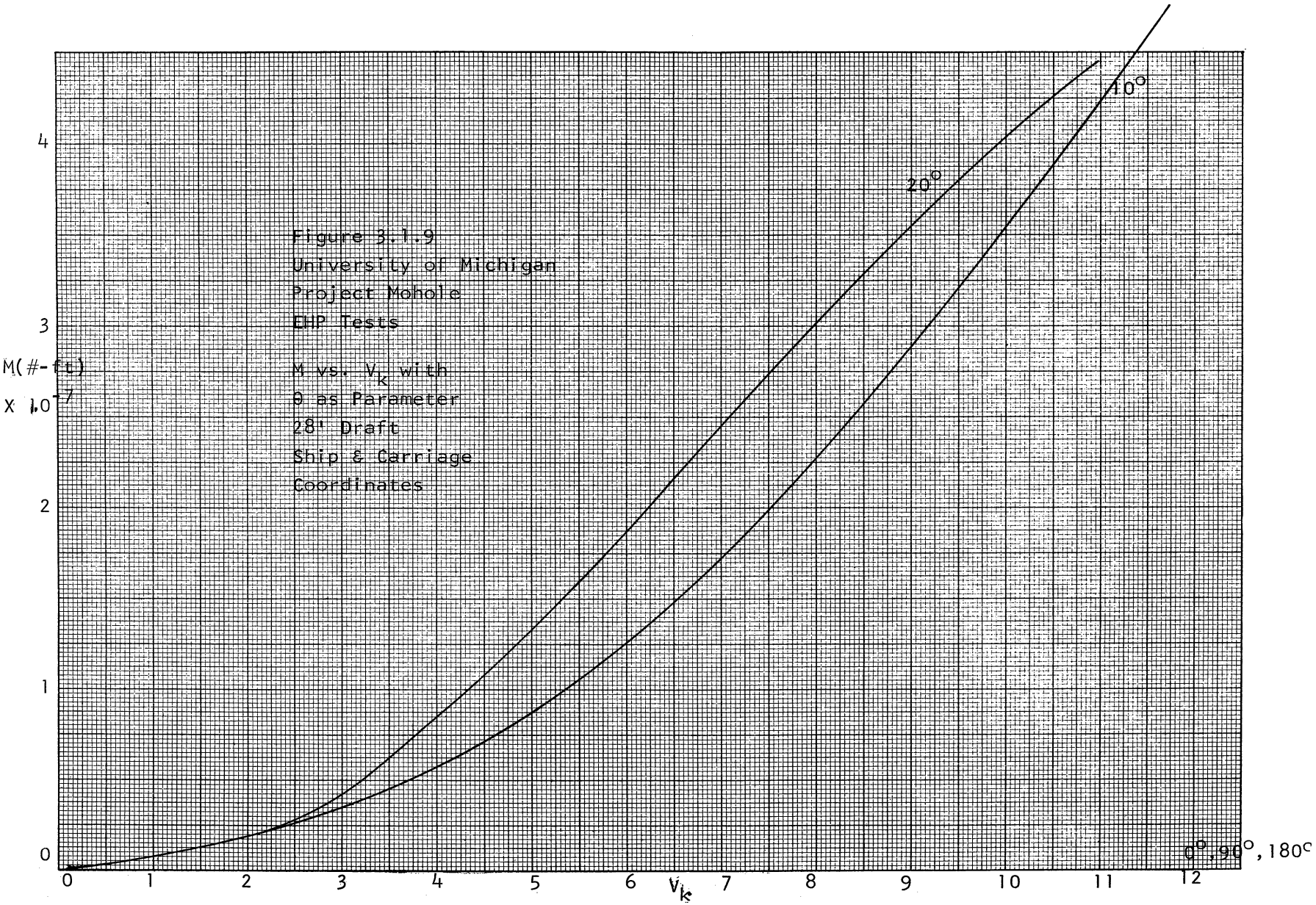
Figure 3.1.9
University of Michigan
Project Mohole
EHP Tests
M vs. V_k with
θ as Parameter
28' Draft
Ship & Carriage
Coordinates
M(#-ft)
X 10^7
V_k
10°
20°
0°, 90°, 180°
0
1
2
3
4
5
6
7
8
9
10
11
12

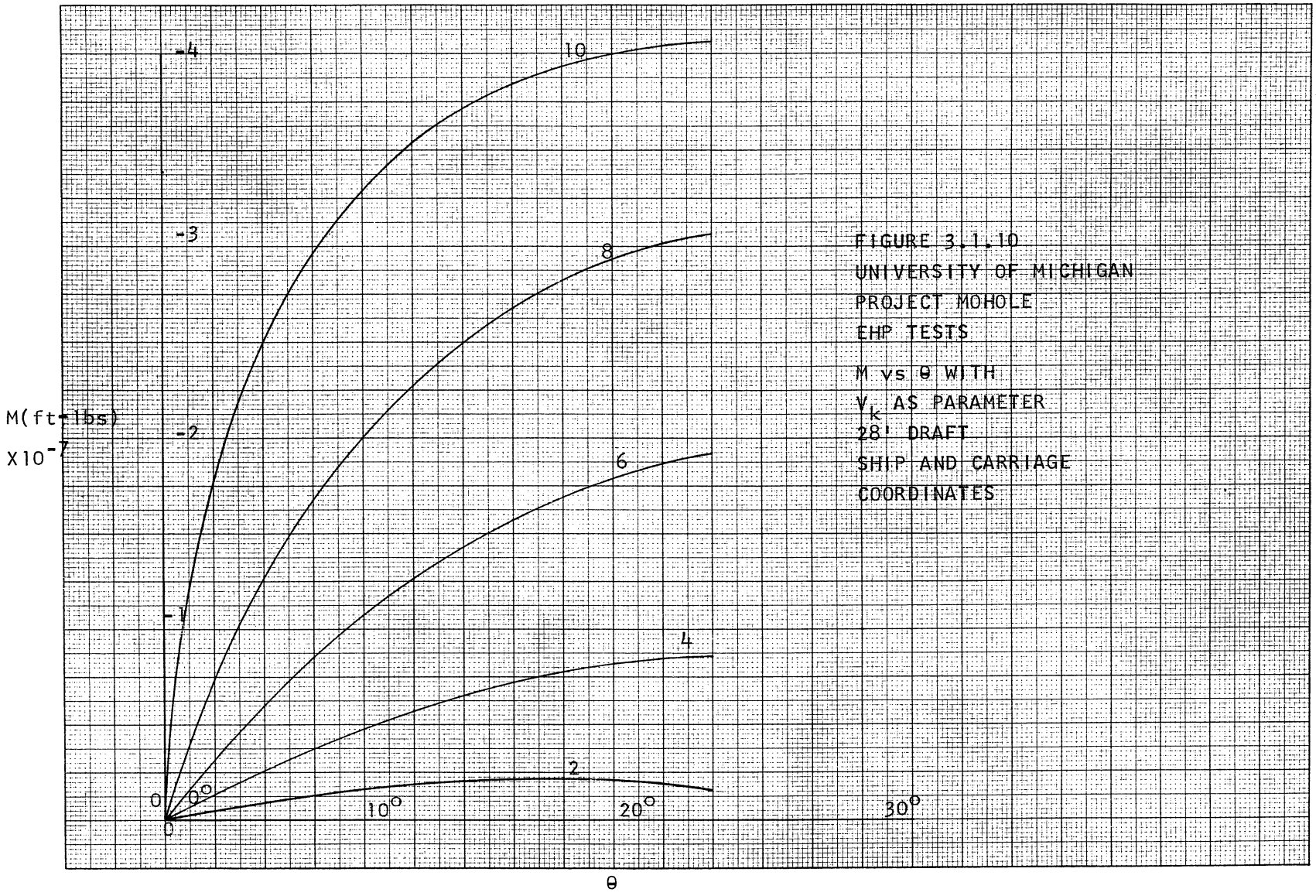
-4
-3
-2
-1
0
M(ft-lbs)
X10-7
10
8
6
4
2
0°
10°
20°
30°
θ
FIGURE 3.1.10
UNIVERSITY OF MICHIGAN
PROJECT MOHOLE
EHP TESTS
M vs θ WITH
Vk AS PARAMETER
28' DRAFT
SHIP AND CARRIAGE
COORDINATES

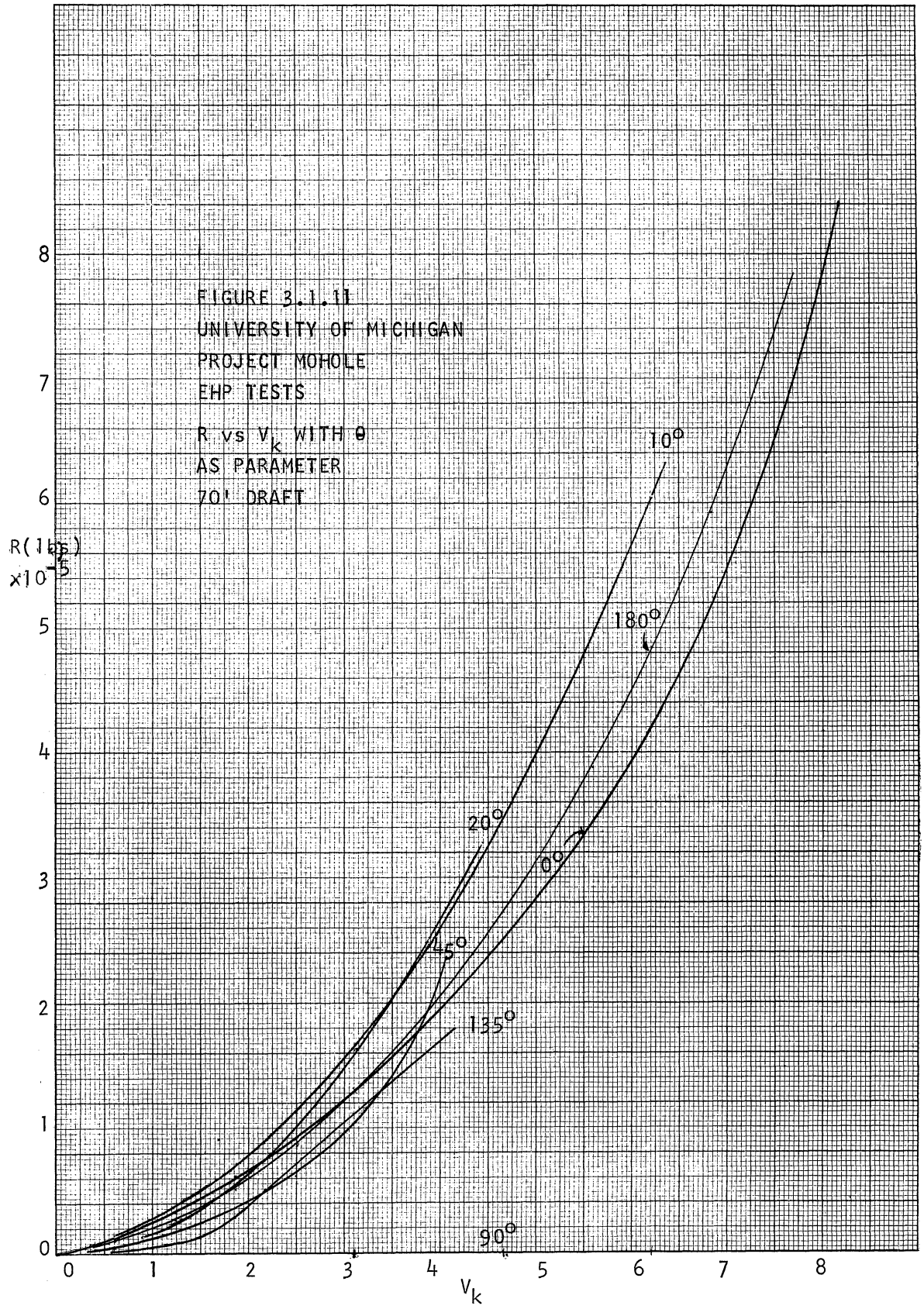
FIGURE 3.1.11
UNIVERSITY OF MICHIGAN
PROJECT MOHOLE
EHP TESTS
R vs V_k WITH θ
AS PARAMETER
70' DRAFT
R(lbs)
$\times 10^{-5}$
V_k
0
1
2
3
4
5
6
7
8
10°
180°
20°
0°
45°
135°
90°

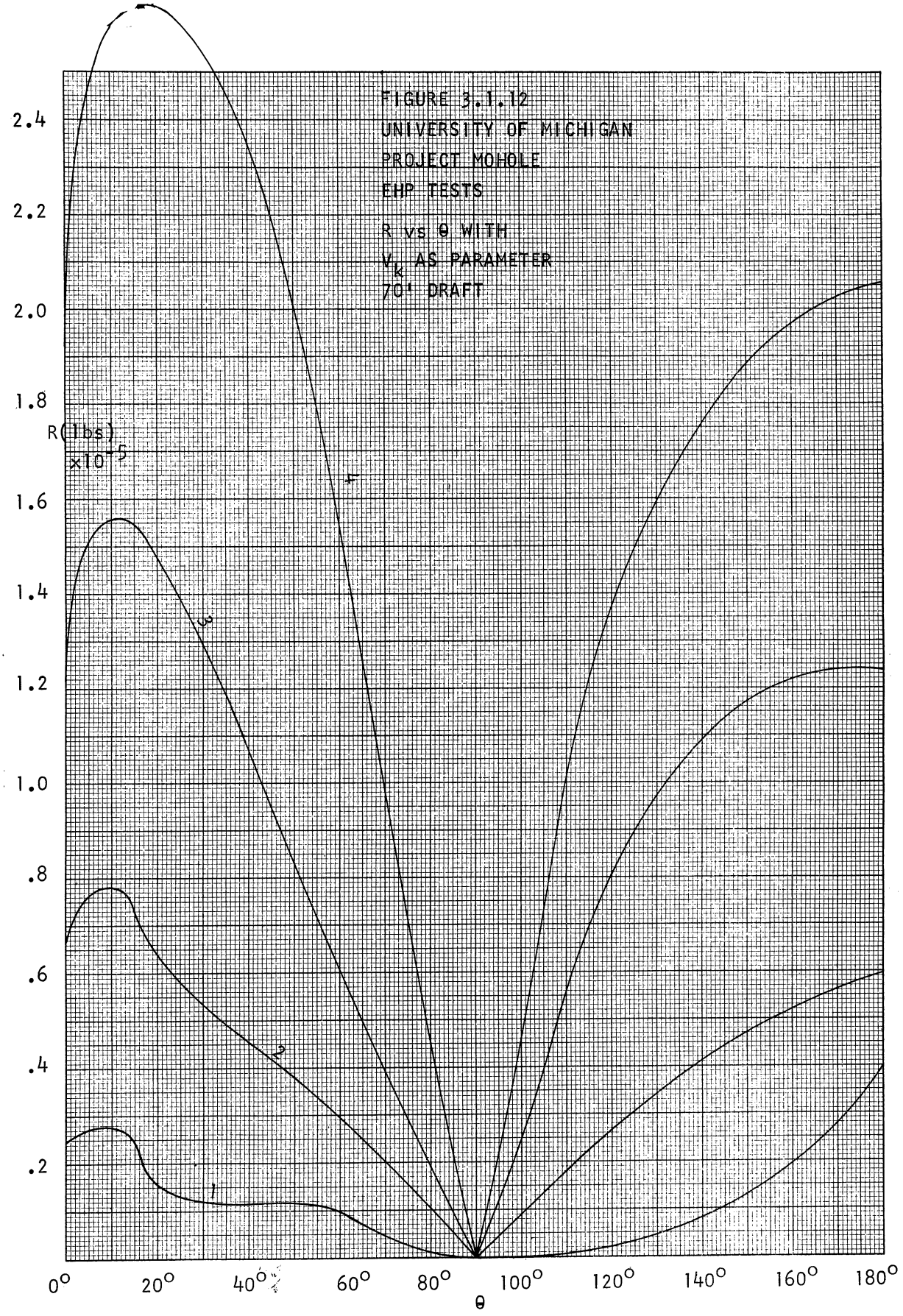
FIGURE 3.1.12
UNIVERSITY OF MICHIGAN
PROJECT MOHOLE
EHP TESTS
R vs θ WITH
V_k AS PARAMETER
70' DRAFT
R(lbs)
×10⁻⁵
2.4
2.2
2.0
1.8
1.6
1.4
1.2
1.0
.8
.6
.4
.2
0°
20°
40°
60°
80°
100°
120°
140°
160°
180°
θ
1
2
3
4

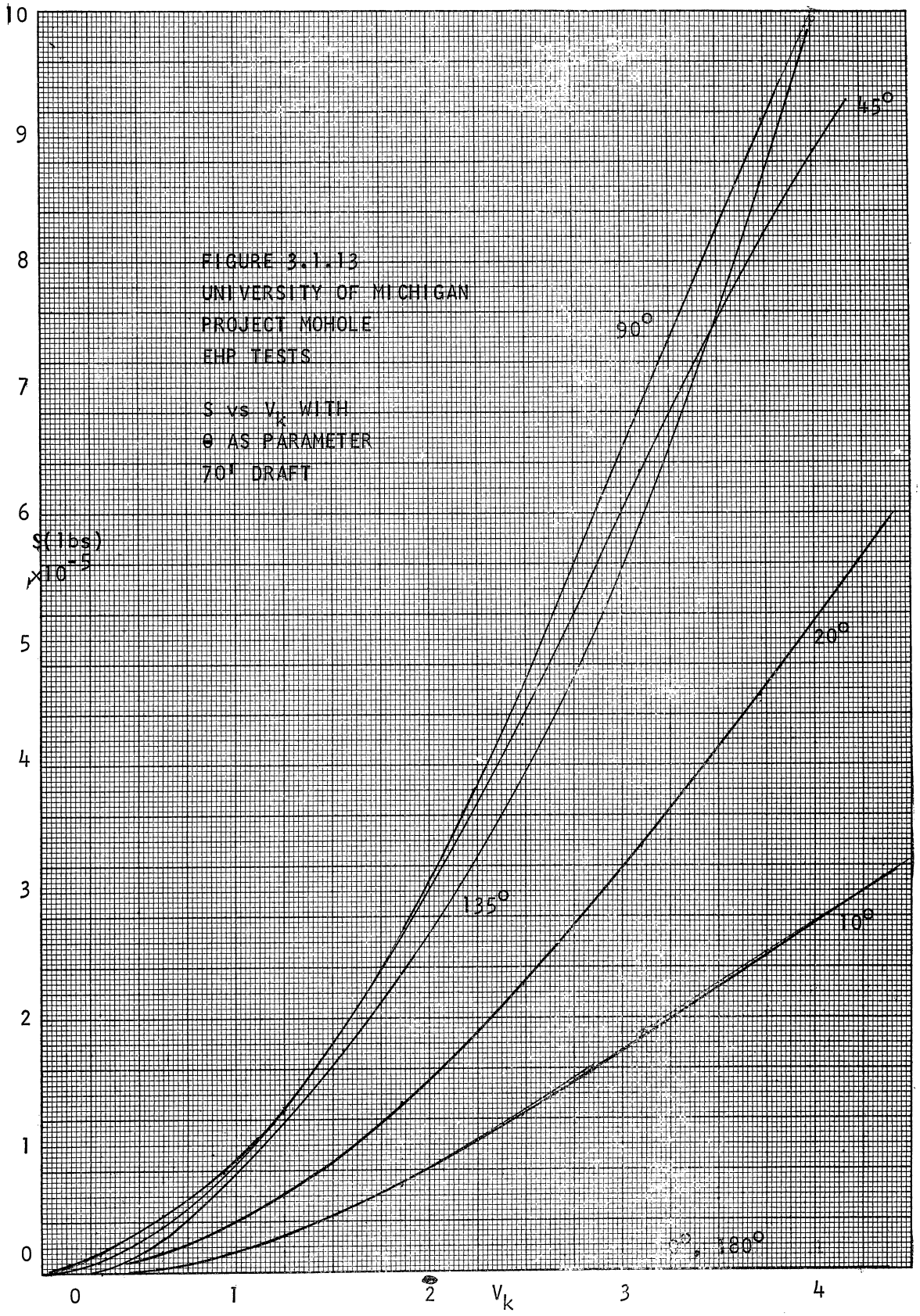
FIGURE 3.1.13
UNIVERSITY OF MICHIGAN
PROJECT MOHOLE
EHP TESTS
S vs V_k WITH
θ AS PARAMETER
70' DRAFT
S(lbs)
$\times 10^{-5}$
10
9
8
7
6
5
4
3
2
1
0
0
1
2
V_k
3
4
90°
45°
135°
20°
10°
180°

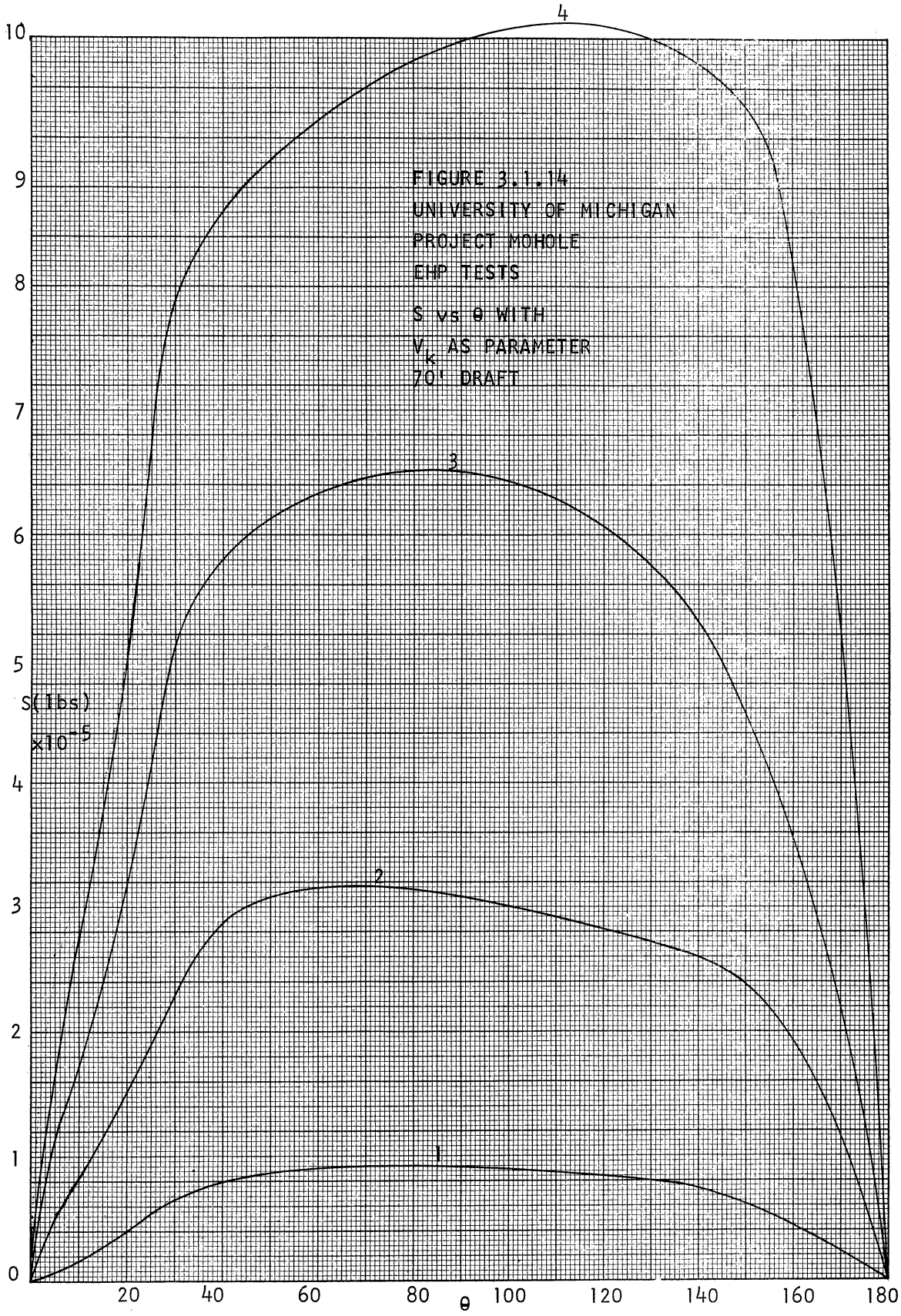
FIGURE 3.1.14
UNIVERSITY OF MICHIGAN
PROJECT MOHOLE
EHP TESTS
S vs θ WITH
V_K AS PARAMETER
70' DRAFT
4
3
2
1
S(lbs)
×10⁻⁵
θ
0
1
2
3
4
5
6
7
8
9
10
20
40
60
80
100
120
140
160
180

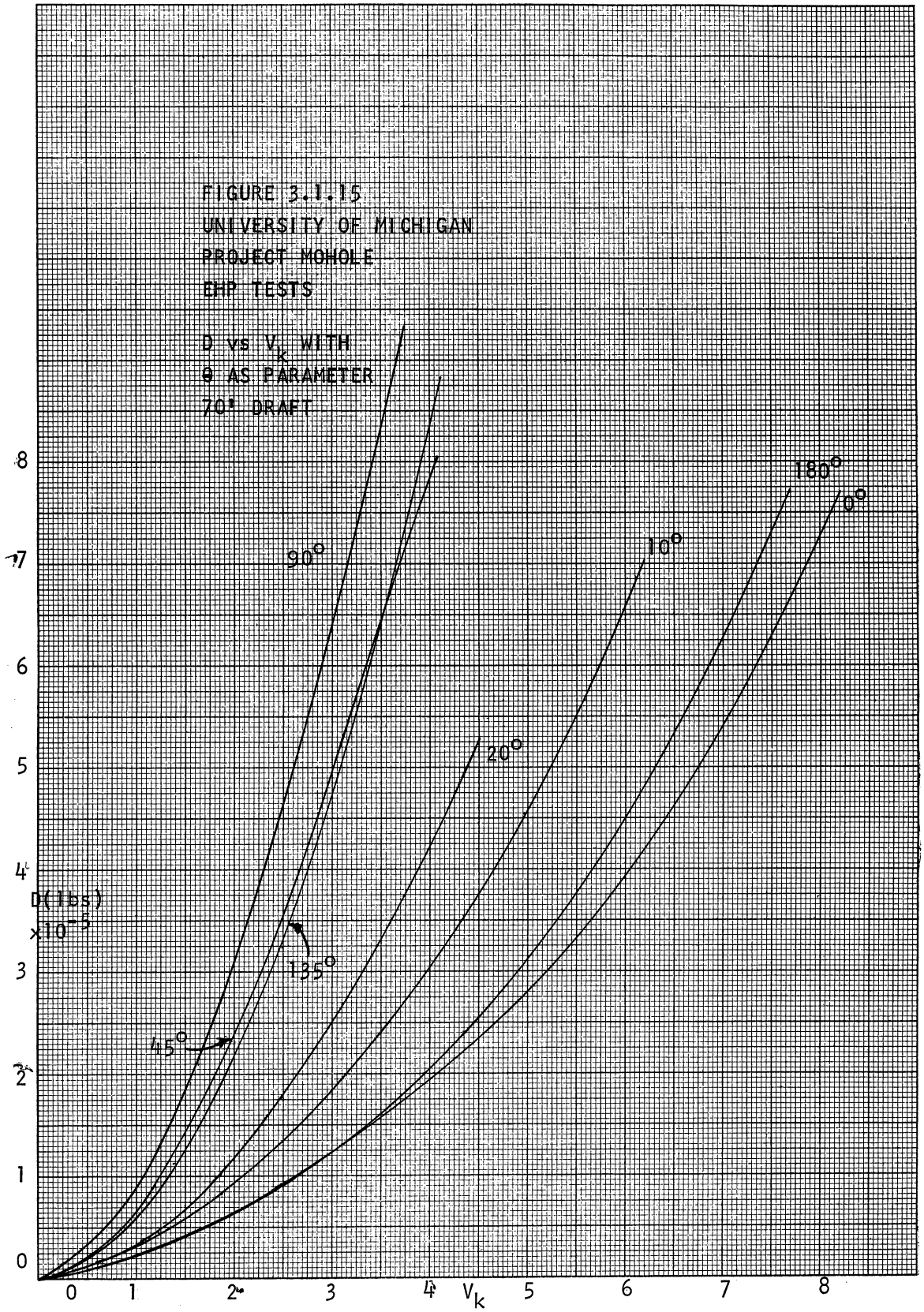
FIGURE 3.1.15
UNIVERSITY OF MICHIGAN
PROJECT MOHOLE
EHP TESTS
D vs V_k WITH
θ AS PARAMETER
70' DRAFT
D(lbs)
$\times 10^{-5}$
V_k
0°
10°
20°
45°
90°
135°
180°
0
1
2
3
4
5
6
7
8

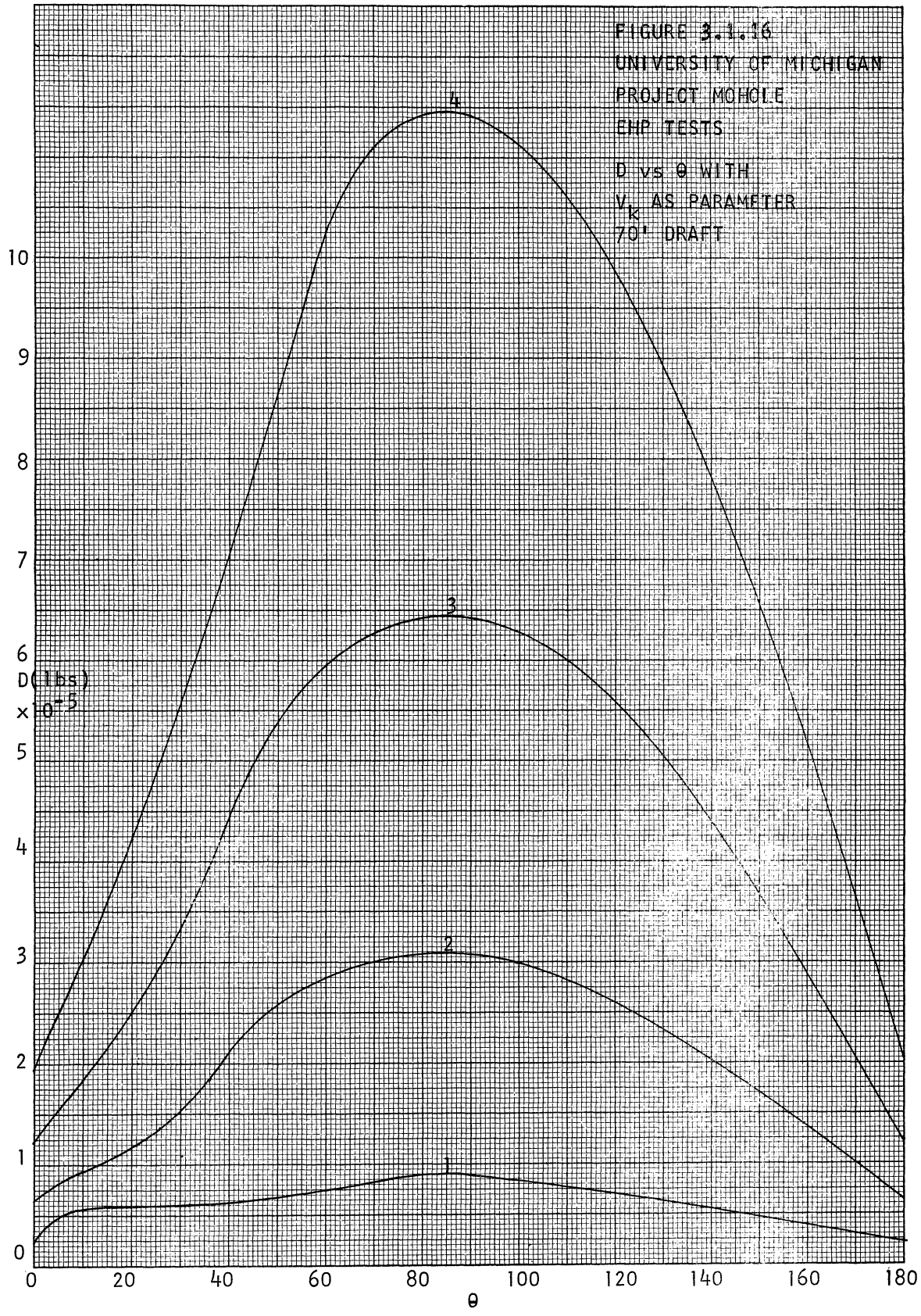
FIGURE 3.1.16
UNIVERSITY OF MICHIGAN
PROJECT MOHOLE
EHP TESTS
D vs θ WITH
V_K AS PARAMETER
70' DRAFT
D(lbs)
x10-5
θ
0
20
40
60
80
100
120
140
160
180
1
2
3
4
5
6
7
8
9
10

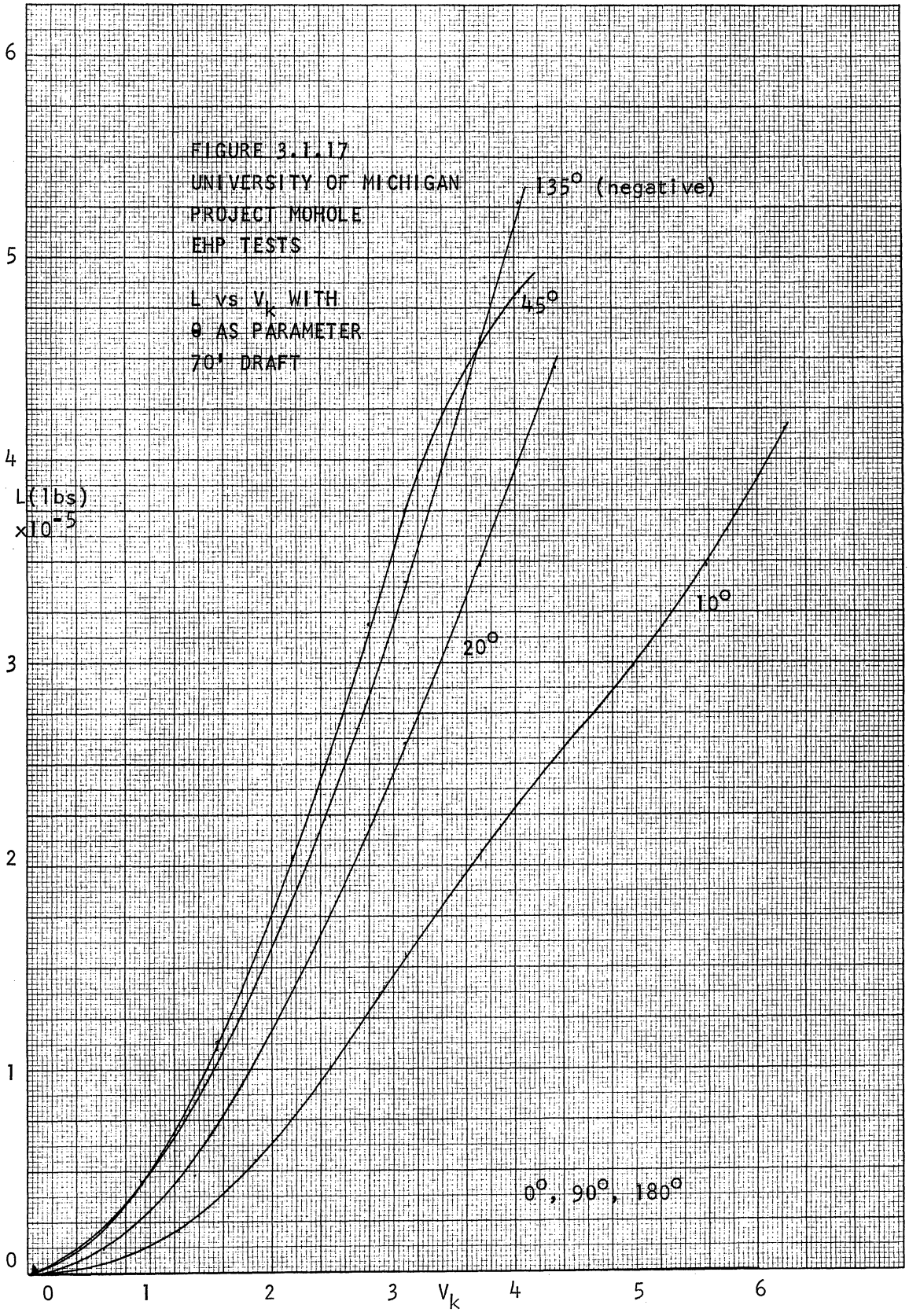
FIGURE 3.1.17
UNIVERSITY OF MICHIGAN
PROJECT MOROLE
EHP TESTS
L vs V_k WITH
θ AS PARAMETER
70' DRAFT
135° (negative)
45°
20°
10°
0°, 90°, 180°
L(lbs)
x10^-5
0
1
2
3
4
5
6
V_k

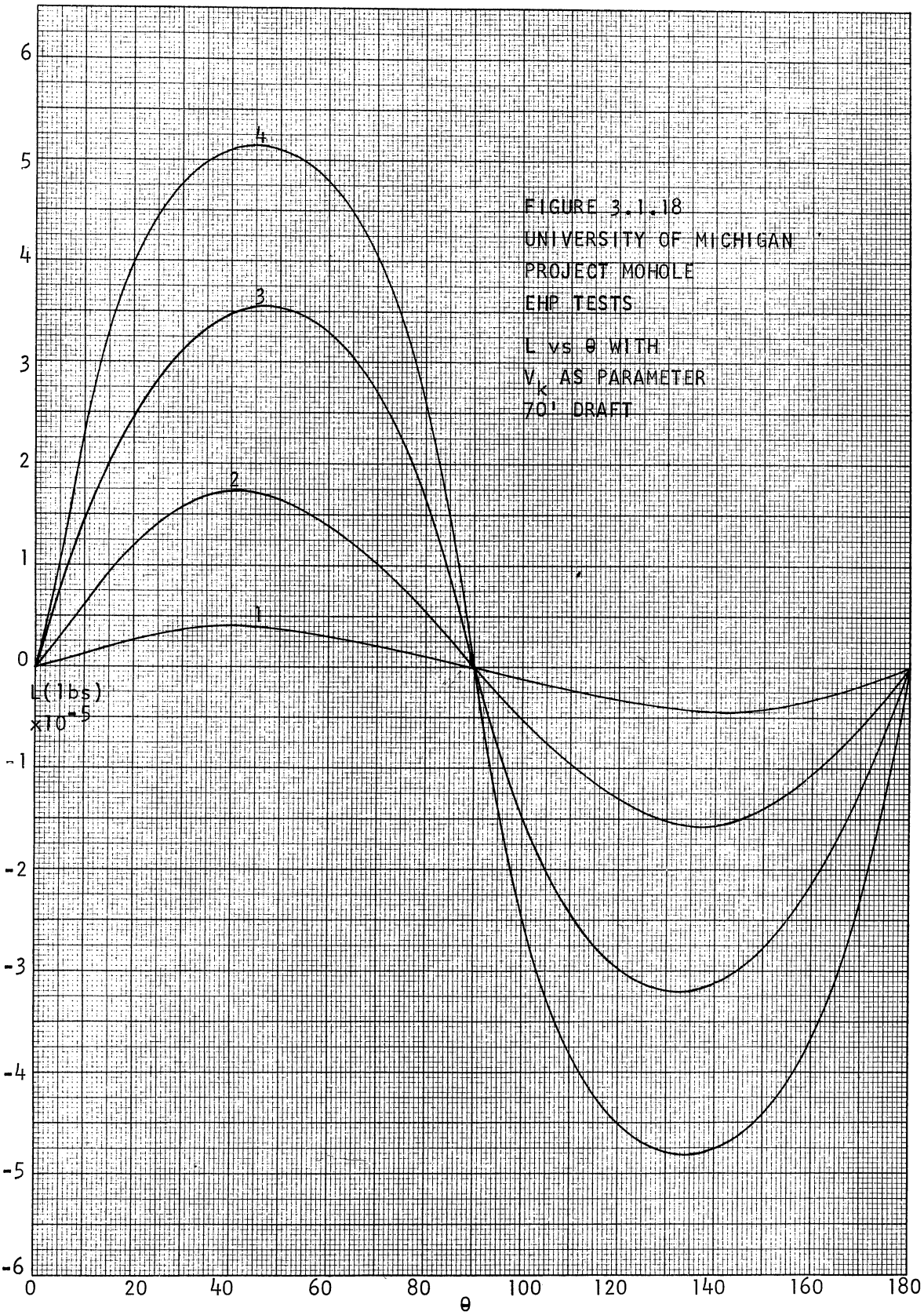
FIGURE 3.1.18
UNIVERSITY OF MICHIGAN
PROJECT MOHOLE
EHP TESTS
L vs θ WITH
V_K AS PARAMETER
70' DRAFT
L(lbs)
x10^-5
θ
1
2
3
4
6
5
4
3
2
1
0
-1
-2
-3
-4
-5
-6
0
20
40
60
80
100
120
140
160
180

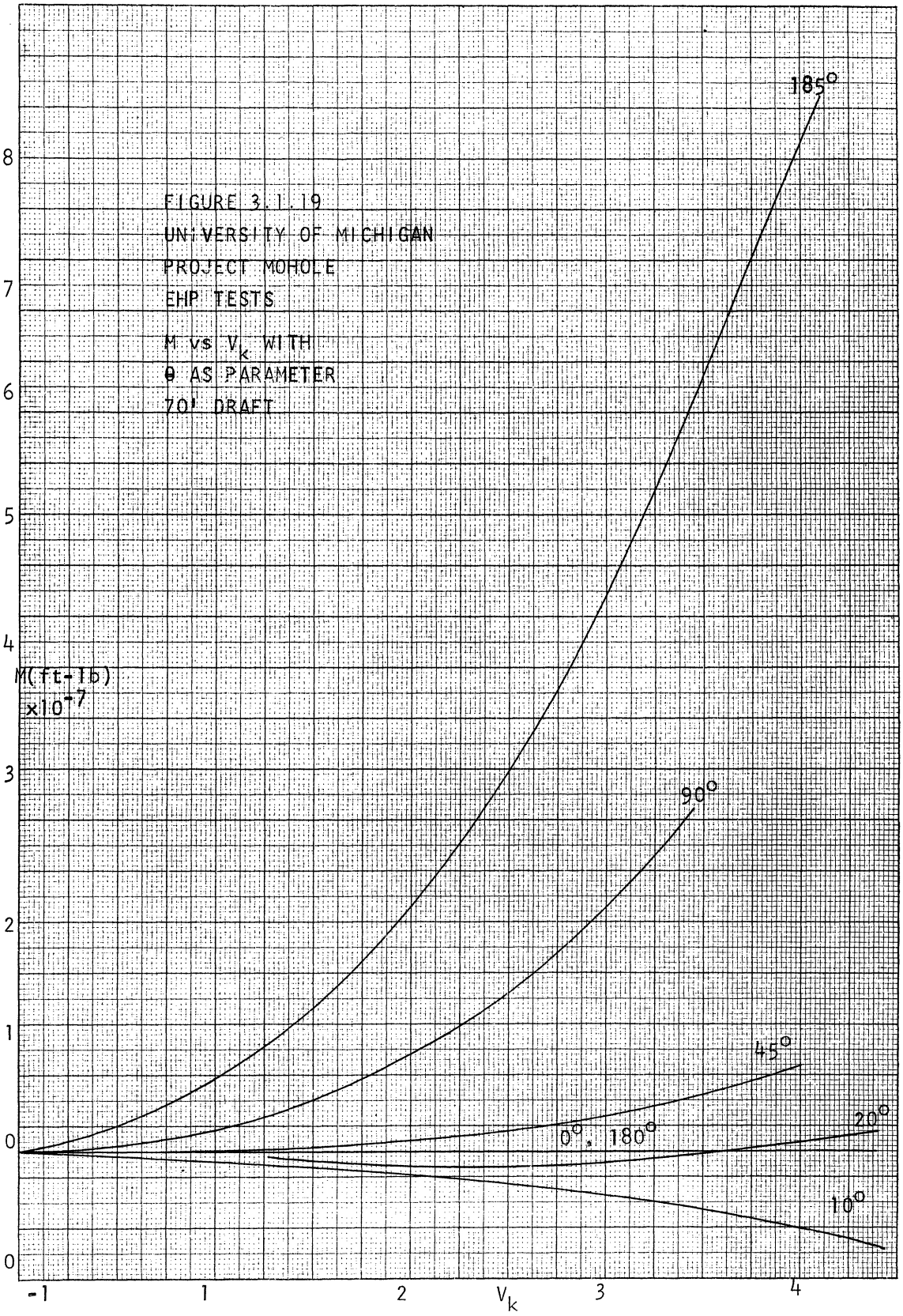
FIGURE 3.1.19
UNIVERSITY OF MICHIGAN
PROJECT MOHOLE
EHP TESTS
M vs V_k WITH
θ AS PARAMETER
70' DRAFT
M(ft-lb)
x10^-7
185°
90°
45°
20°
0°, 180°
10°
8
7
6
5
4
3
2
1
0
0
-1
1
2
3
4
V_k

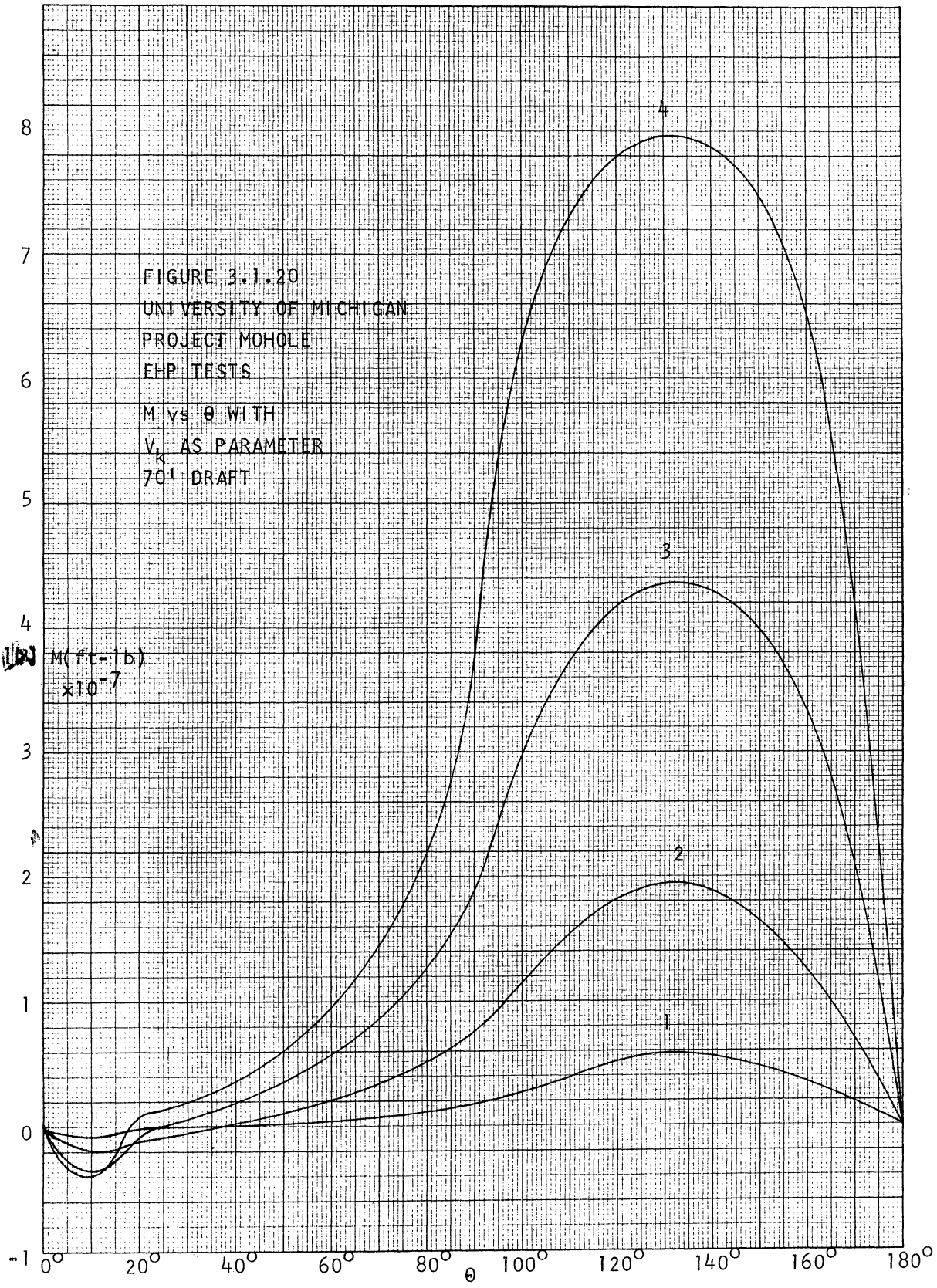
FIGURE 3.1.20
UNIVERSITY OF MICHIGAN
PROJECT MOHOLE
EHP TESTS
M vs θ WITH
V_k AS PARAMETER
70' DRAFT
M(ft-lb)
×10⁻⁷
8
7
6
5
4
3
2
1
0
-1
0°
20°
40°
60°
80°
100°
120°
140°
160°
180°
θ
1
2
3
4

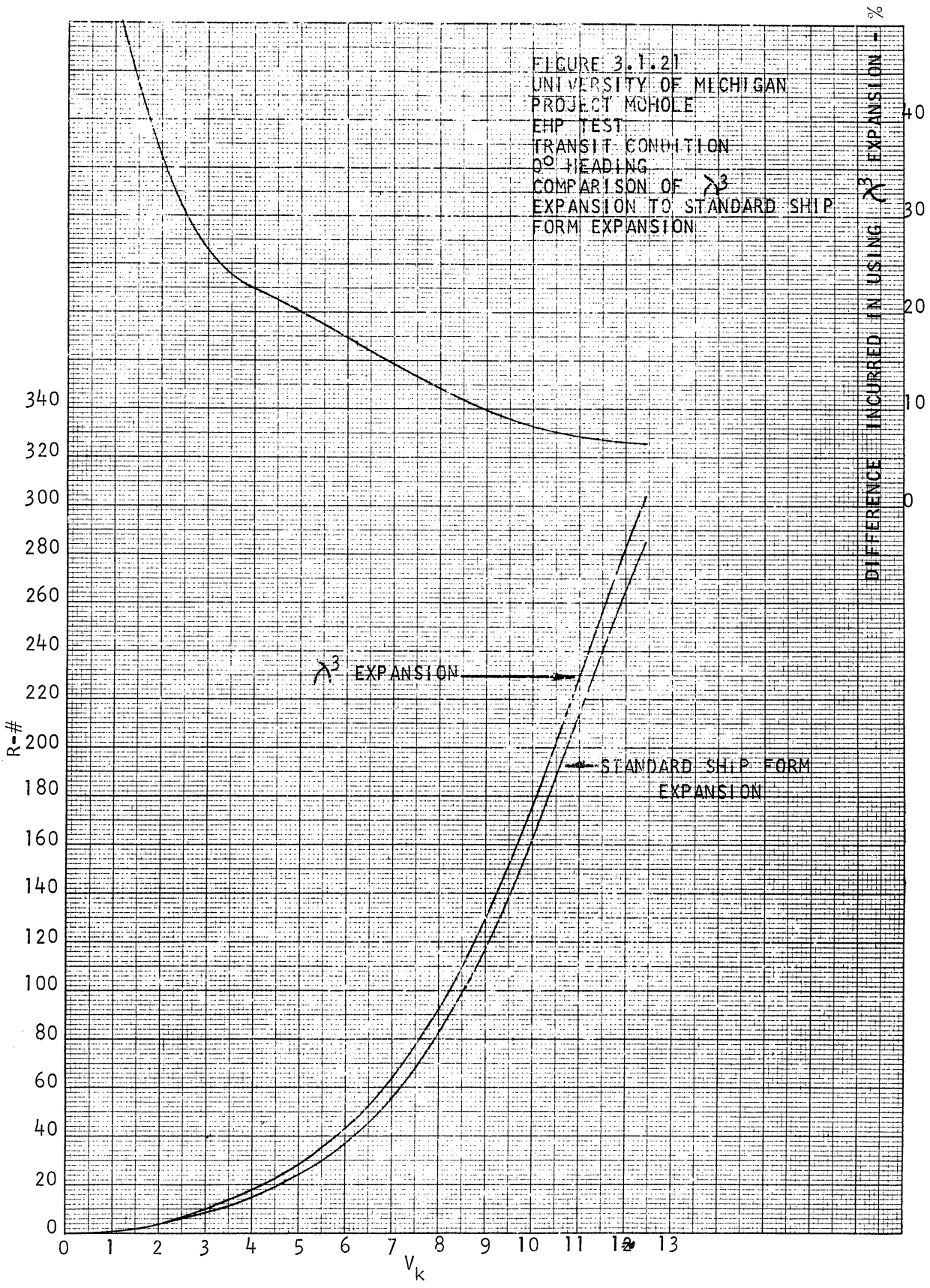
FIGURE 3.1.21
UNIVERSITY OF MICHIGAN
PROJECT MOHOLE
EHP TEST
TRANSIT CONDITION
0° HEADING
COMPARISON OF λ³ EXPANSION TO STANDARD SHIP FORM EXPANSION
DIFFERENCE INCURRED IN USING λ³ EXPANSION - %
R-#
V_k
λ³ EXPANSION
STANDARD SHIP FORM EXPANSION
0
20
40
60
80
100
120
140
160
180
200
220
240
260
280
300
320
340
0
10
20
30
40
0 1 2 3 4 5 6 7 8 9 10 11 12 13

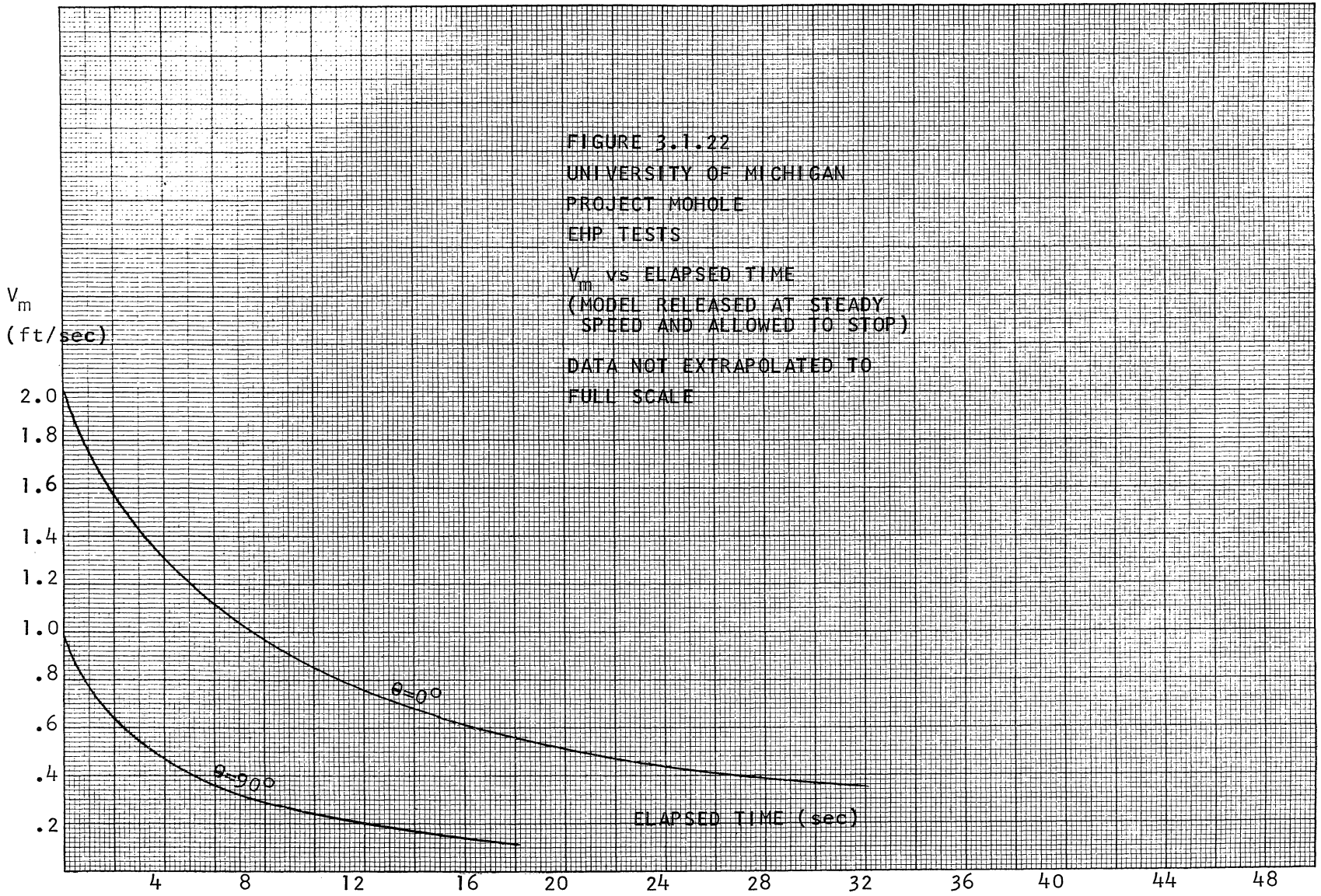
FIGURE 3.1.22
UNIVERSITY OF MICHIGAN
PROJECT MOHOLE
EHP TESTS
V_m vs ELAPSED TIME
(MODEL RELEASED AT STEADY SPEED AND ALLOWED TO STOP)
DATA NOT EXTRAPOLATED TO FULL SCALE
V_m (ft/sec)
2.0
1.8
1.6
1.4
1.2
1.0
.8
.6
.4
.2
θ=0°
θ=90°
ELAPSED TIME (sec)
4
8
12
16
20
24
28
32
36
40
44
48

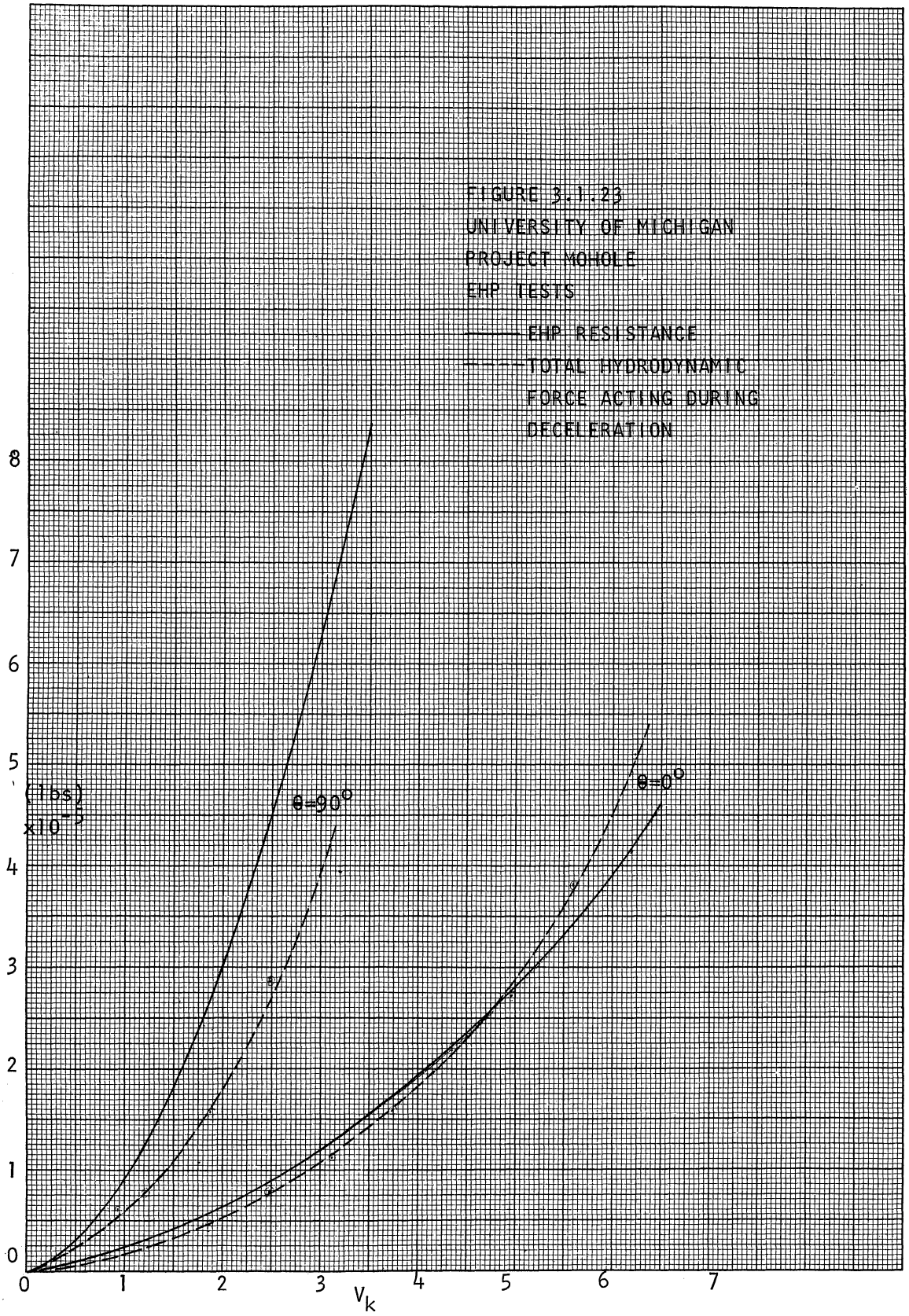
FIGURE 3.1.23
UNIVERSITY OF MICHIGAN
PROJECT MOHOLE
EHP TESTS
——— EHP RESISTANCE
– – – – TOTAL HYDRODYNAMIC FORCE ACTING DURING DECELERATION
θ=90°
θ=0°
(lbs) x10⁻⁵
V_k
0
1
2
3
4
5
6
7
8

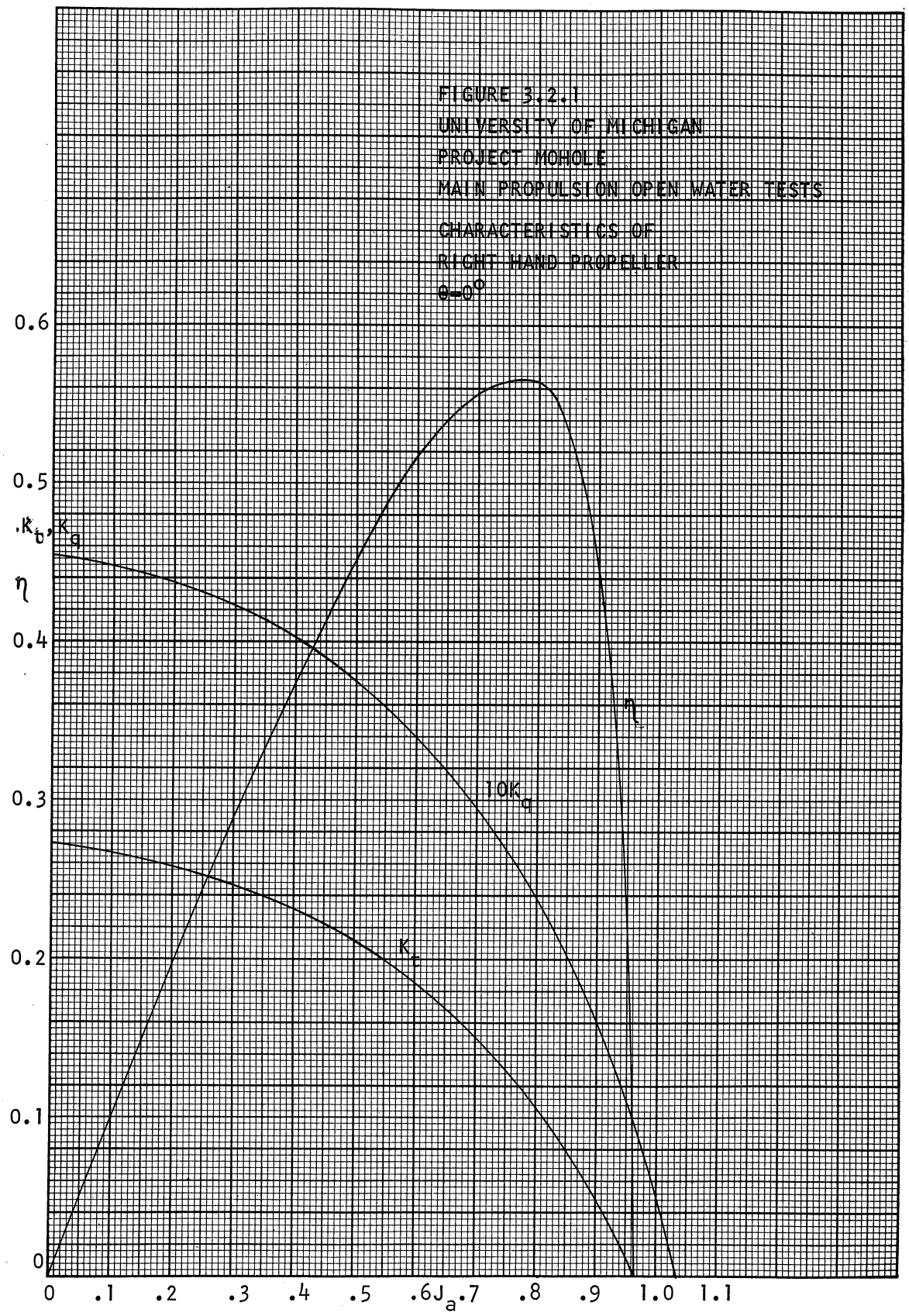
FIGURE 3.2.1
UNIVERSITY OF MICHIGAN
PROJECT MOHOLE
MAIN PROPULSION OPEN WATER TESTS
CHARACTERISTICS OF
RIGHT HAND PROPELLER
θ=0°
0.6
0.5
K_t, K_q
η
0.4
0.3
0.2
0.1
0
$10K_q$
K_t
η
0 .1 .2 .3 .4 .5 .6 J_a .7 .8 .9 1.0 1.1

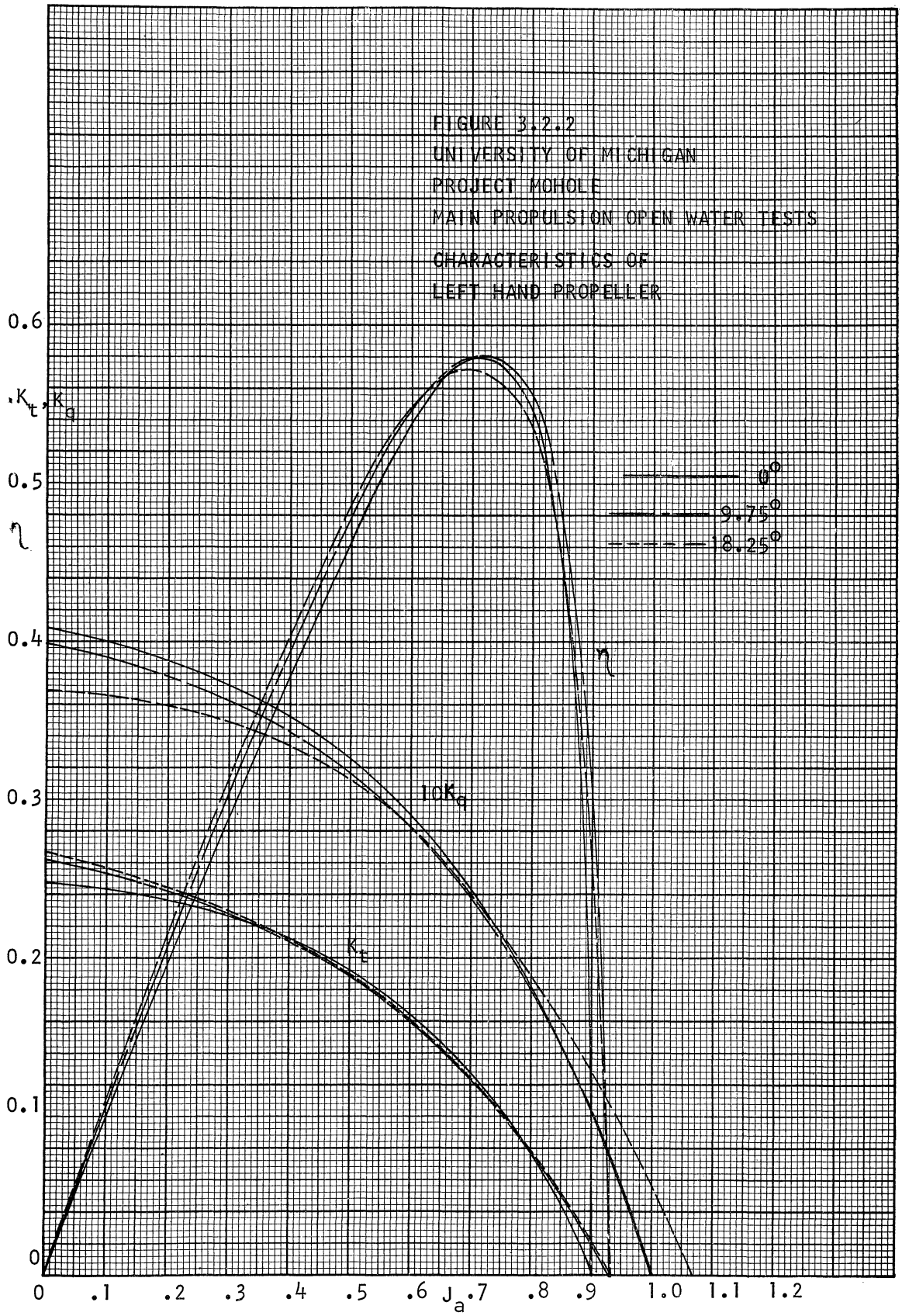
FIGURE 3.2.2
UNIVERSITY OF MICHIGAN
PROJECT MOHOLE
MAIN PROPULSION OPEN WATER TESTS
CHARACTERISTICS OF
LEFT HAND PROPELLER
0.6
K_t, K_q
0.5
η
0.4
0.3
0.2
0.1
0
$10K_q$
K_t
η
0°
9.75°
18.25°
0 .1 .2 .3 .4 .5 .6 J_a .7 .8 .9 1.0 1.1 1.2

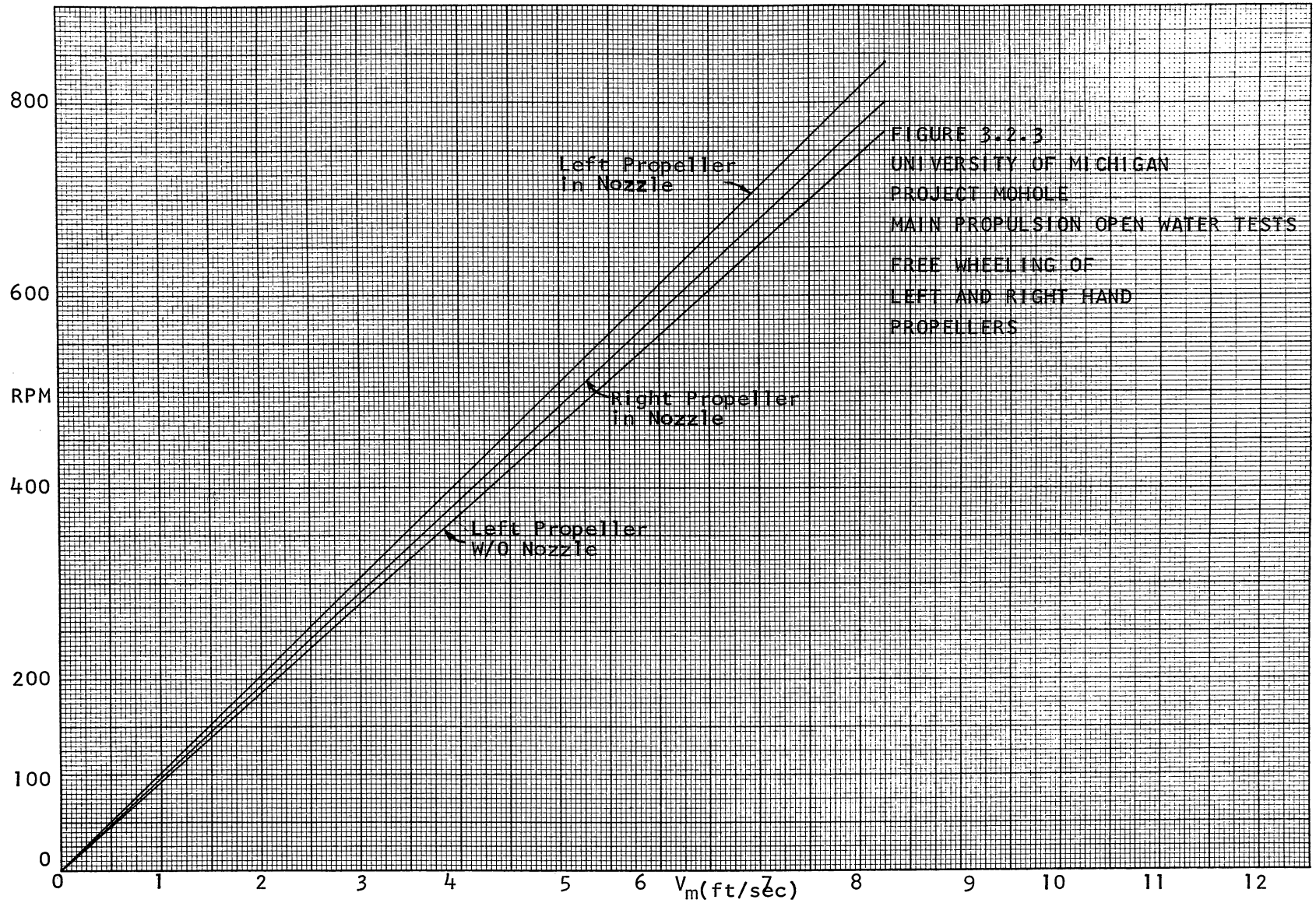
800
600
RPM
400
200
100
0
0
1
2
3
4
5
6
7
8
9
10
11
12
V_m(ft/sec)
Left Propeller in Nozzle
Right Propeller in Nozzle
Left Propeller W/O Nozzle
FIGURE 3.2.3
UNIVERSITY OF MICHIGAN
PROJECT MOHOLE
MAIN PROPULSION OPEN WATER TESTS
FREE WHEELING OF
LEFT AND RIGHT HAND
PROPELLERS

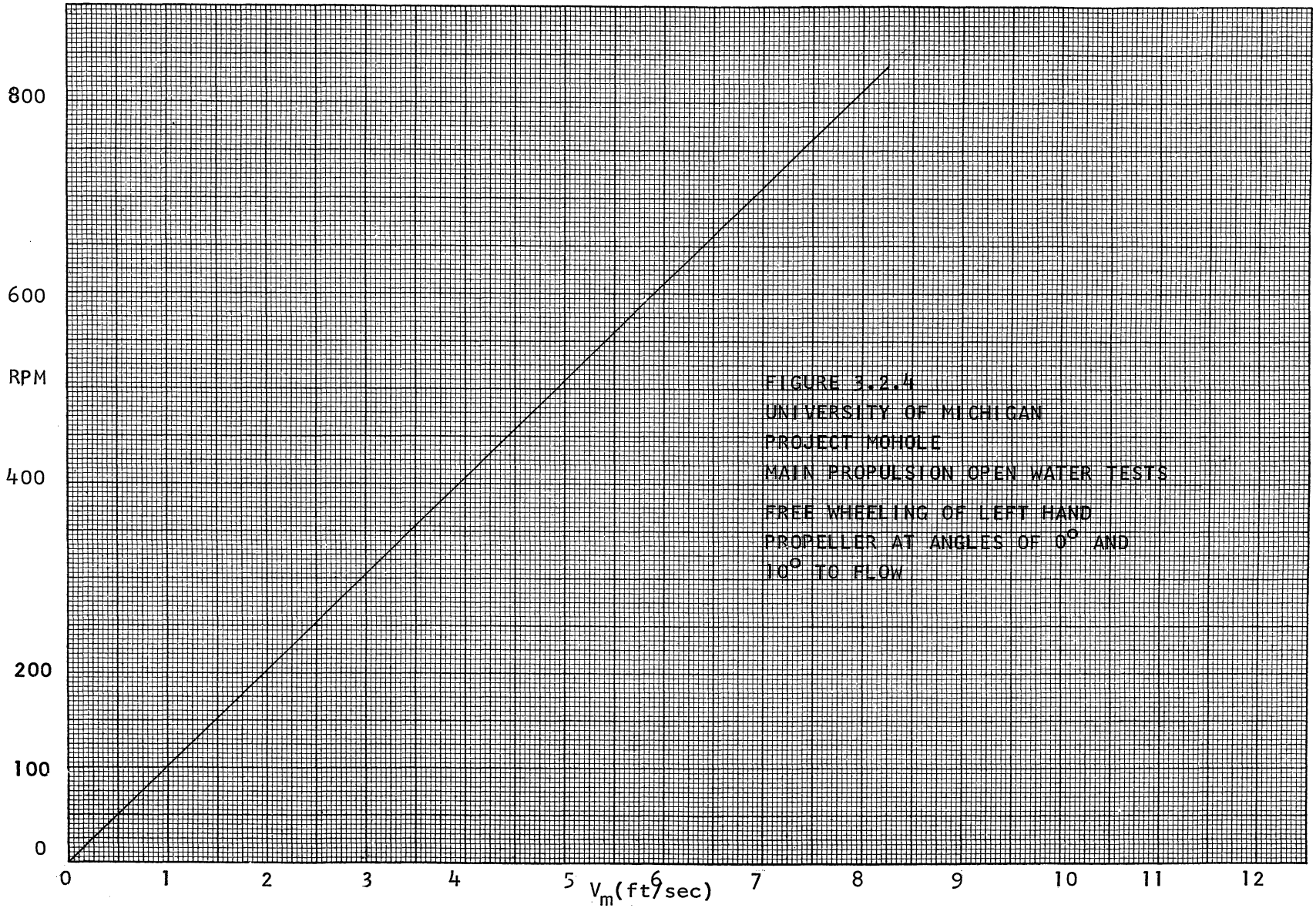

FIGURE 3.2.4
UNIVERSITY OF MICHIGAN
PROJECT MOHOLE
MAIN PROPULSION OPEN WATER TESTS
FREE WHEELING OF LEFT HAND PROPELLER AT ANGLES OF 0° AND 10° TO FLOW

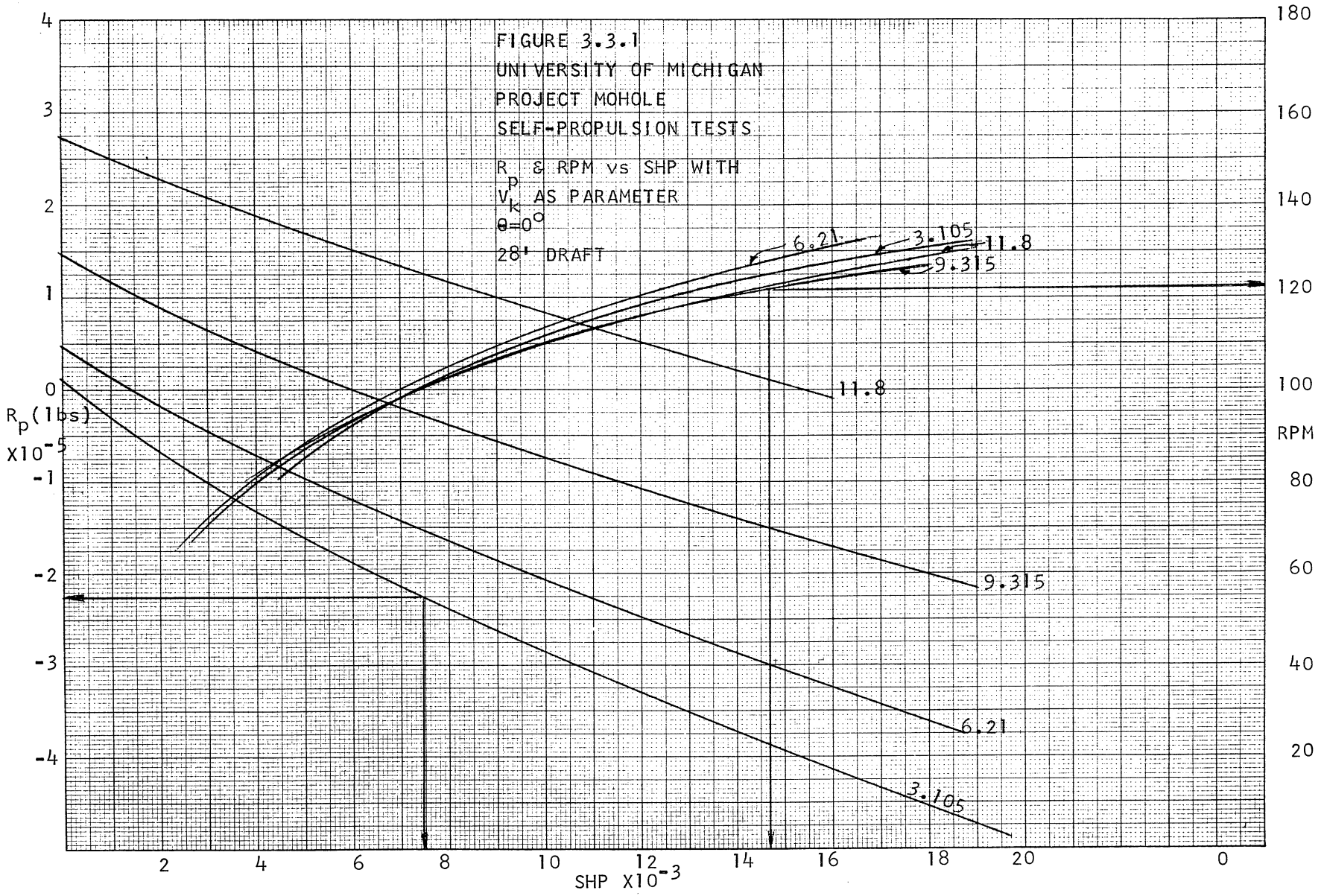
FIGURE 3.3.1
UNIVERSITY OF MICHIGAN
PROJECT MOHOLE
SELF-PROPULSION TESTS
R_p & RPM vs SHP WITH
V_k AS PARAMETER
θ=0°
28' DRAFT
6.21
3.105
11.8
9.315
11.8
9.315
6.21
3.105
R_p (lbs) X10^{-5}
RPM
SHP X10^{-3}
4
3
2
1
0
-1
-2
-3
-4
180
160
140
120
100
80
60
40
20
2
4
6
8
10
12
14
16
18
20
0

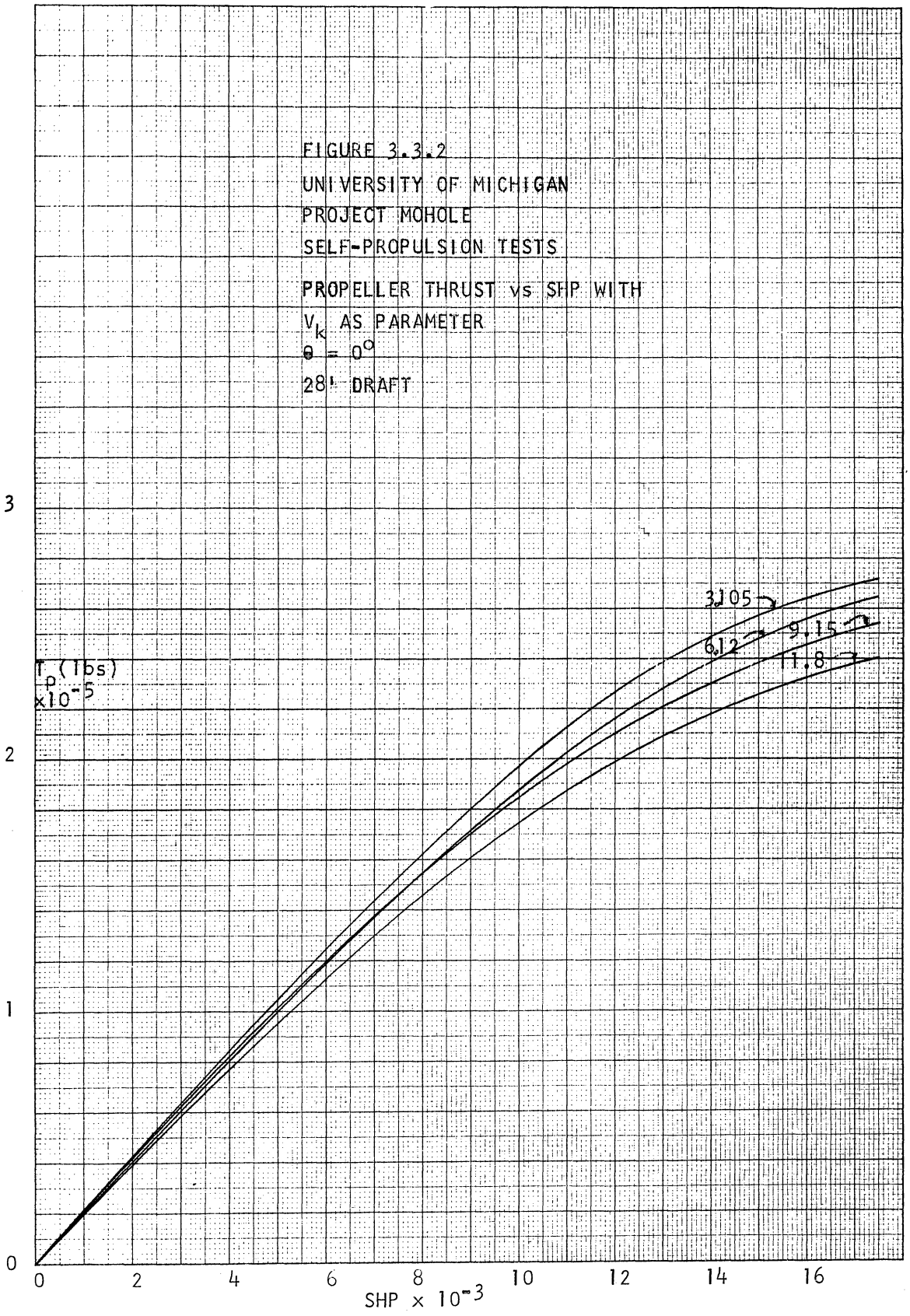
FIGURE 3.3.2
UNIVERSITY OF MICHIGAN
PROJECT MOHOLE
SELF-PROPULSION TESTS
PROPELLER THRUST vs SHP WITH
V_k AS PARAMETER
$\theta = 0^o$
28' DRAFT
3.105
6.12
9.15
11.8
T_p (lbs) $\times 10^{-5}$
0
1
2
3
0
2
4
6
8
10
12
14
16
SHP $\times 10^{-3}$

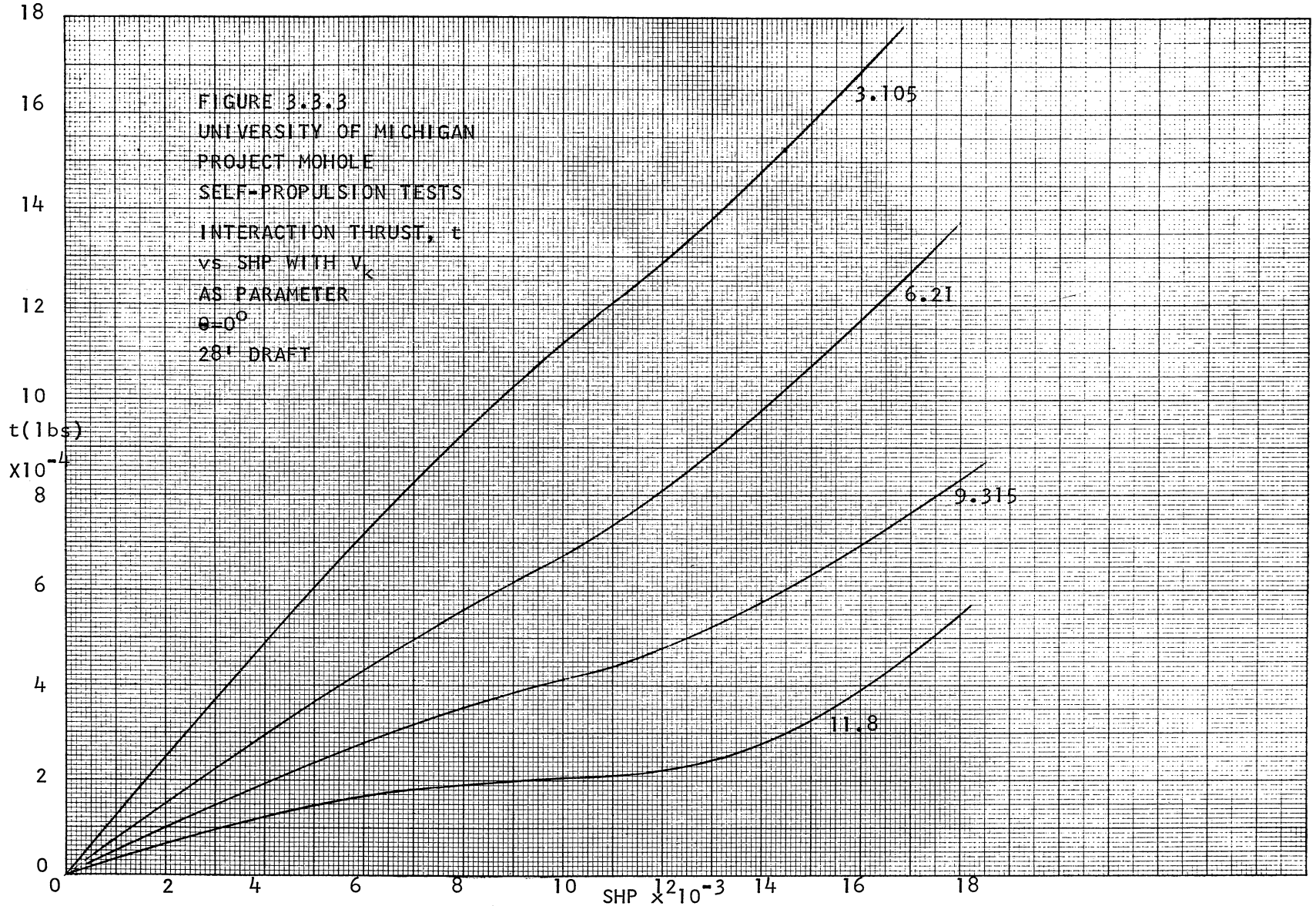
FIGURE 3.3.3
UNIVERSITY OF MICHIGAN
PROJECT MOHOLE
SELF-PROPULSION TESTS
INTERACTION THRUST, t
vs SHP WITH V_K
AS PARAMETER
$\theta=0^o$
28' DRAFT
3.105
6.21
9.315
11.8
t(lbs)
X10^{-4}
SHP X10^{-3}
0
2
4
6
8
10
12
14
16
18

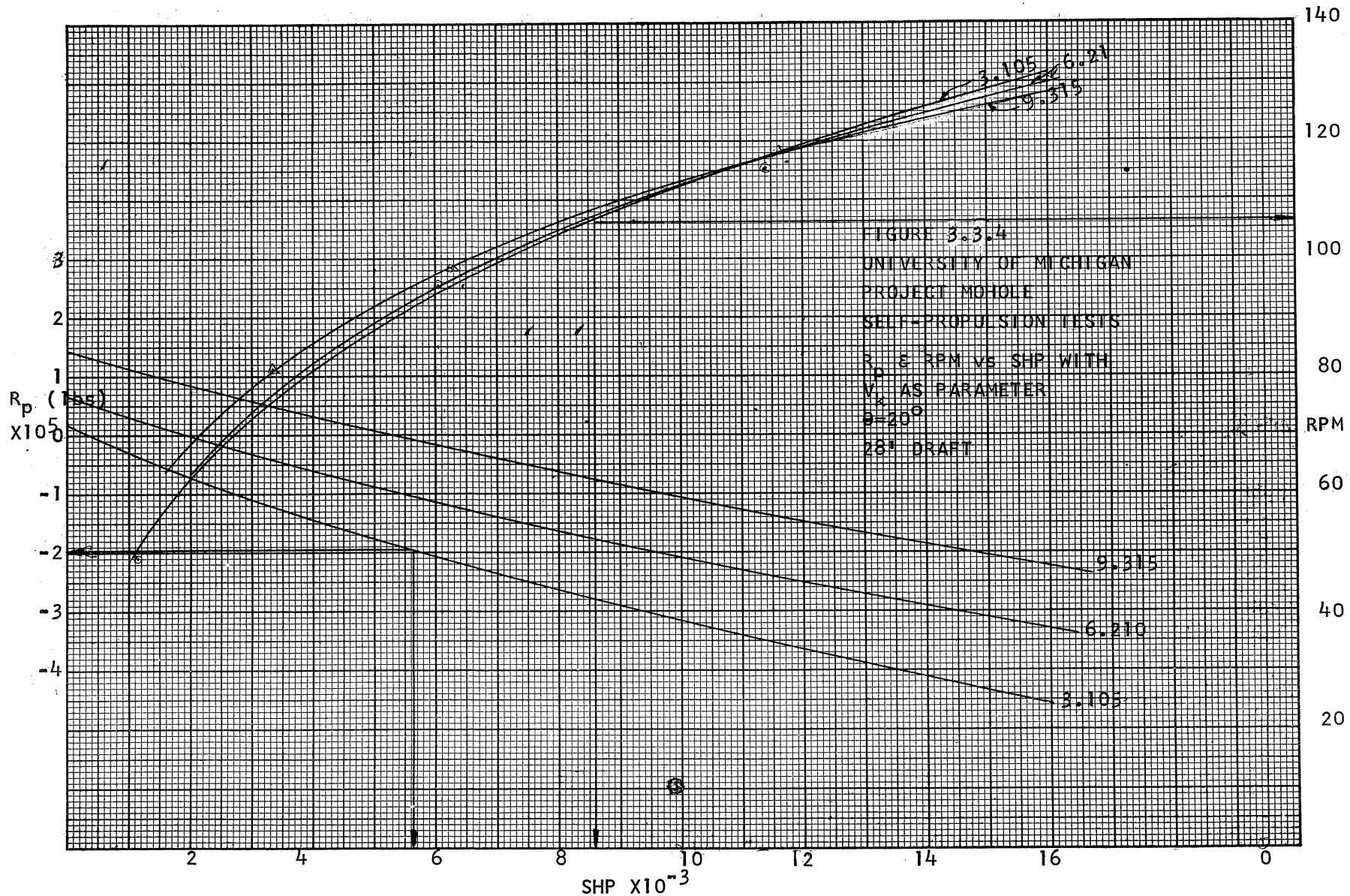
3.105
6.21
9.315
FIGURE 3.3.4
UNIVERSITY OF MICHIGAN
PROJECT MOHOLE
SELF-PROPULSION TESTS
R_p & RPM vs SHP WITH
V_k AS PARAMETER
β=20°
28' DRAFT
R_p (lbs)
X10^5
3
2
1
0
-1
-2
-3
-4
9.315
6.210
3.105
140
120
100
80
RPM
60
40
20
2
4
6
8
10
12
14
16
0
SHP X10^{-3}

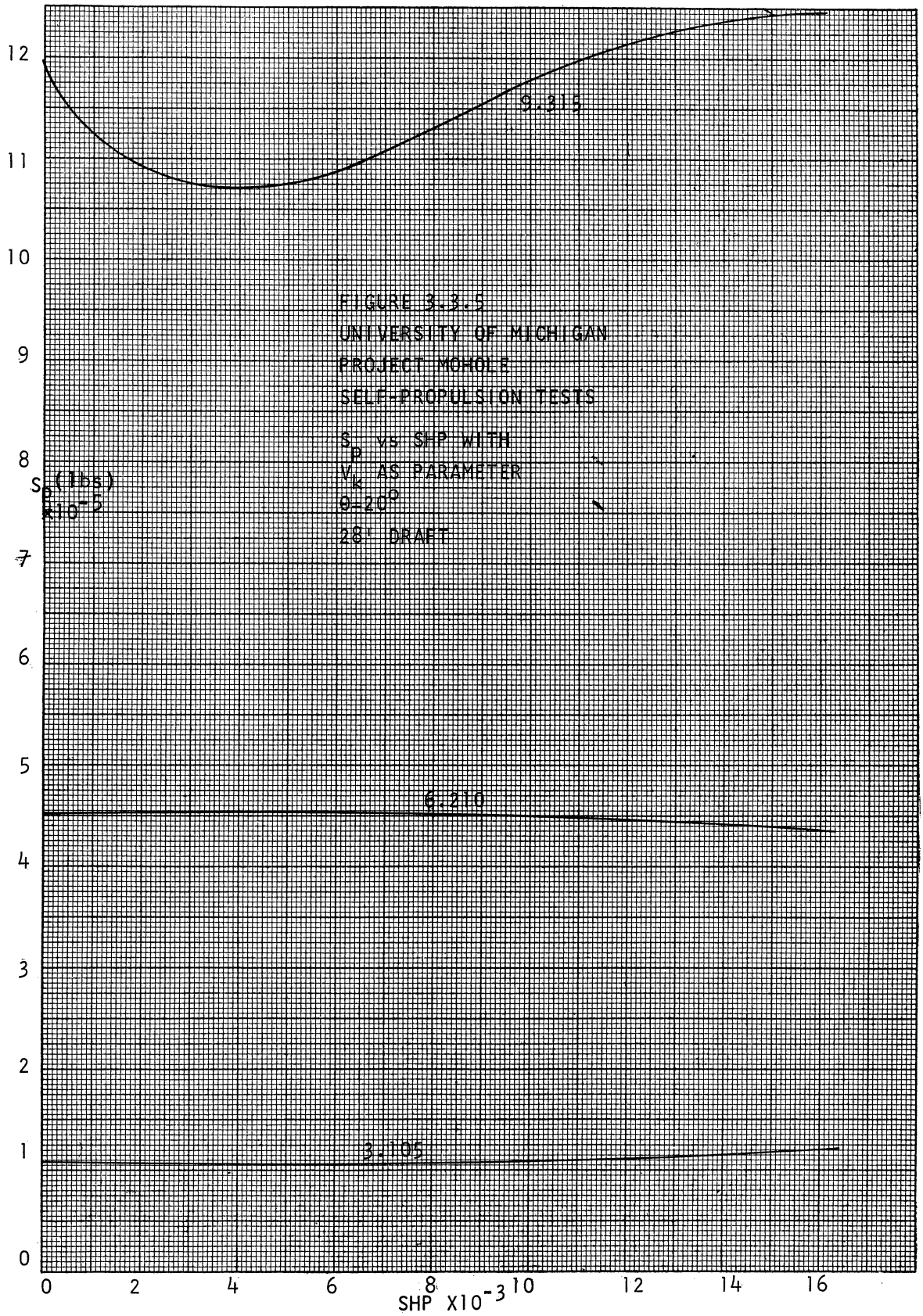

FIGURE 3.3.5
UNIVERSITY OF MICHIGAN
PROJECT MOHOLE
SELF-PROPULSION TESTS

S_p vs SHP WITH
V_k AS PARAMETER
$\theta = 20^\circ$
28' DRAFT

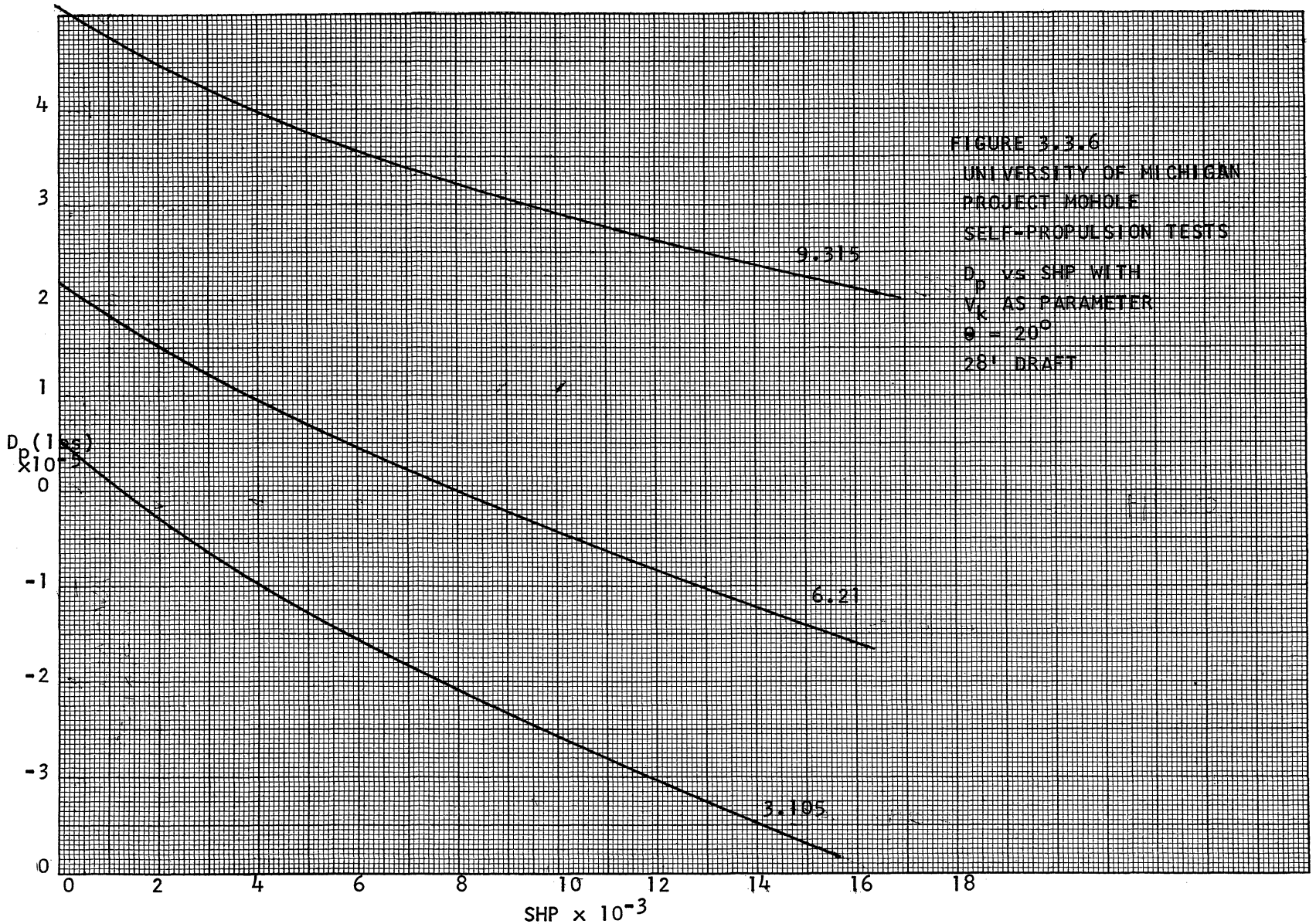
FIGURE 3.3.6
UNIVERSITY OF MICHIGAN
PROJECT MOHOLE
SELF-PROPULSION TESTS
D_p vs SHP WITH
V_K AS PARAMETER
$\theta = 20^\circ$
28' DRAFT
9.315
6.21
3.105
D_p (lbs) $\times 10^{-3}$
SHP $\times 10^{-3}$
4
3
2
1
0
-1
-2
-3
0
2
4
6
8
10
12
14
16
18

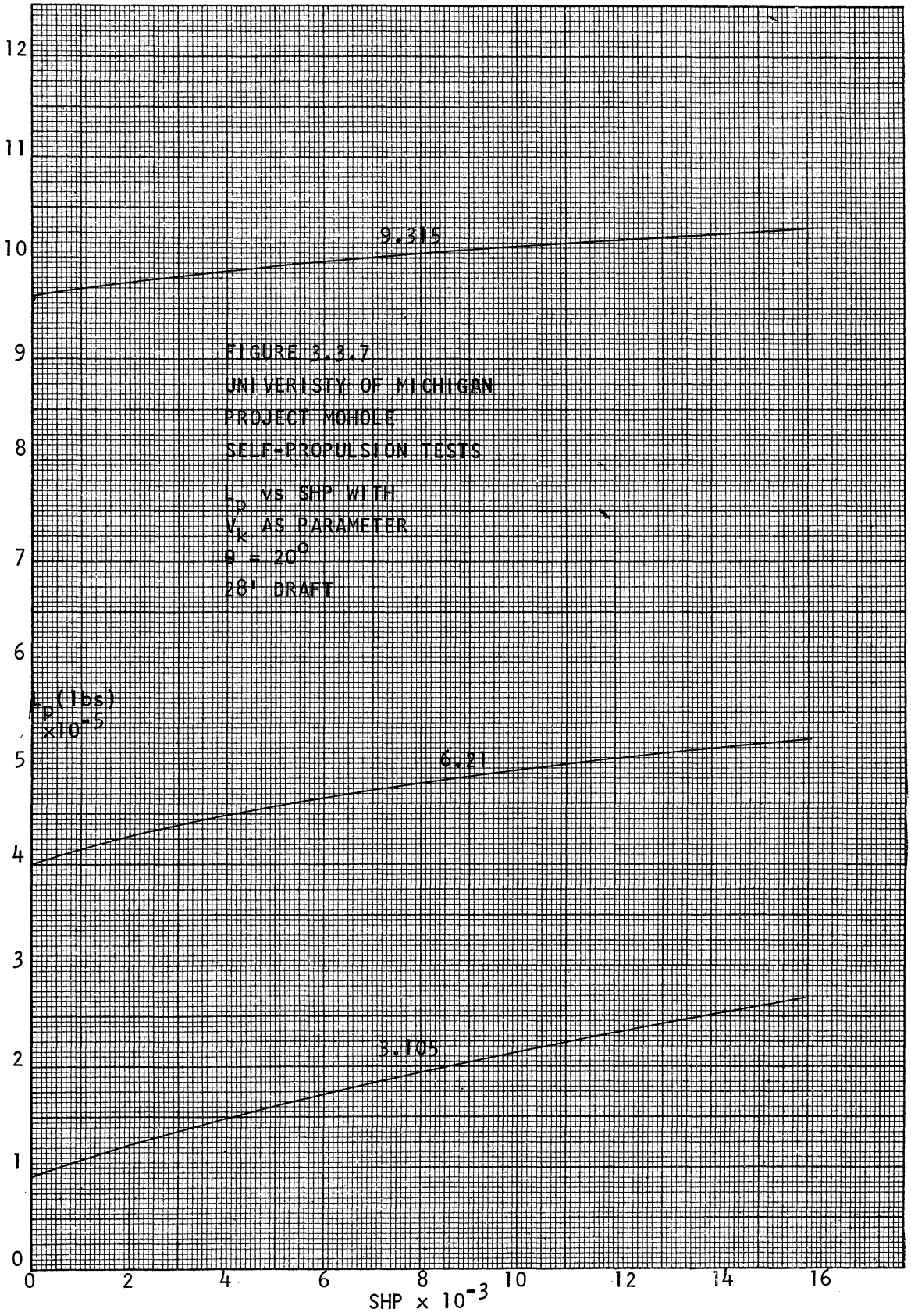
12
11
10
9
8
7
6
5
4
3
2
1
0
9.315
6.21
3.105
FIGURE 3.3.7
UNIVERISTY OF MICHIGAN
PROJECT MOHOLE
SELF-PROPULSION TESTS
L_p vs SHP WITH
V_K AS PARAMETER
$\theta = 20^o$
28' DRAFT
L_p (lbs)
x10^{-5}
0
2
4
6
8
10
12
14
16
SHP x 10^{-3}

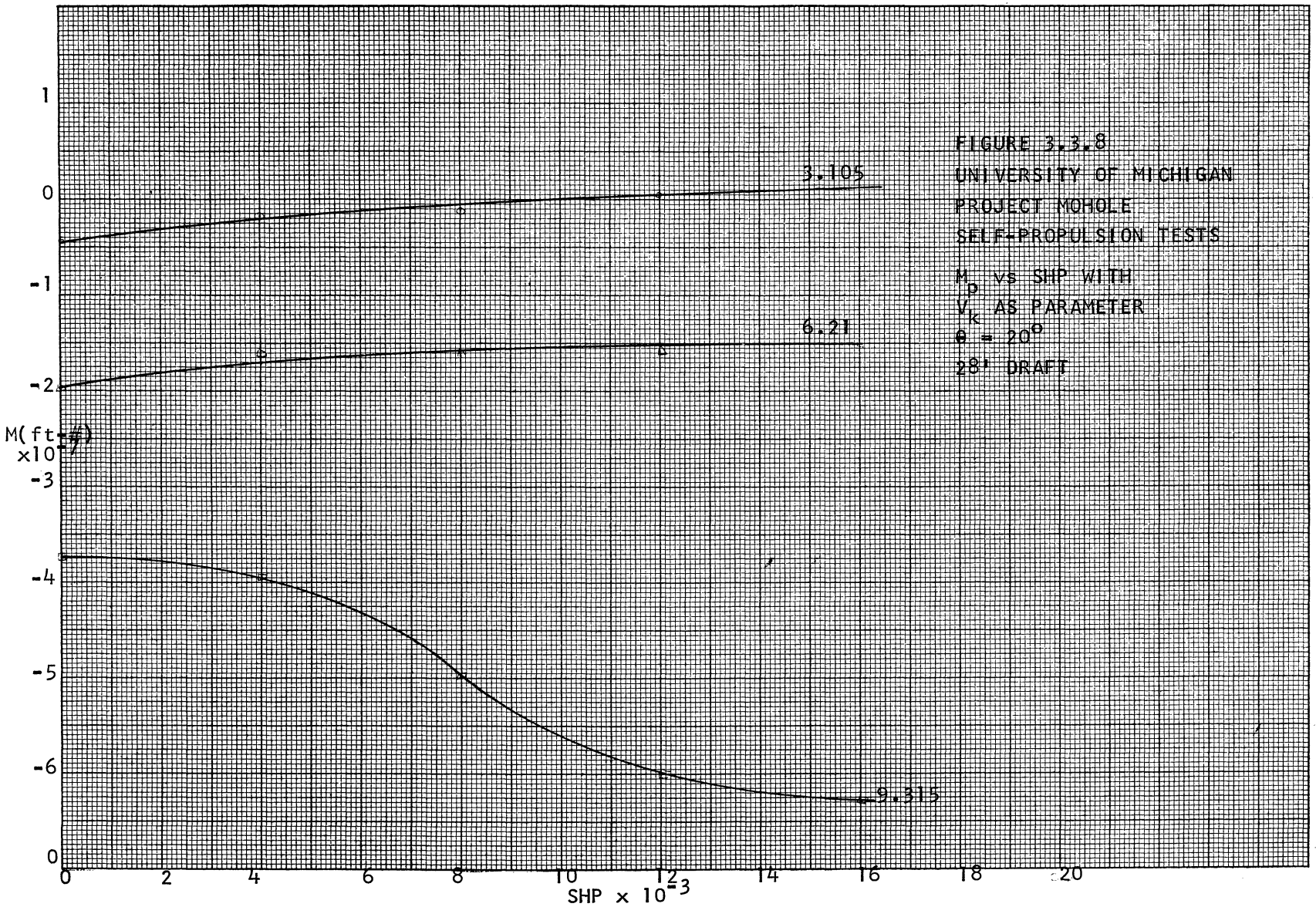

FIGURE 3.3.8
UNIVERSITY OF MICHIGAN
PROJECT MOHOLE
SELF-PROPULSION TESTS

M_p vs SHP WITH
V_K AS PARAMETER
$\theta = 20^0$
28' DRAFT

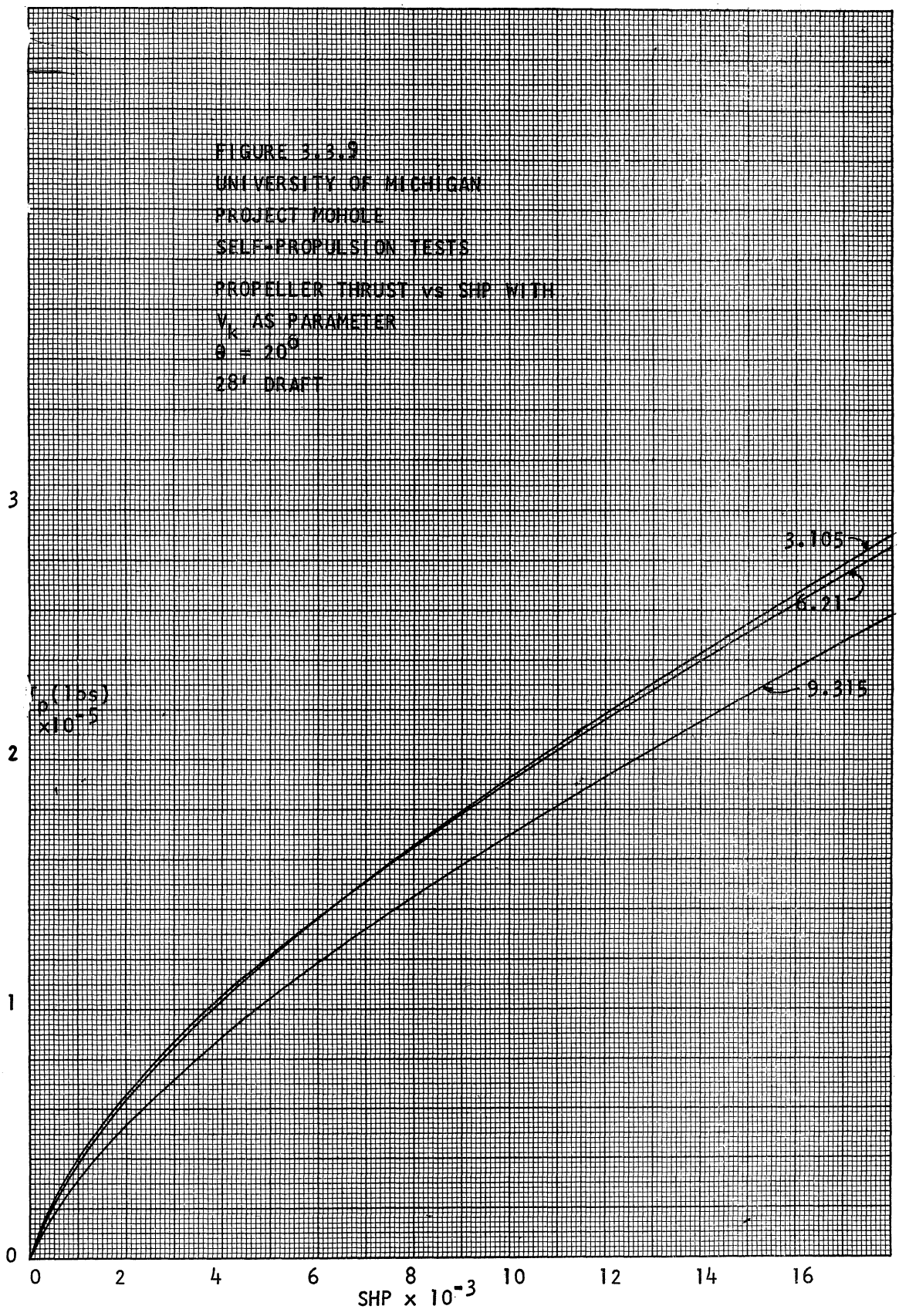
FIGURE 3.3.9
UNIVERSITY OF MICHIGAN
PROJECT MOHOLE
SELF-PROPULSION TESTS
PROPELLER THRUST vs SHP WITH
V_K AS PARAMETER
$\theta = 20^\circ$
28' DRAFT
3.105
6.21
9.315
T_p (lbs) $\times 10^{-5}$
0
1
2
3
0
2
4
6
8
10
12
14
16
SHP $\times 10^{-3}$

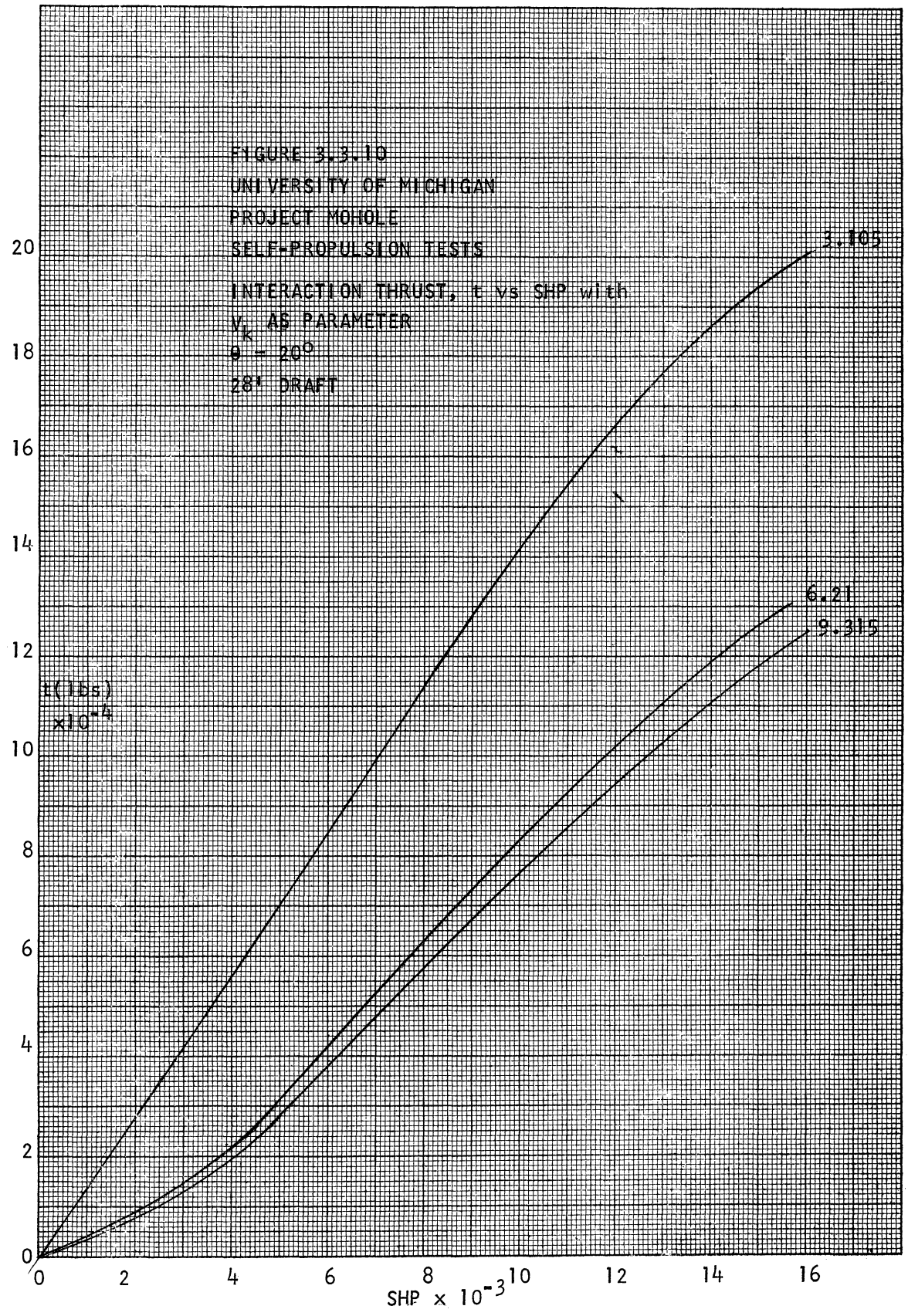
FIGURE 3.3.10
UNIVERSITY OF MICHIGAN
PROJECT MOHOLE
SELF-PROPULSION TESTS
INTERACTION THRUST, t vs SHP with
V_K AS PARAMETER
$\theta = 20^0$
28' DRAFT
3.105
6.21
9.315
t(lbs)
$\times 10^{-4}$
SHP $\times 10^{-3}$
0
2
4
6
8
10
12
14
16
18
20

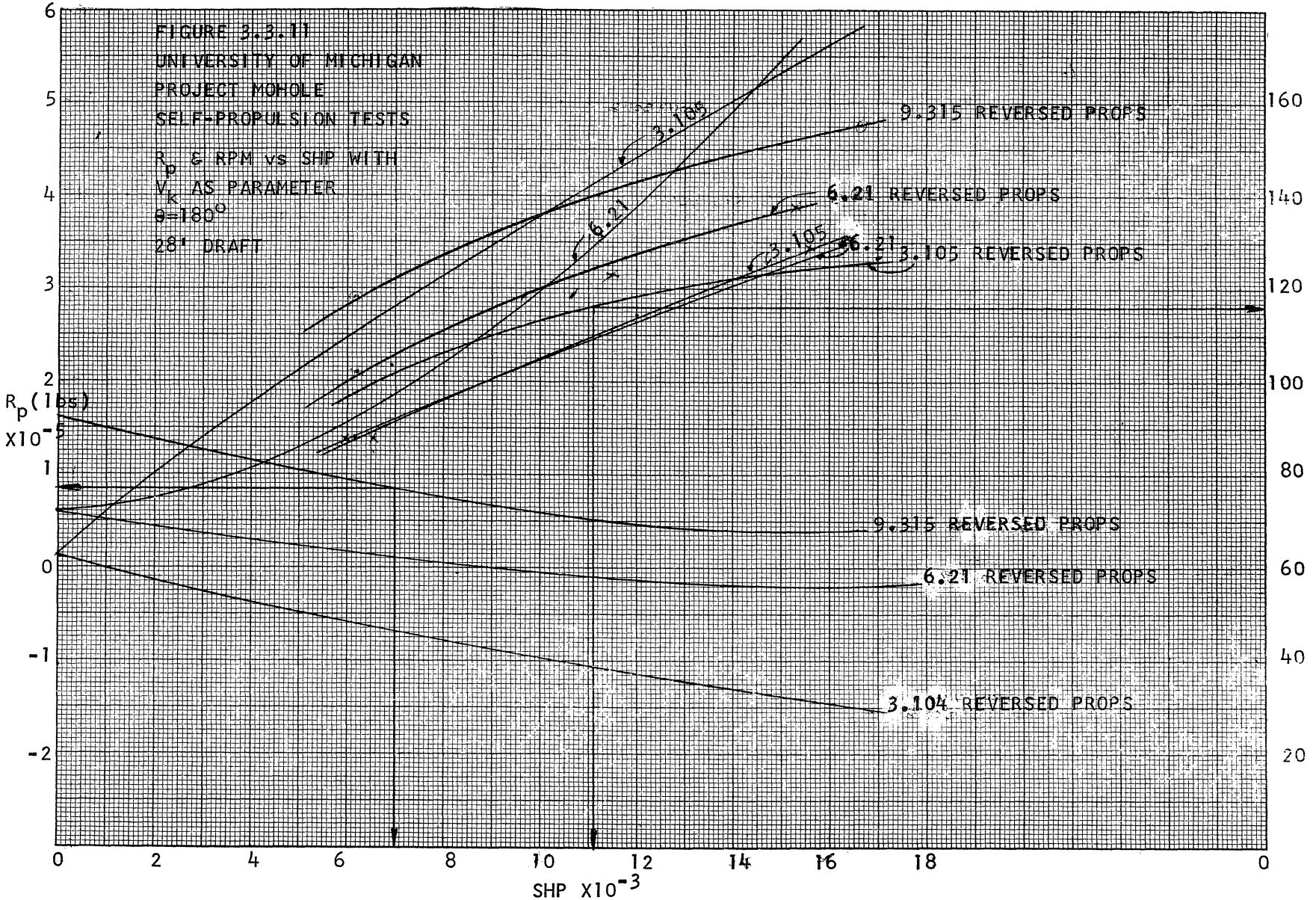
FIGURE 3.3.11
UNIVERSITY OF MICHIGAN
PROJECT MOHOLE
SELF-PROPULSION TESTS
R_p & RPM vs SHP WITH
V_k AS PARAMETER
θ=180°
28' DRAFT
9.315 REVERSED PROPS
6.21 REVERSED PROPS
3.105 REVERSED PROPS
3.104 REVERSED PROPS
R_p (lbs) X10^{-5}
SHP X10^{-3}
6
5
4
3
2
1
0
-1
-2
160
140
120
100
80
60
40
20
0
2
4
6
8
10
12
14
16
18

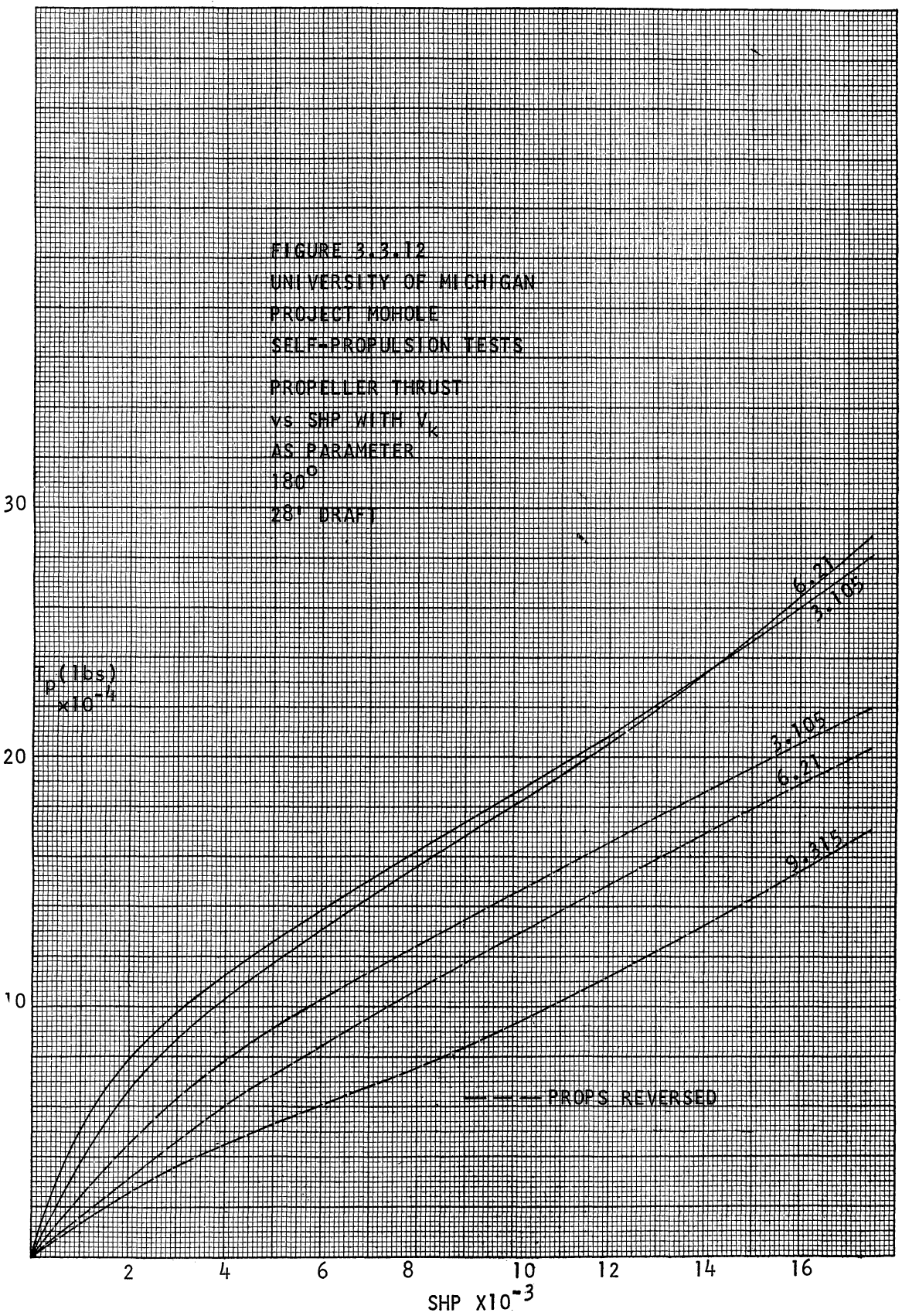
FIGURE 3.3.12
UNIVERSITY OF MICHIGAN
PROJECT MOHOLE
SELF-PROPULSION TESTS
PROPELLER THRUST
vs SHP WITH V_K
AS PARAMETER
180°
28' DRAFT
30
20
10
T_p (lbs) x10^{-4}
6.21
3.105
3.105
6.21
9.315
PROPS REVERSED
2
4
6
8
10
12
14
16
SHP X10^{-3}

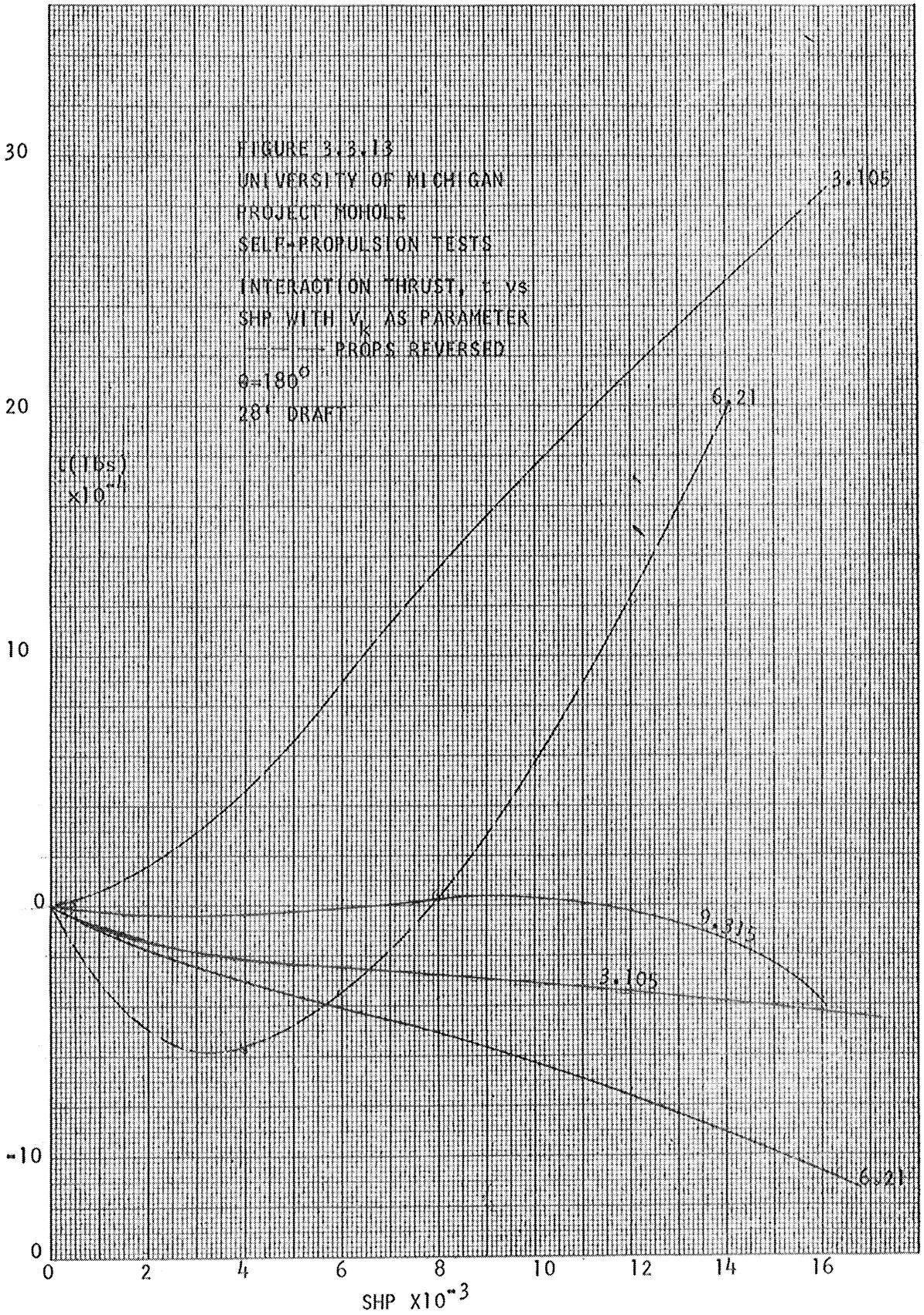
FIGURE 3.3.13
UNIVERSITY OF MICHIGAN
PROJECT MOHOLE
SELF-PROPULSION TESTS
INTERACTION THRUST, t VS
SHP WITH V_k AS PARAMETER
PROPS REVERSED
θ=180°
28' DRAFT
3.105
6.21
9.315
3.105
6.21
t(lbs)
X10^-4
30
20
10
0
-10
0
0
2
4
6
8
10
12
14
16
SHP X10^-3

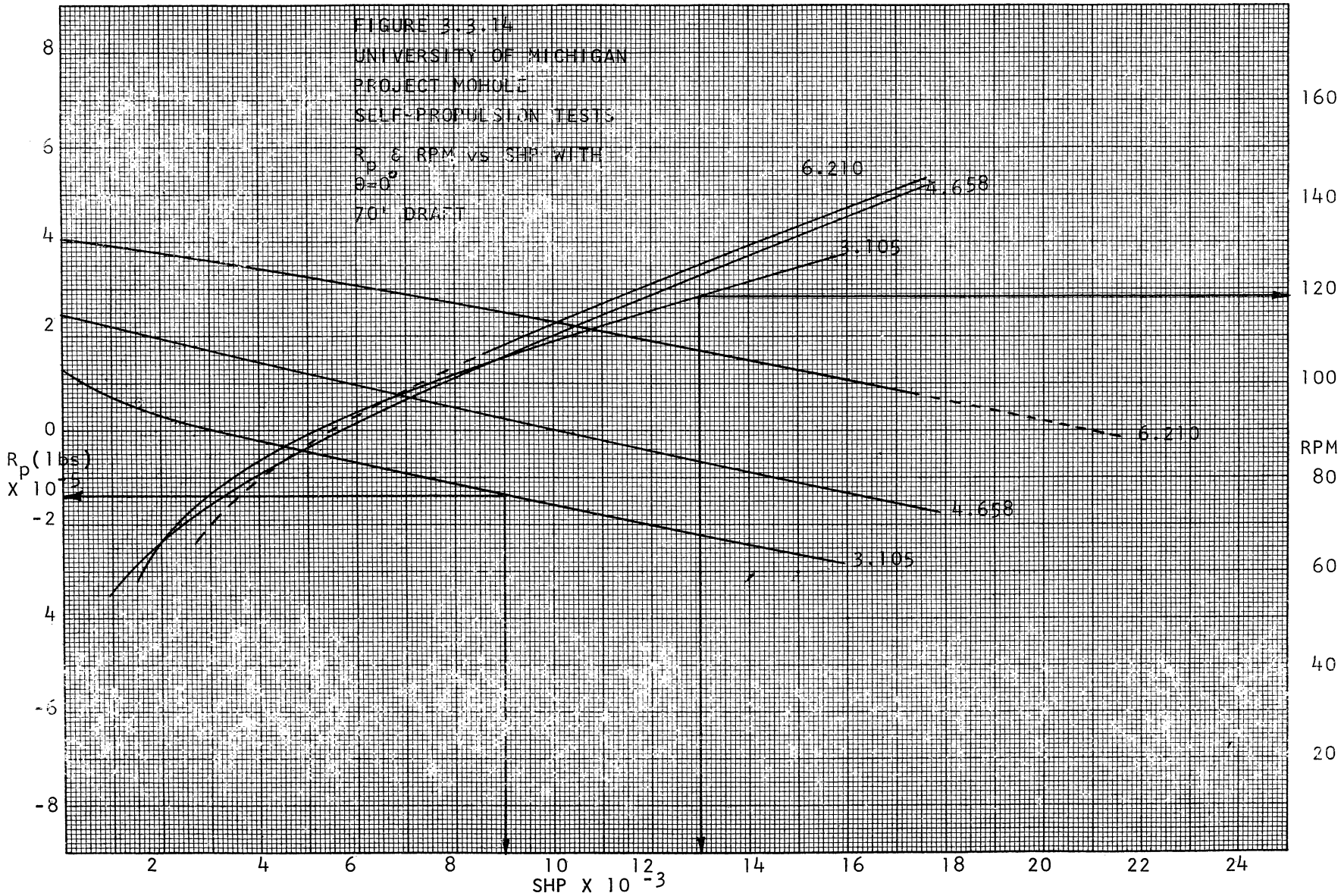
FIGURE 3.3.14
UNIVERSITY OF MICHIGAN
PROJECT MOHOLE
SELF-PROPULSION TESTS
R_p & RPM vs SHP WITH
$\theta=0^\circ$
70' DRAFT
6.210
4.658
3.105
6.210
4.658
3.105
R_p (lbs)
X 10^{-3}
RPM
SHP X 10^{-3}
8
6
4
2
0
-2
4
-6
-8
160
140
120
100
80
60
40
20
2
4
6
8
10
12
14
16
18
20
22
24

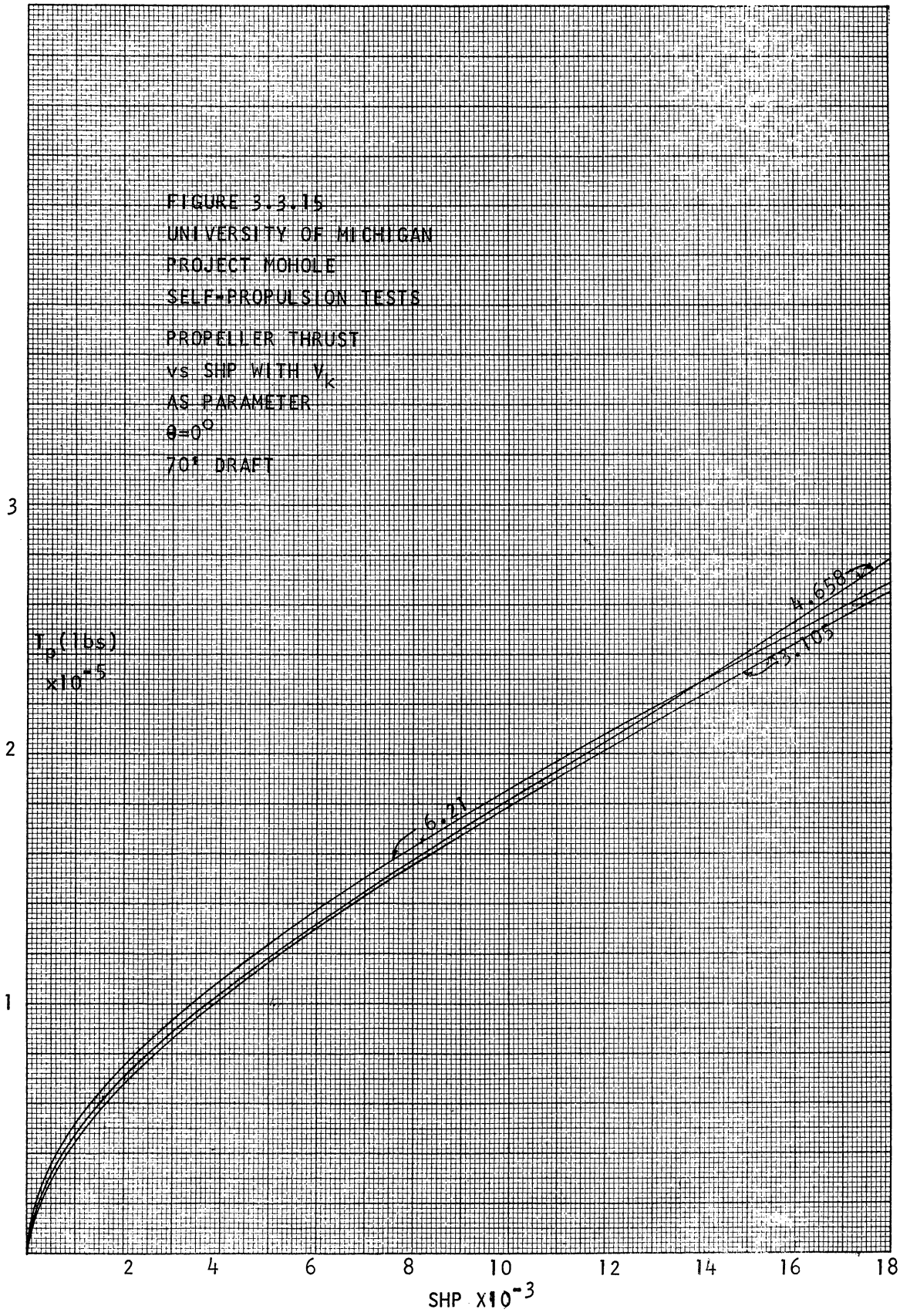
FIGURE 3.3.15
UNIVERSITY OF MICHIGAN
PROJECT MOHOLE
SELF-PROPULSION TESTS
PROPELLER THRUST
vs SHP WITH V_k
AS PARAMETER
$\theta=0^\circ$
70' DRAFT
T_p (lbs)
$\times 10^{-5}$
3
2
1
6.21
6.658
6.105
2
4
6
8
10
12
14
16
18
SHP $\times 10^{-3}$

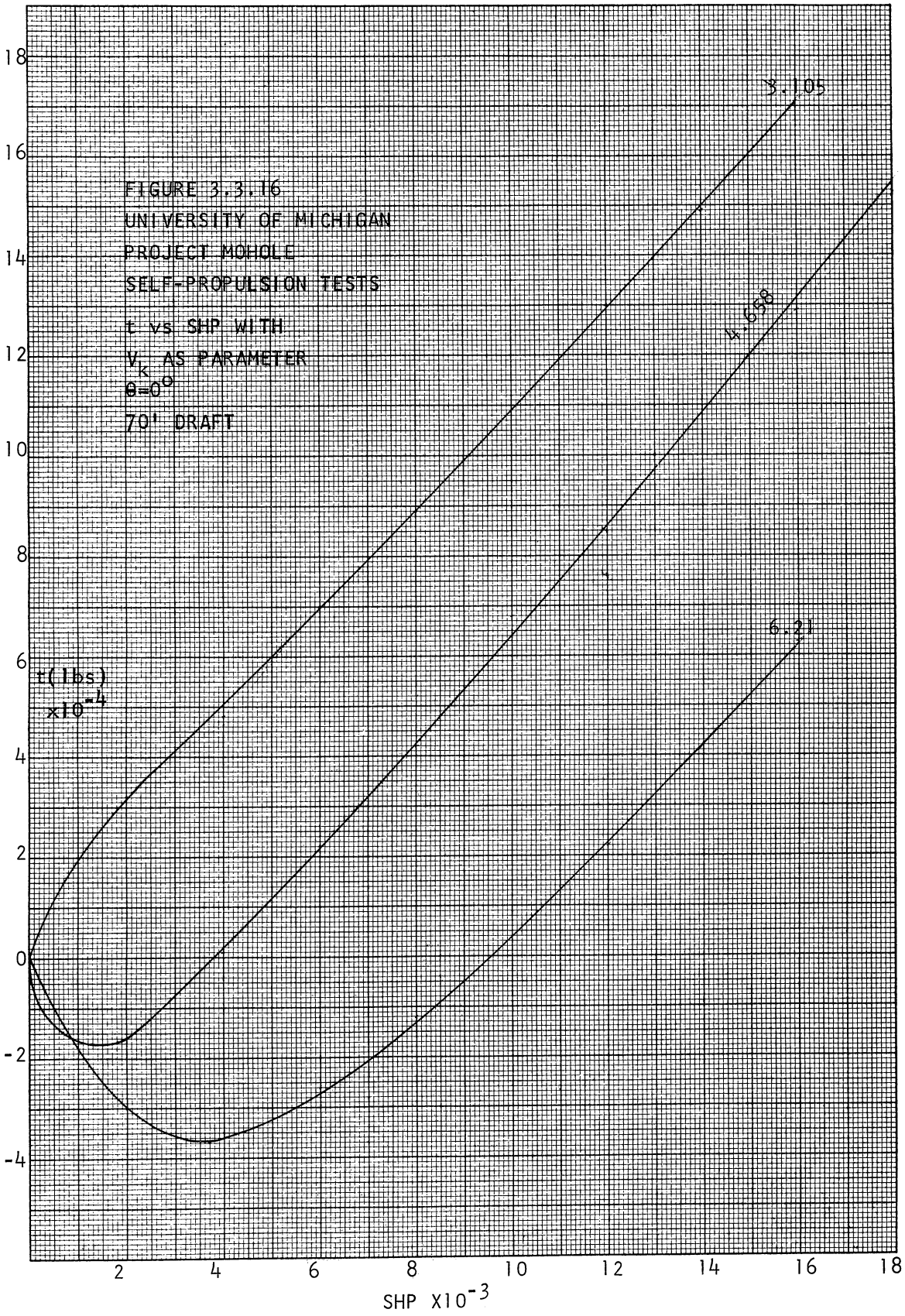
FIGURE 3.3.16
UNIVERSITY OF MICHIGAN
PROJECT MOHOLE
SELF-PROPULSION TESTS
t vs SHP WITH
V_K AS PARAMETER
θ=0°
70' DRAFT
8.105
6.68
6.21
t(lbs)
x10⁻⁴
SHP X10⁻³
18
16
14
12
10
8
6
4
2
0
-2
-4
2
4
6
8
10
12
14
16
18

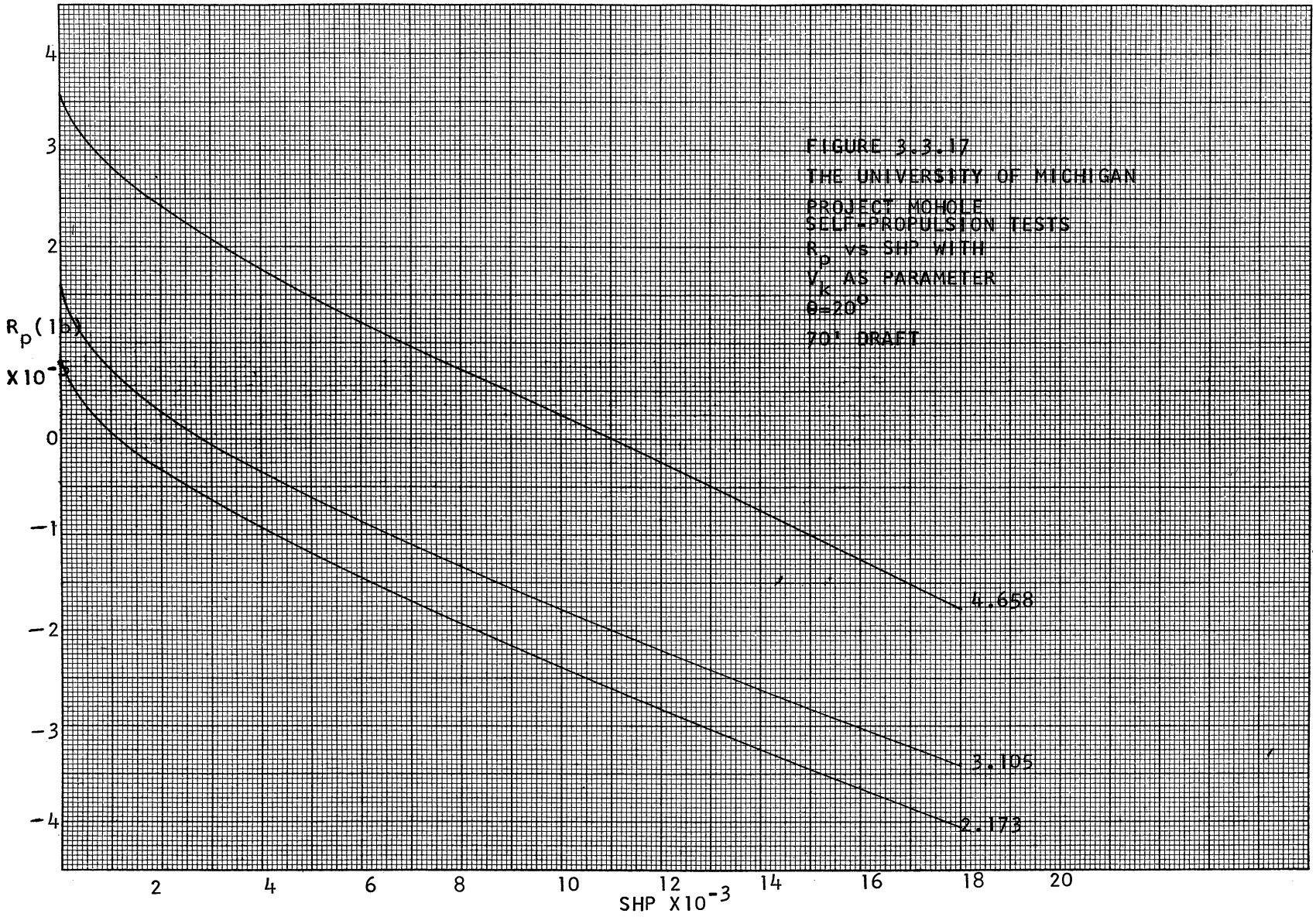
FIGURE 3.3.17
THE UNIVERSITY OF MICHIGAN
PROJECT MOHOLE
SELF-PROPULSION TESTS
R_p vs SHP WITH
V_k AS PARAMETER
$\theta=20^o$
70' DRAFT
R_p (lb)
X 10^{-3}
4
3
2
0
−1
−2
−3
−4
2
4
6
8
10
12
14
16
18
20
SHP X 10^{-3}
4.658
3.105
2.173

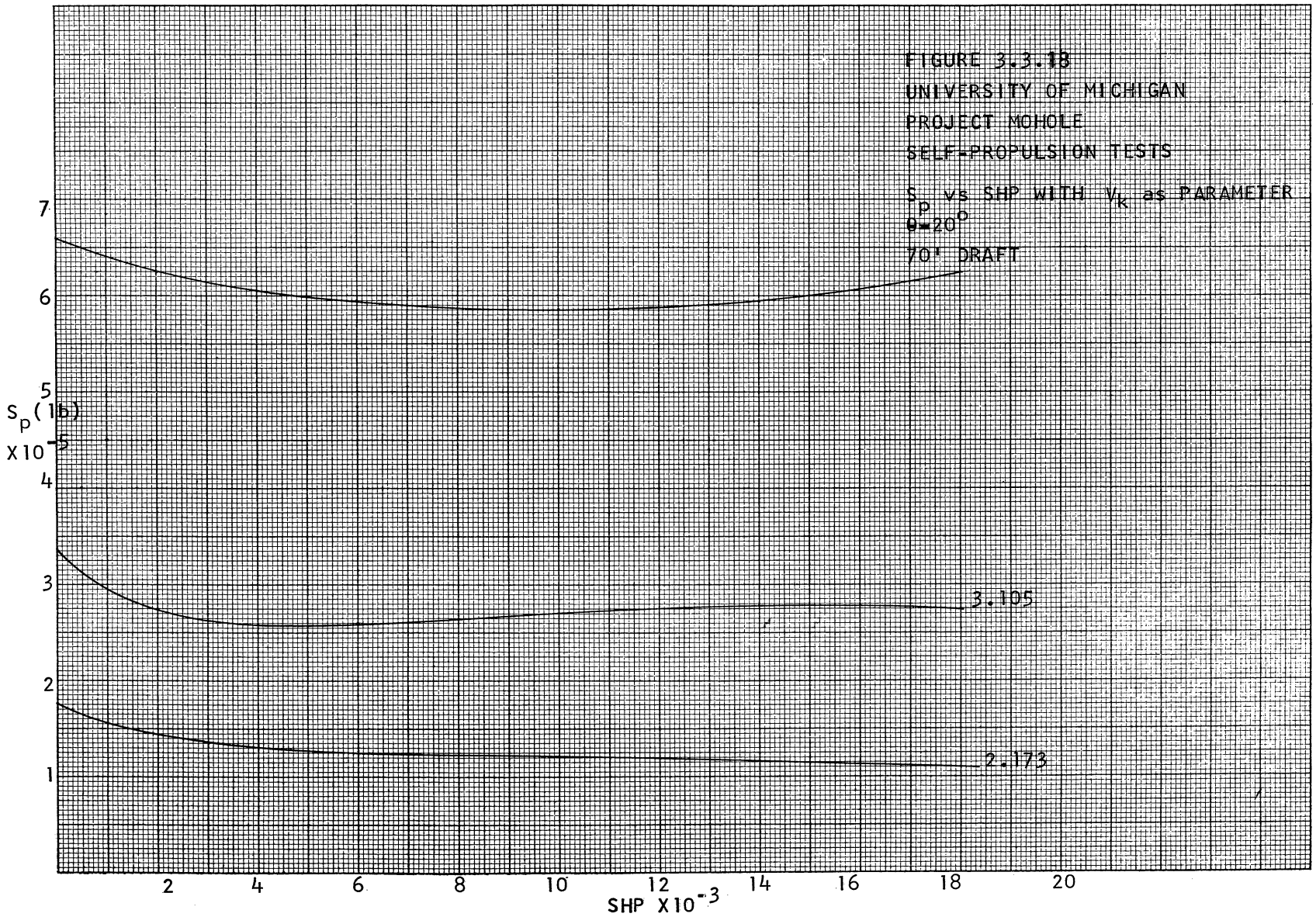
FIGURE 3.3.18
UNIVERSITY OF MICHIGAN
PROJECT MOHOLE
SELF-PROPULSION TESTS
S_p vs SHP WITH V_k as PARAMETER
$\theta = 20^o$
70' DRAFT
S_p (lb)
X 10^{-5}
SHP X 10^{-3}
3.105
2.173
1
2
3
4
5
6
7
2
4
6
8
10
12
14
16
18
20

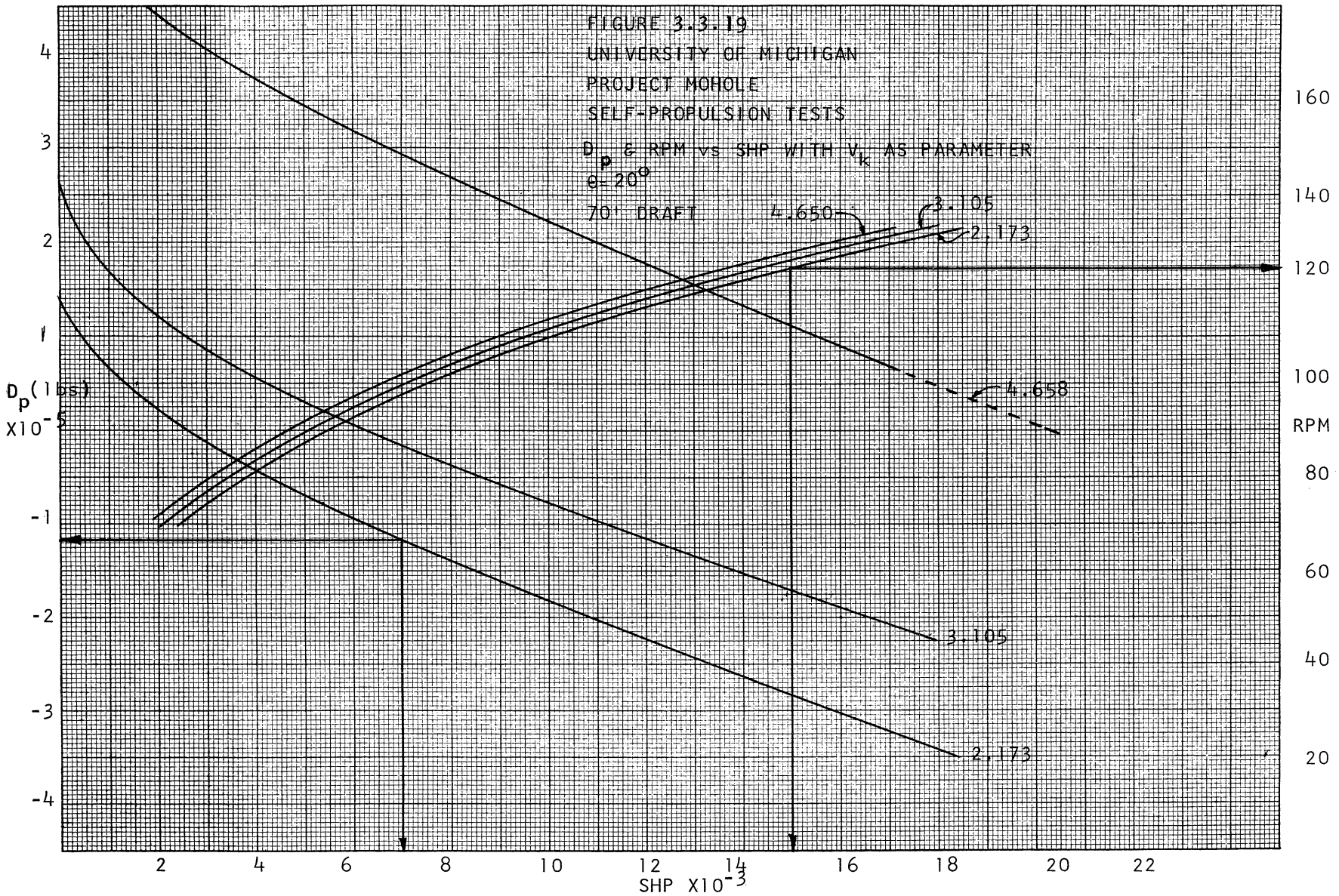
FIGURE 3.3.19
UNIVERSITY OF MICHIGAN
PROJECT MOHOLE
SELF-PROPULSION TESTS
D_p & RPM vs SHP WITH V_k AS PARAMETER
$\theta = 20^\circ$
70' DRAFT
4.650
3.105
2.173
4.658
3.105
2.173
D_p (lbs) $X10^{-5}$
SHP $X10^{-3}$
RPM
4
3
2
1
-1
-2
-3
-4
2
4
6
8
10
12
14
16
18
20
22
160
140
120
100
80
60
40
20

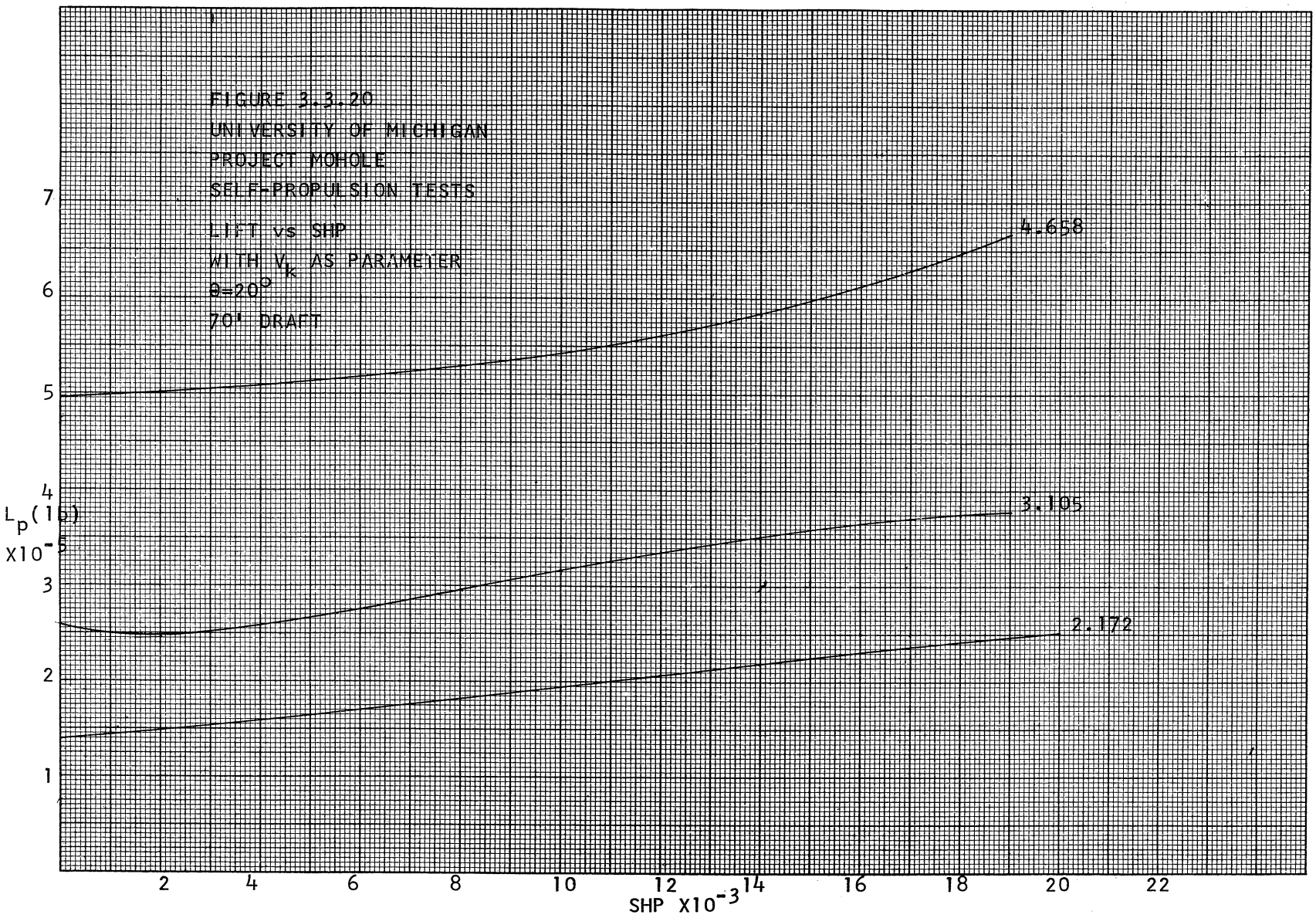
FIGURE 3.3.20
UNIVERSITY OF MICHIGAN
PROJECT MOHOLE
SELF-PROPULSION TESTS
LIFT vs SHP
WITH V_k AS PARAMETER
$\theta=20^0$
70' DRAFT
4.658
3.105
2.172
L_p (lb)
X10^{-5}
SHP X10^{-3}
1
2
3
4
5
6
7
2
4
6
8
10
12
14
16
18
20
22

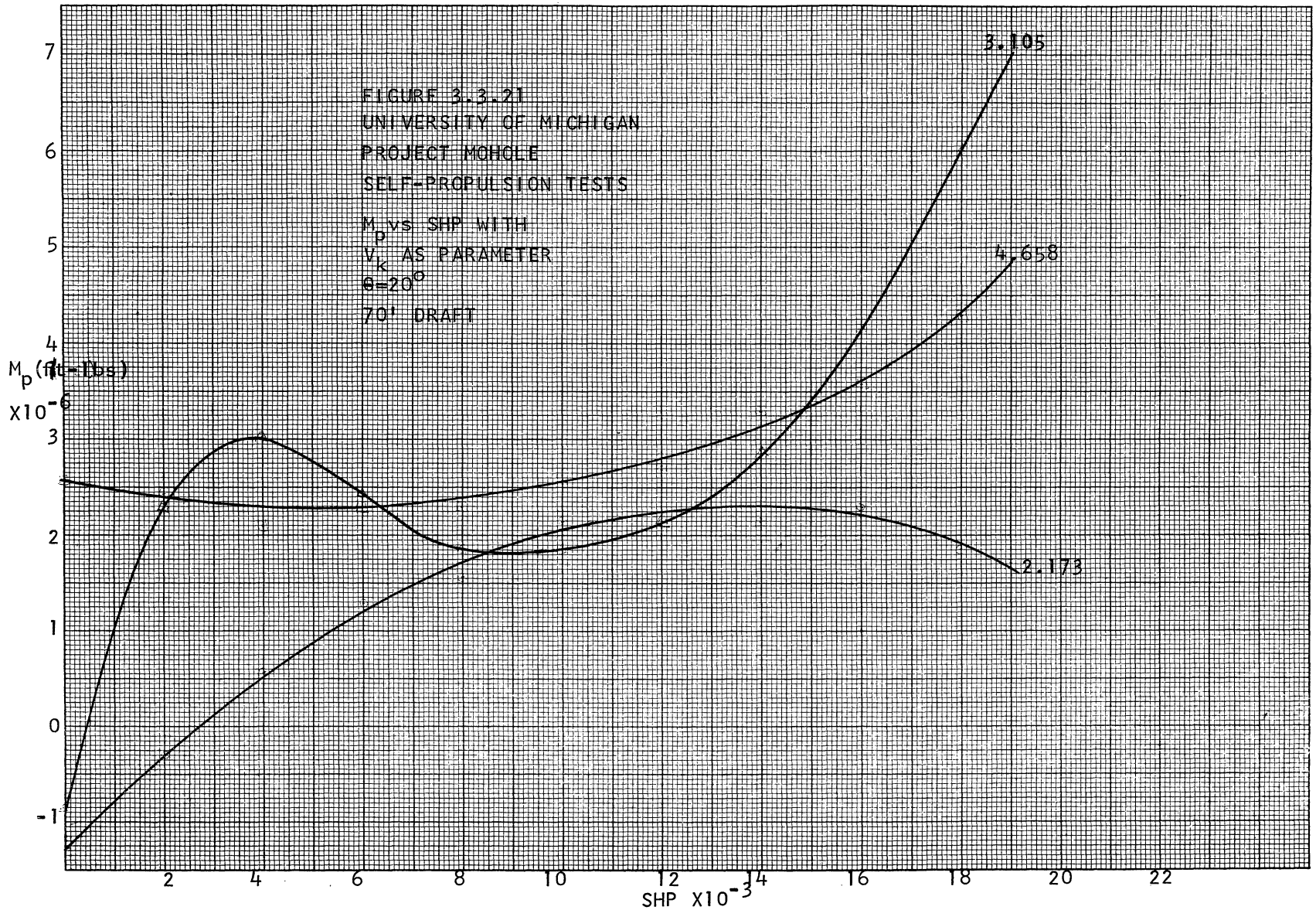
FIGURE 3.3.21
UNIVERSITY OF MICHIGAN
PROJECT MOHOLE
SELF-PROPULSION TESTS
M_p vs SHP WITH
V_K AS PARAMETER
θ=20°
70' DRAFT
3.105
4.658
2.173
M_p (ft-lbs)
X10^{-6}
SHP X10^{-3}
7
6
5
4
3
2
1
0
-1
2
4
6
8
10
12
14
16
18
20
22

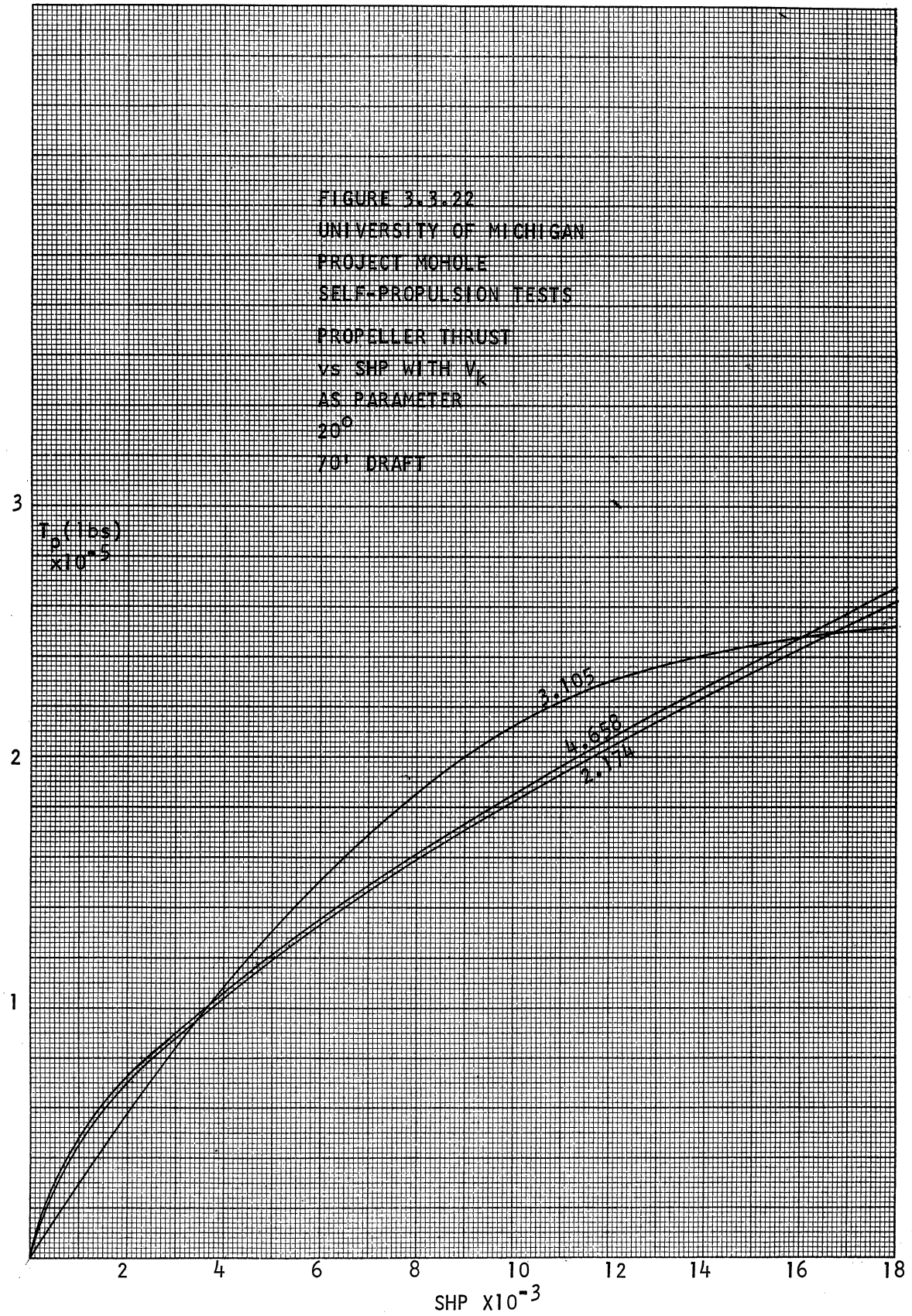
FIGURE 3.3.22
UNIVERSITY OF MICHIGAN
PROJECT MOHOLE
SELF-PROPULSION TESTS
PROPELLER THRUST
VS SHP WITH V_K
AS PARAMETER
20°
70' DRAFT
T_p(lbs)
X10^{-5}
3
2
1
3.105
2.668
2.114
2
4
6
8
10
12
14
16
18
SHP X10^{-3}

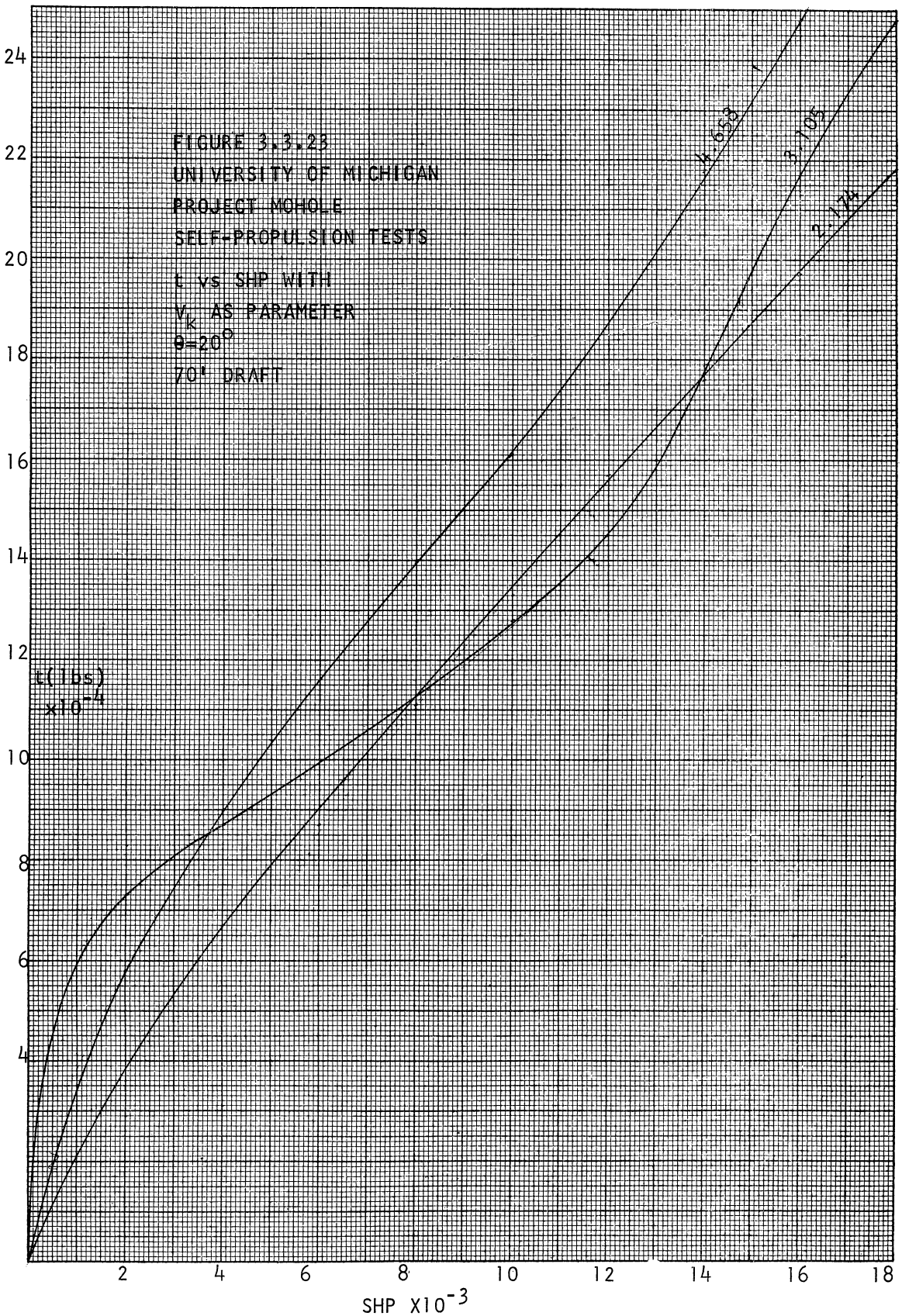
FIGURE 3.3.23
UNIVERSITY OF MICHIGAN
PROJECT MOHOLE
SELF-PROPULSION TESTS
t vs SHP WITH
V_k AS PARAMETER
$\theta=20^0$
70' DRAFT
V_k 6.53
3.105
2.138
t(lbs) x10^{-4}
SHP X10^{-3}
24
22
20
18
16
14
12
10
8
6
4
2
4
6
8
10
12
14
16
18

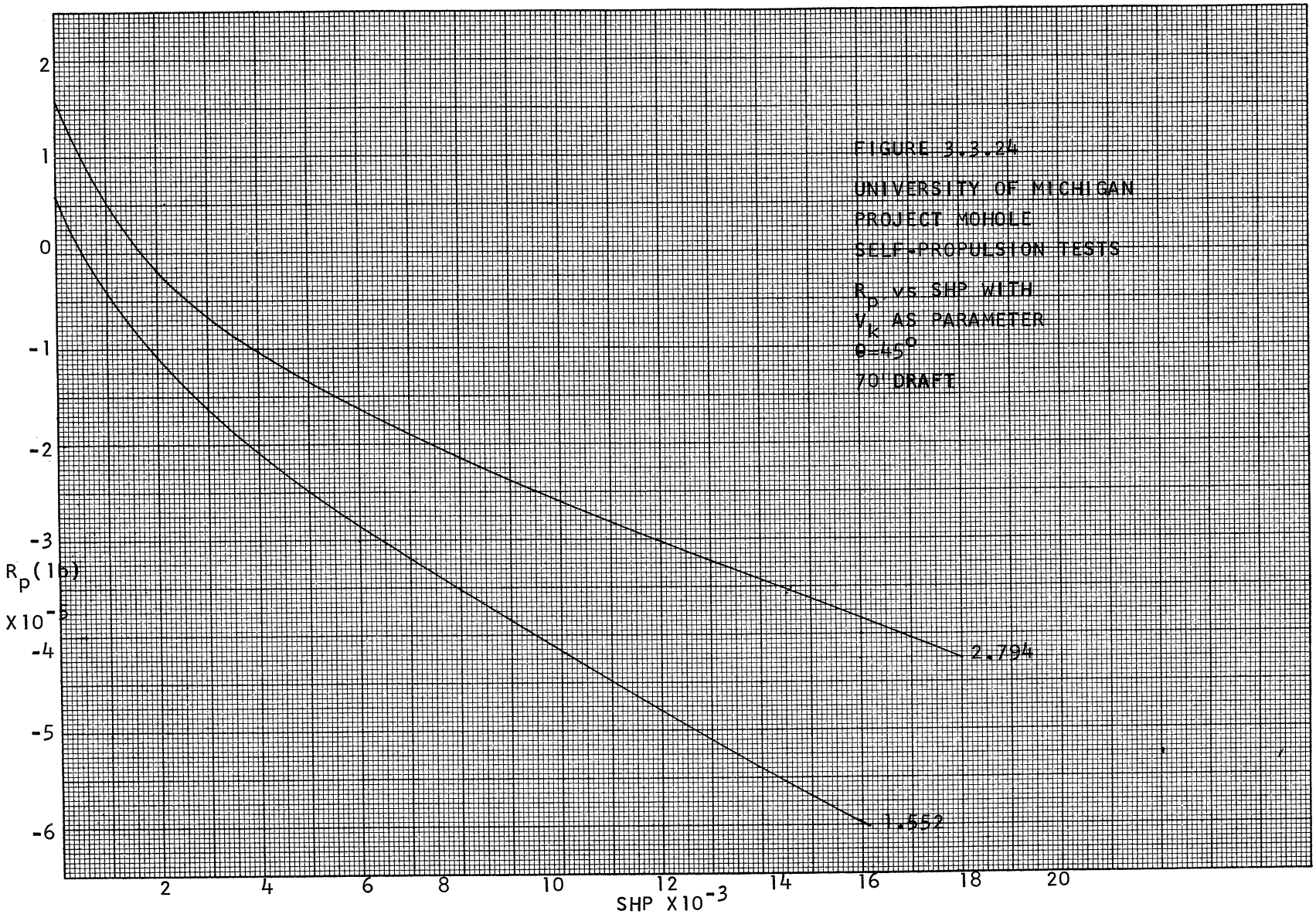
FIGURE 3.3.24
UNIVERSITY OF MICHIGAN
PROJECT MOHOLE
SELF-PROPULSION TESTS
R_p vs SHP WITH
V_K AS PARAMETER
θ=45°
70' DRAFT
2.794
1.552
R_p (lb)
X10^{-5}
SHP X10^{-3}
2
1
0
-1
-2
-3
-4
-5
-6
2
4
6
8
10
12
14
16
18
20

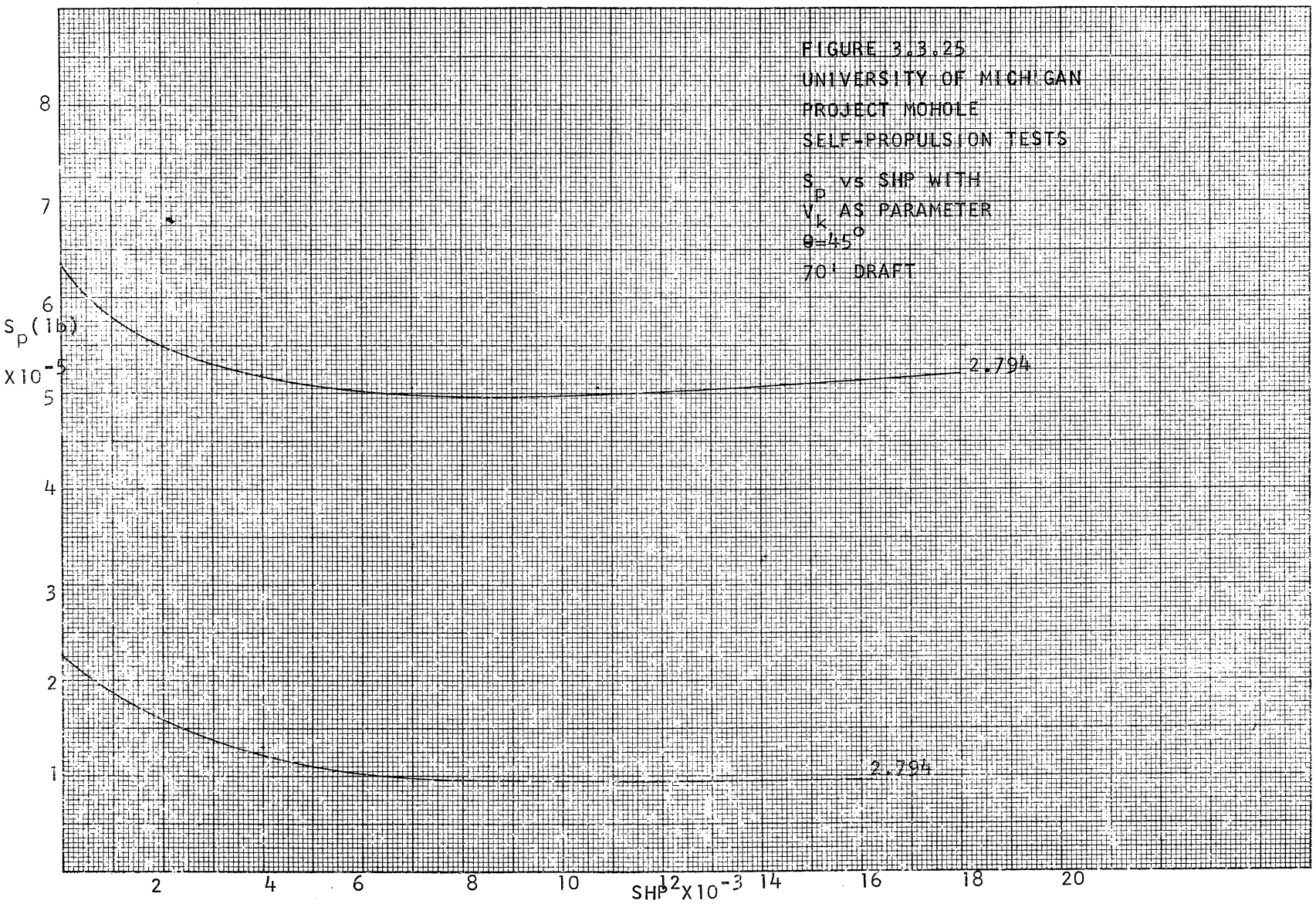
FIGURE 3.3.25
UNIVERSITY OF MICHIGAN
PROJECT MOHOLE
SELF-PROPULSION TESTS
S_p vs SHP WITH
V_k AS PARAMETER
$\theta=45^\circ$
70' DRAFT
S_p (lb)
X10^{-5}
8
7
6
5
4
3
2
1
2.794
2.794
2
4
6
8
10
12
14
16
18
20
SHP X10^{-3}

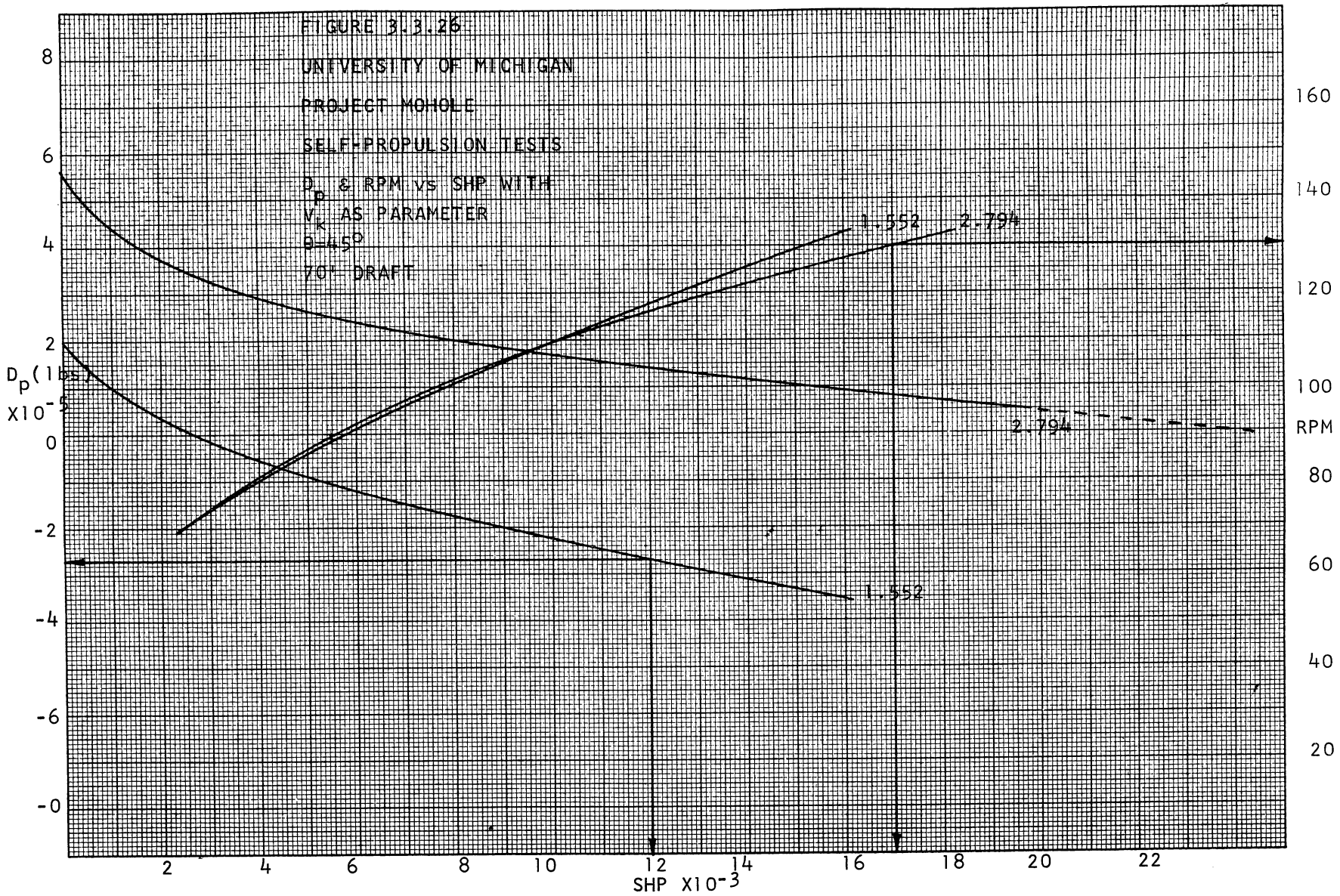
FIGURE 3.3.26
UNIVERSITY OF MICHIGAN
PROJECT MOHOLE
SELF-PROPULSION TESTS
D_p & RPM vs SHP WITH
V_k AS PARAMETER
$\theta=45^D$
70' DRAFT
1.552
2.794
2.794
1.552
D_p (lbs) X10^{-3}
SHP X10^{-3}
RPM
8
6
4
2
0
-2
-4
-6
-0
2
4
6
8
10
12
14
16
18
20
22
160
140
120
100
80
60
40
20

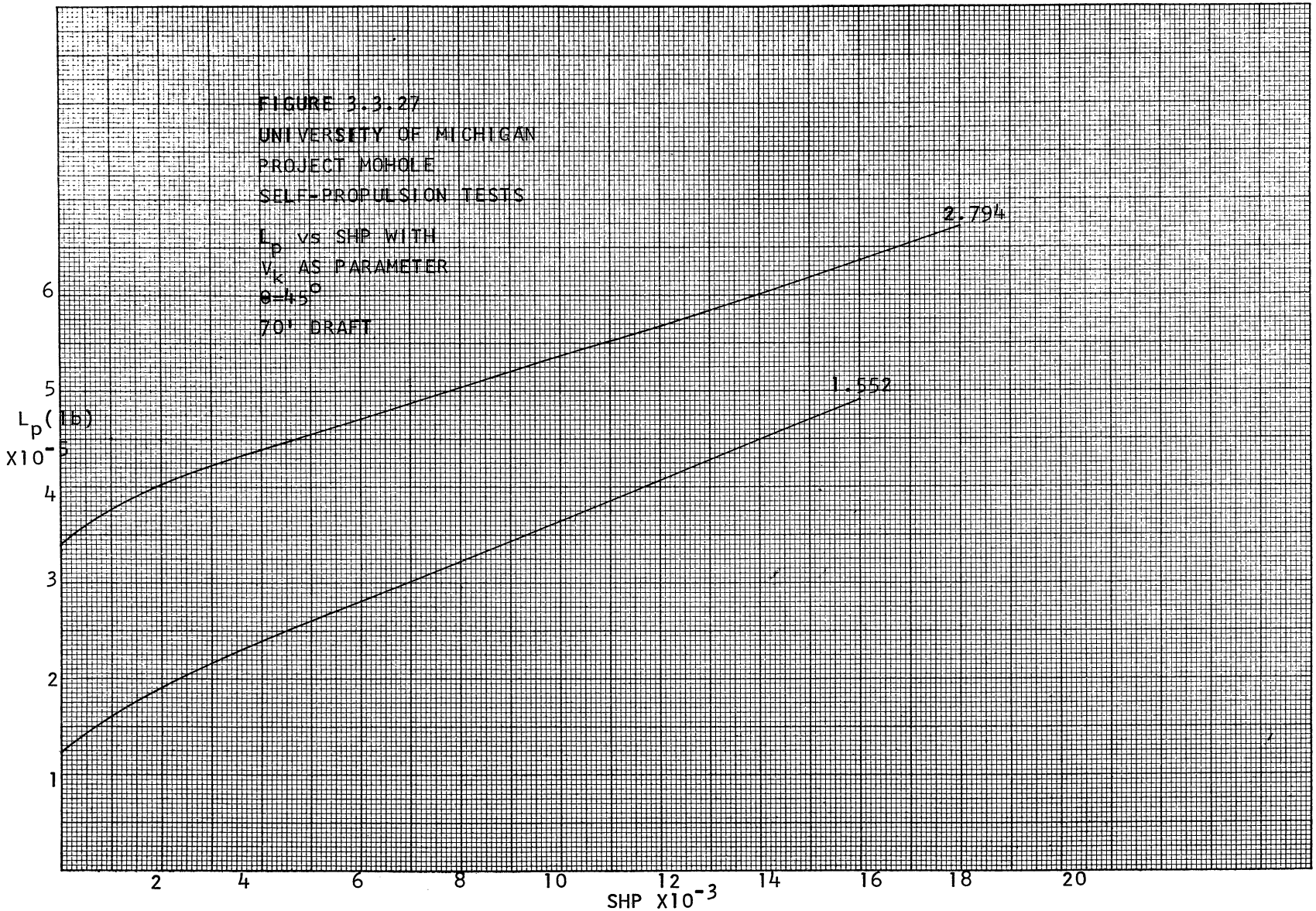
FIGURE 3.3.27
UNIVERSITY OF MICHIGAN
PROJECT MOHOLE
SELF-PROPULSION TESTS
L_p VS SHP WITH
V_K AS PARAMETER
θ=45°
70' DRAFT
2.794
1.552
L_p (lb)
X10^{-5}
SHP X10^{-3}
1
2
3
4
5
6
2
4
6
8
10
12
14
16
18
20

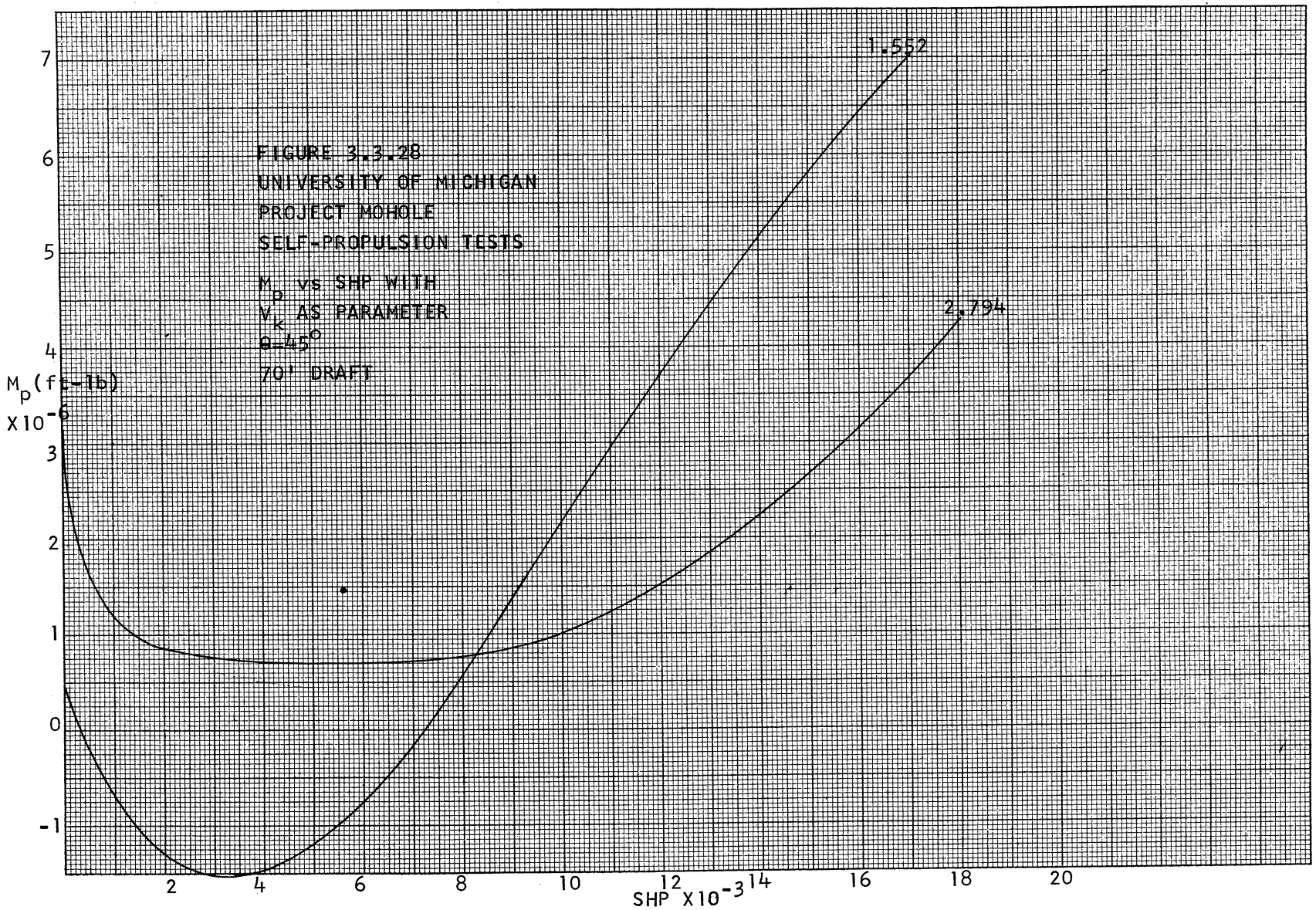
FIGURE 3.3.28
UNIVERSITY OF MICHIGAN
PROJECT MOHOLE
SELF-PROPULSION TESTS
M_p vs SHP WITH
V_K AS PARAMETER
θ=45°
70' DRAFT
1.552
2.794
M_p (ft-lb)
X10^{-6}
SHP X10^{-3}
7
6
5
4
3
2
1
0
-1
2
4
6
8
10
12
14
16
18
20

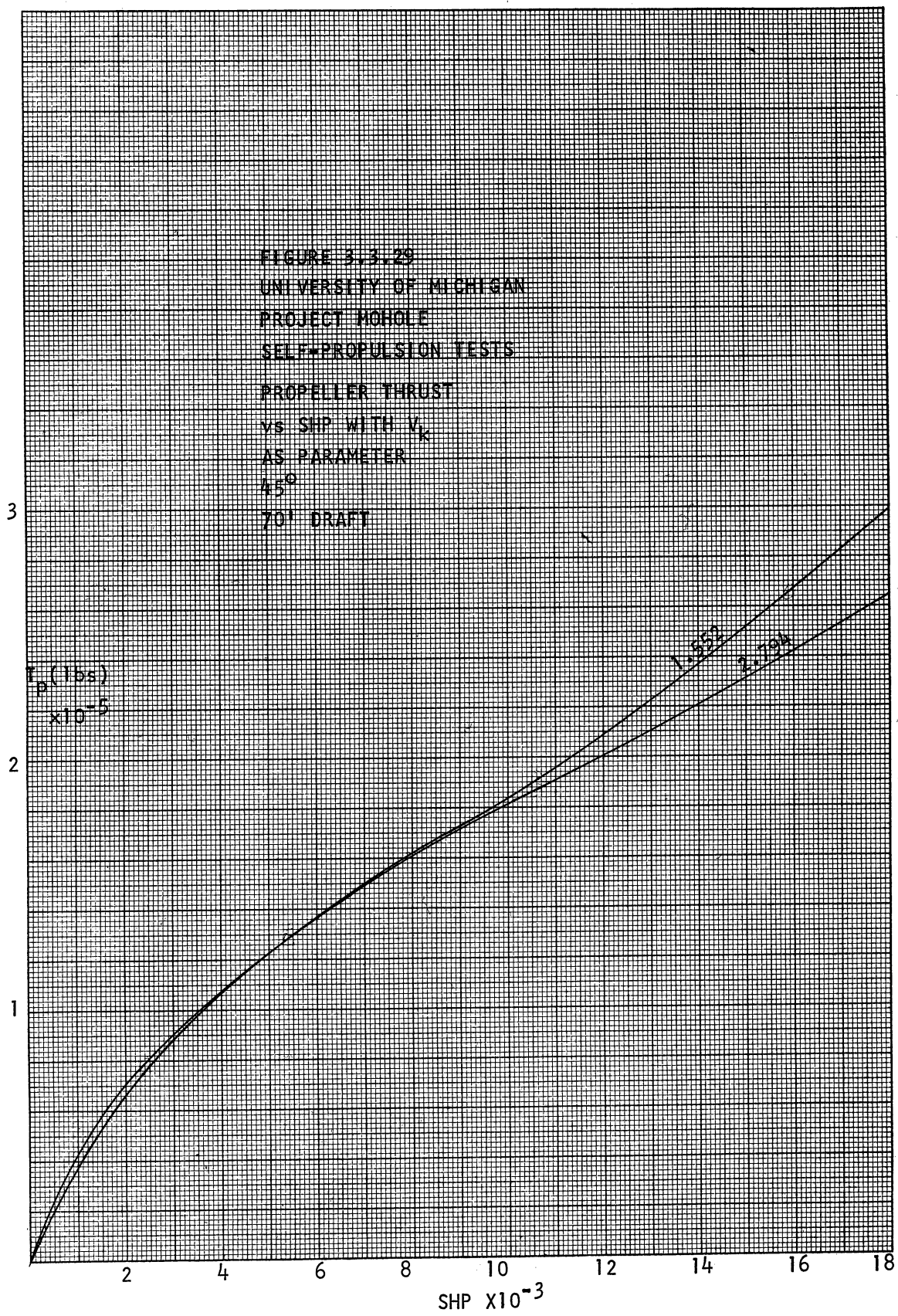
FIGURE 3.3.29
UNIVERSITY OF MICHIGAN
PROJECT MOHOLE
SELF-PROPULSION TESTS
PROPELLER THRUST
vs SHP WITH V_K
AS PARAMETER
45°
70' DRAFT
T_p (lbs)
x10^{-5}
3
2
1
2
4
6
8
10
12
14
16
18
SHP X10^{-3}
V_K = 15.0 kts
V_K = 14.0 kts

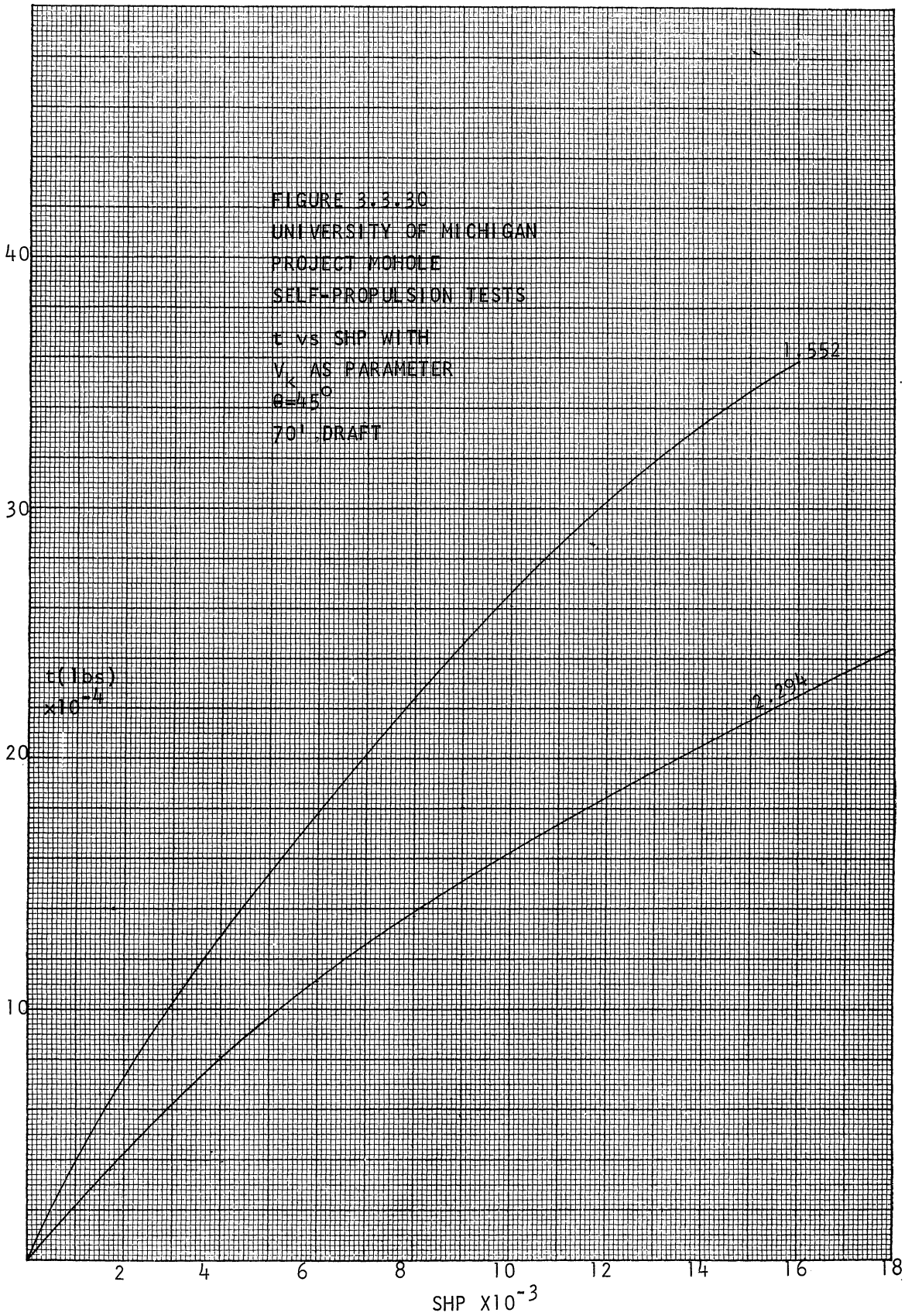
FIGURE 3.3.30
UNIVERSITY OF MICHIGAN
PROJECT MOHOLE
SELF-PROPULSION TESTS
t vs SHP WITH
V_k AS PARAMETER
θ=45°
70' DRAFT
1.552
2.20k
t(lbs)
×10⁻⁴
40
30
20
10
2
4
6
8
10
12
14
16
18
SHP X10⁻³

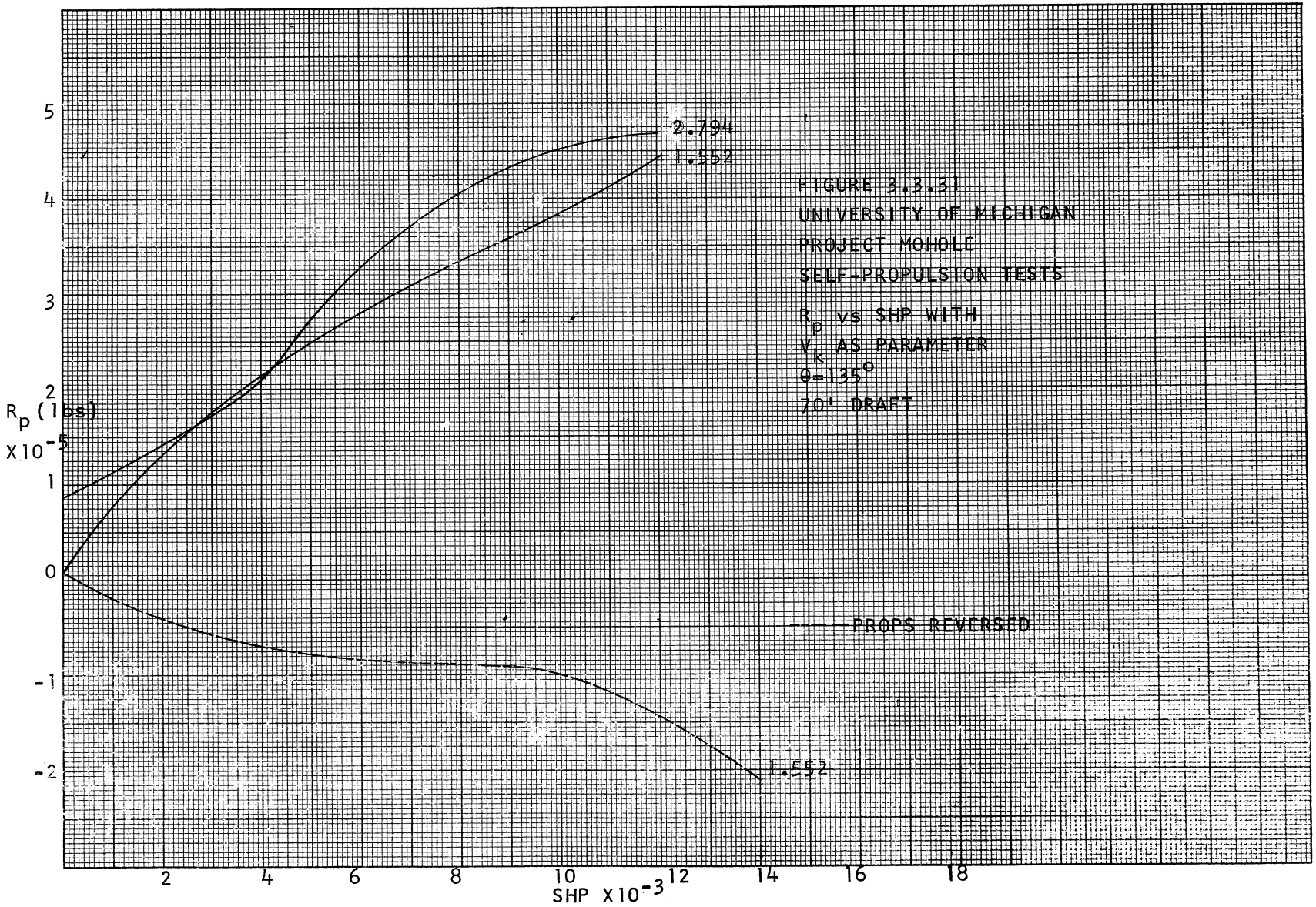

FIGURE 3.3.31
UNIVERSITY OF MICHIGAN
PROJECT MOHOLE
SELF-PROPULSION TESTS

R_p vs SHP WITH
V_K AS PARAMETER
θ=135°
70' DRAFT

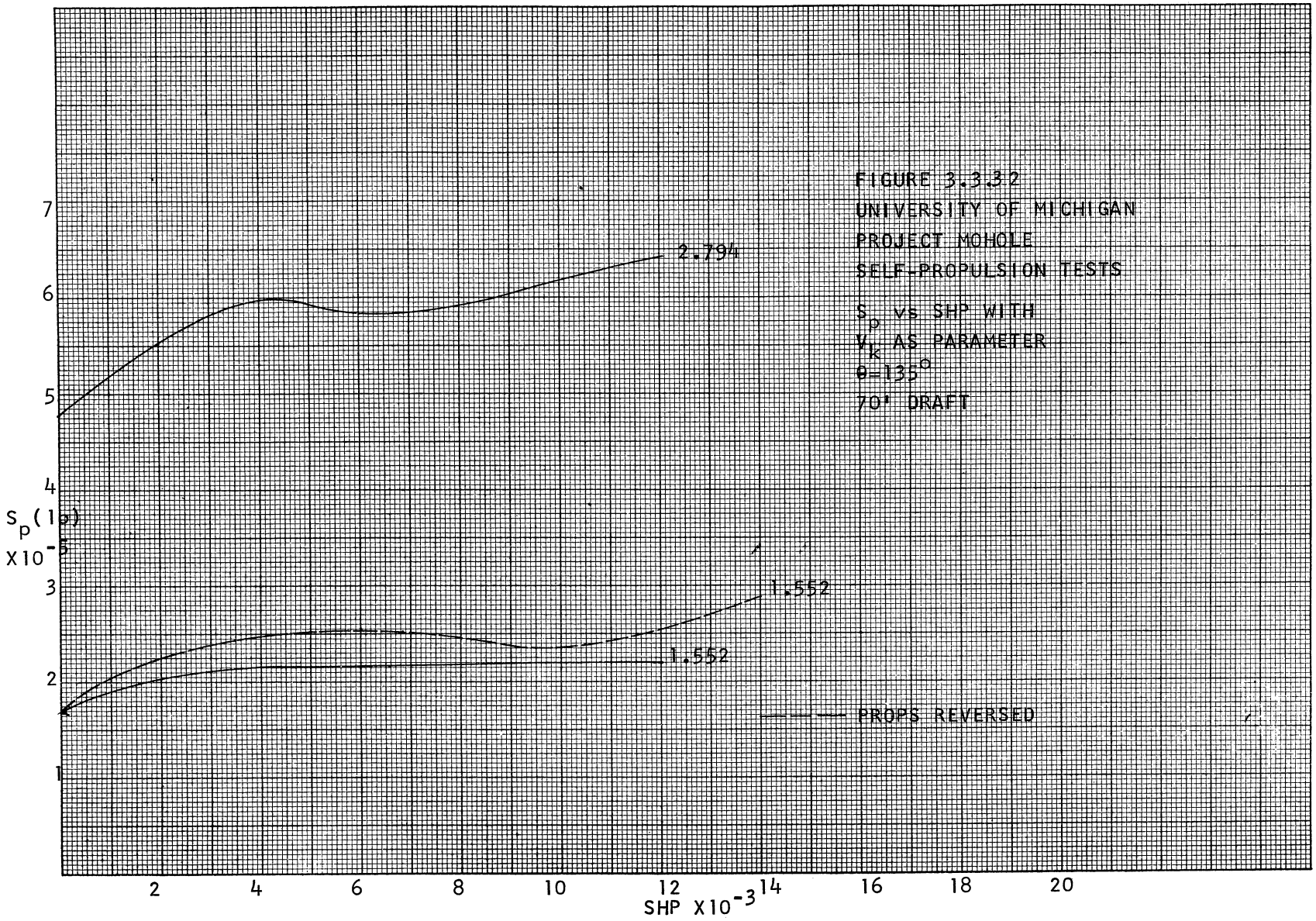
FIGURE 3.3.32
UNIVERSITY OF MICHIGAN
PROJECT MOHOLE
SELF-PROPULSION TESTS
S_p vs SHP WITH
V_k AS PARAMETER
θ=135°
70' DRAFT
2.794
1.552
1.552
PROPS REVERSED
S_p (lb)
X10^{-5}
SHP X10^{-3}
1
2
3
4
5
6
7
2
4
6
8
10
12
14
16
18
20

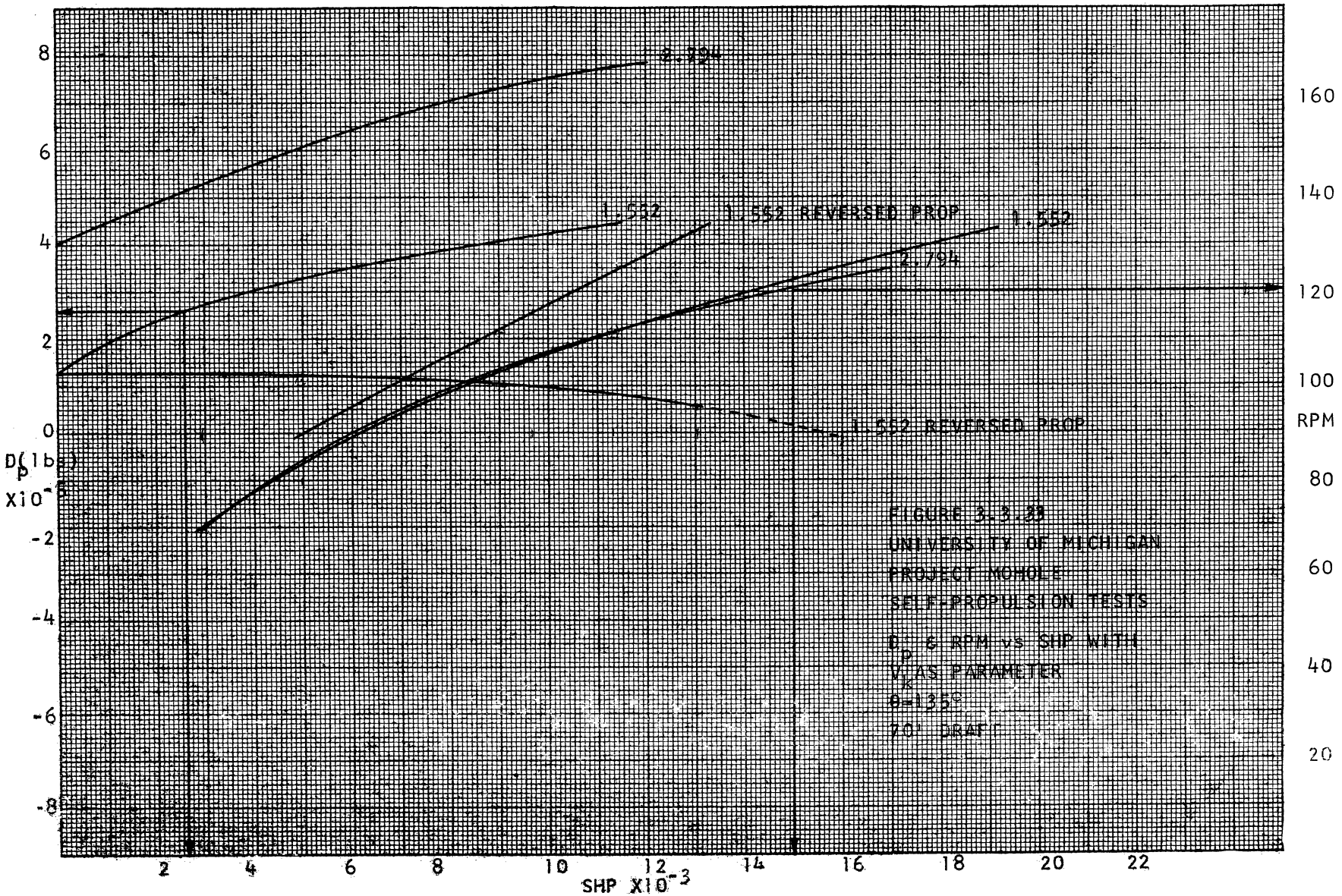
2.794
1.552
1.552 REVERSED PROP
1.552
2.794
1.552 REVERSED PROP
8
6
4
2
0
-2
-4
-6
-8
160
140
120
100
RPM
80
60
40
20
2
4
6
8
10
12
14
16
18
20
22
SHP X10-3
D(lbs)
X10-3
FIGURE 3.3.23
UNIVERSITY OF MICHIGAN
PROJECT NOHOLE
SELF-PROPULSION TESTS
δp & RPM vs SHP WITH
Vk AS PARAMETER
θ=135°
70' DRAFT

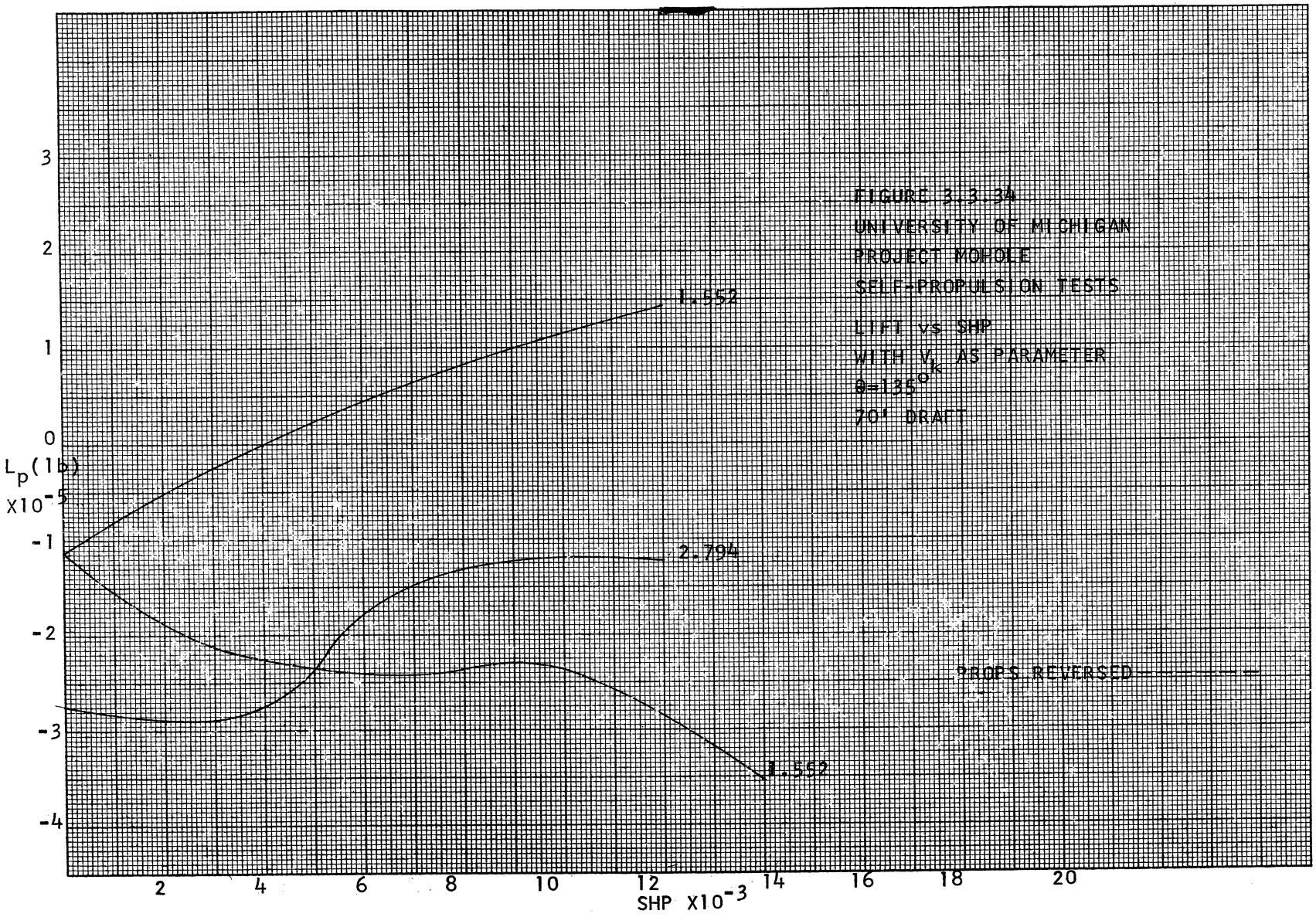
FIGURE 3.3.34
UNIVERSITY OF MICHIGAN
PROJECT MOHOLE
SELF-PROPULSION TESTS
LIFT vs SHP
WITH V_k AS PARAMETER
θ=135°
70' DRAFT
1.552
2.794
1.552
PROPS REVERSED
L_p (lb)
X10^{-5}
SHP X10^{-3}
3
2
1
0
-1
-2
-3
-4
2
4
6
8
10
12
14
16
18
20

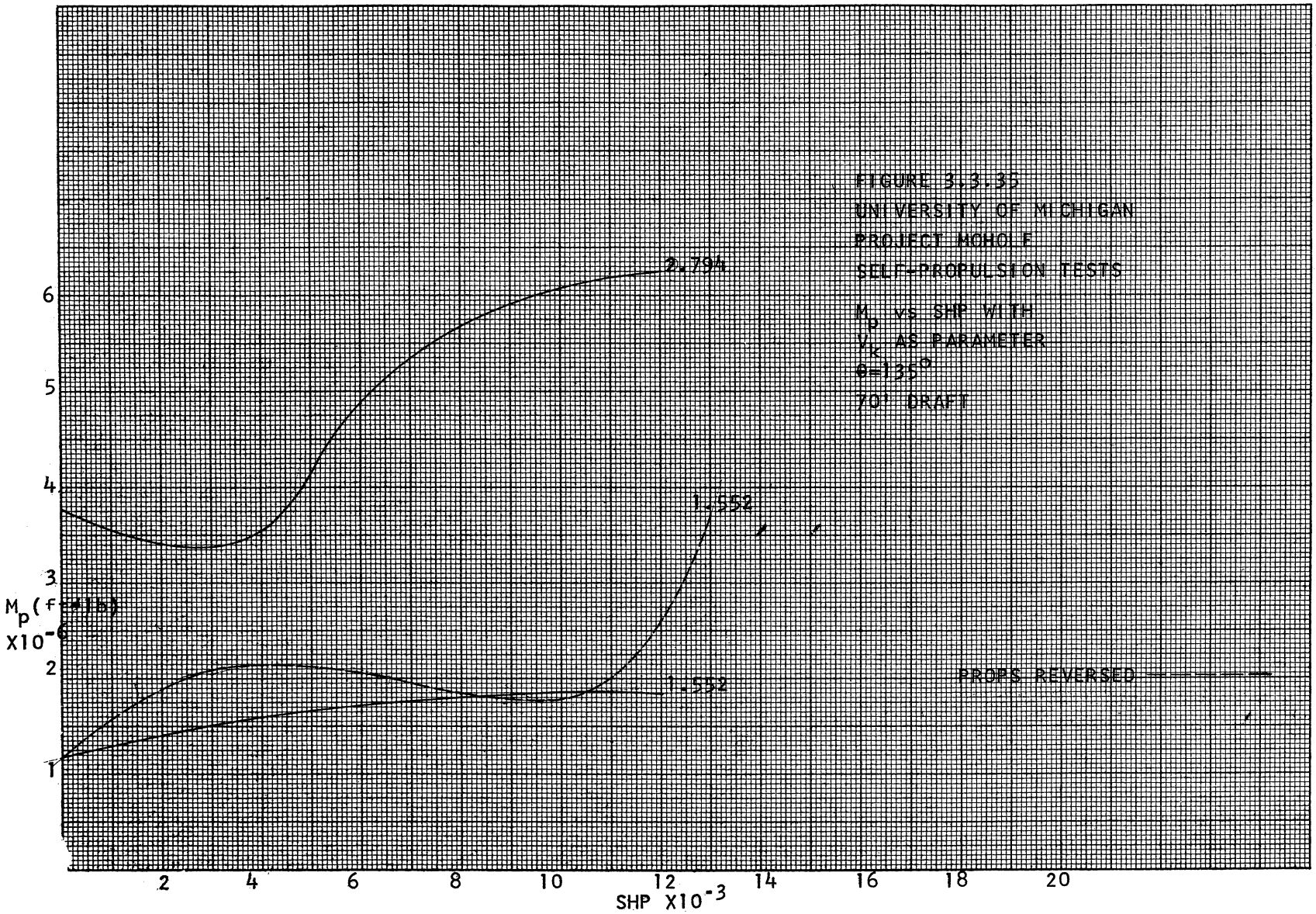
FIGURE 3.3.35
UNIVERSITY OF MICHIGAN
PROJECT MOHOLE
SELF-PROPULSION TESTS
M_p vs SHP WITH
V_K AS PARAMETER
θ=135°
70' DRAFT
2.794
1.552
1.552
PROPS REVERSED
M_p (ft-lbs)
X10^{-6}
SHP X10^{-3}
1
2
3
4
5
6
2
4
6
8
10
12
14
16
18
20

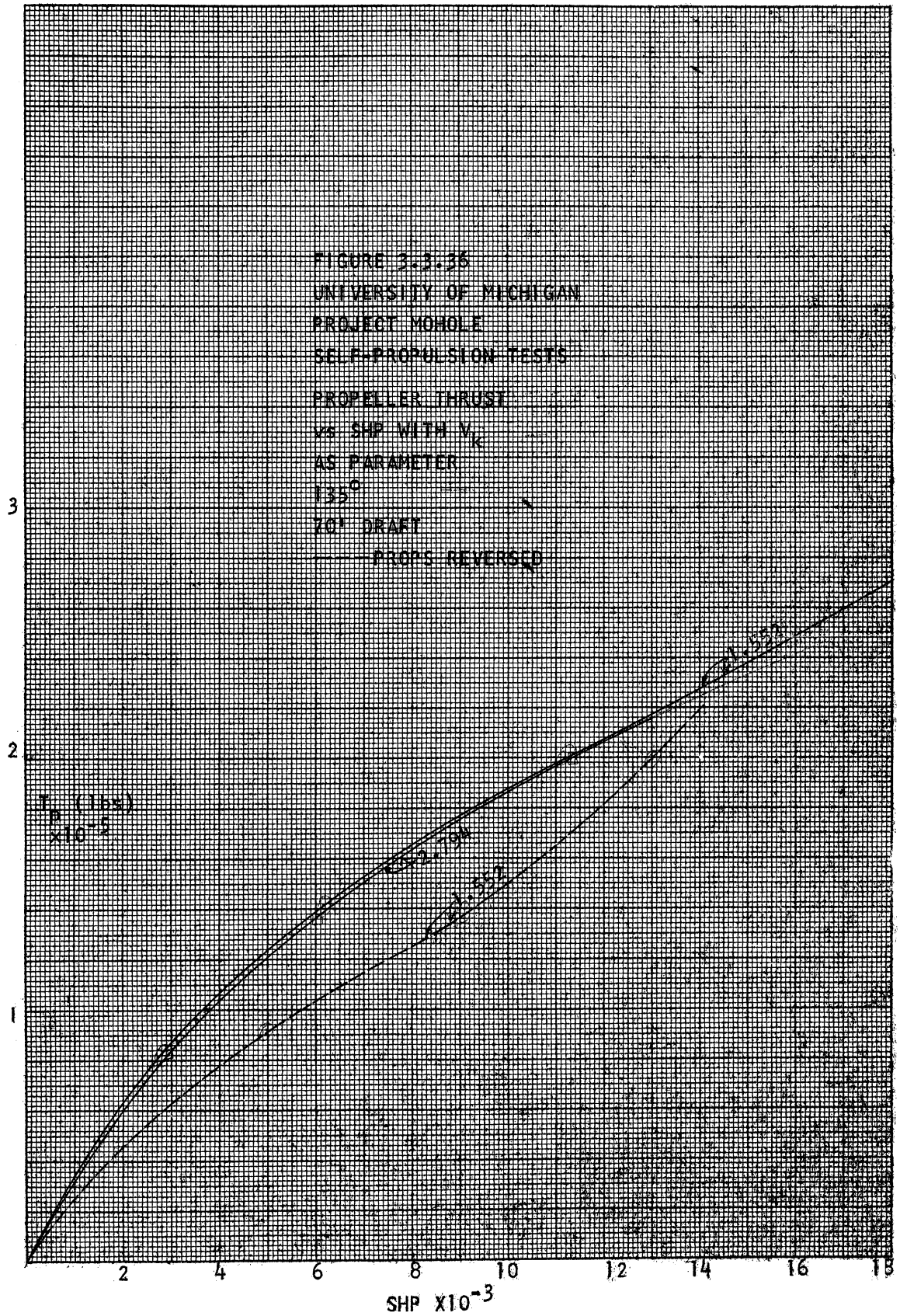
FIGURE 3.3.36
UNIVERSITY OF MICHIGAN
PROJECT MOHOLE
SELF-PROPULSION TESTS
PROPELLER THRUST
vs SHP WITH V_K
AS PARAMETER
135°
20' DRAFT
----PROPS REVERSED
T_P (lbs)
$\times 10^{-5}$
SHP $X10^{-3}$
1
2
3
2
4
6
8
10
12
14
16
18

FIGURE 3.3.37

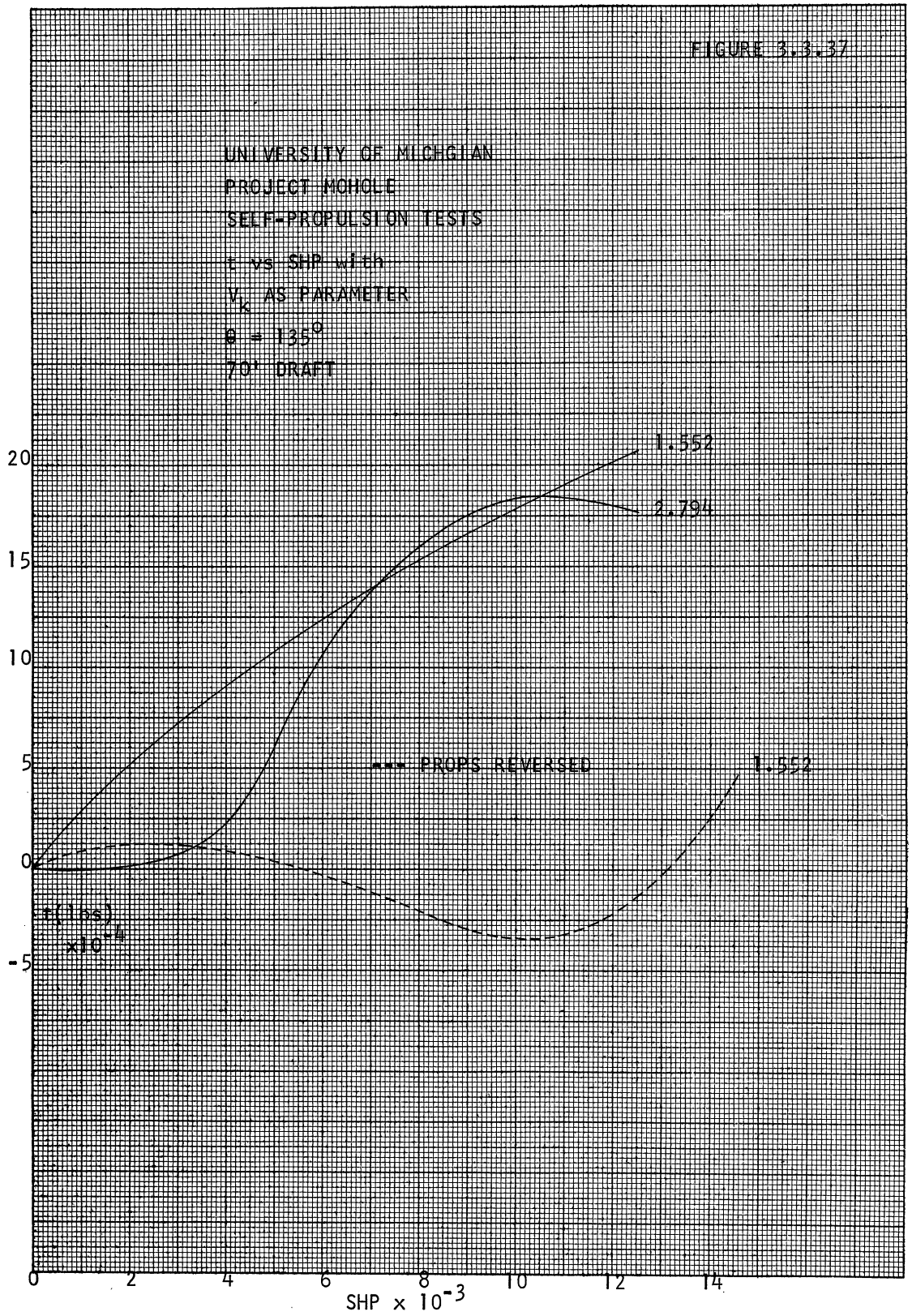
UNIVERSITY OF MICHIGAN
PROJECT MOHOLE
SELF-PROPULSION TESTS
τ vs SHP with
V_k AS PARAMETER
θ = 135°
70' DRAFT
1.552
2.794
--- PROPS REVERSED
1.552
20
15
10
5
0
-5
τ(lbs)
×10⁻⁴
0
2
4
6
8
10
12
14
SHP x 10⁻³

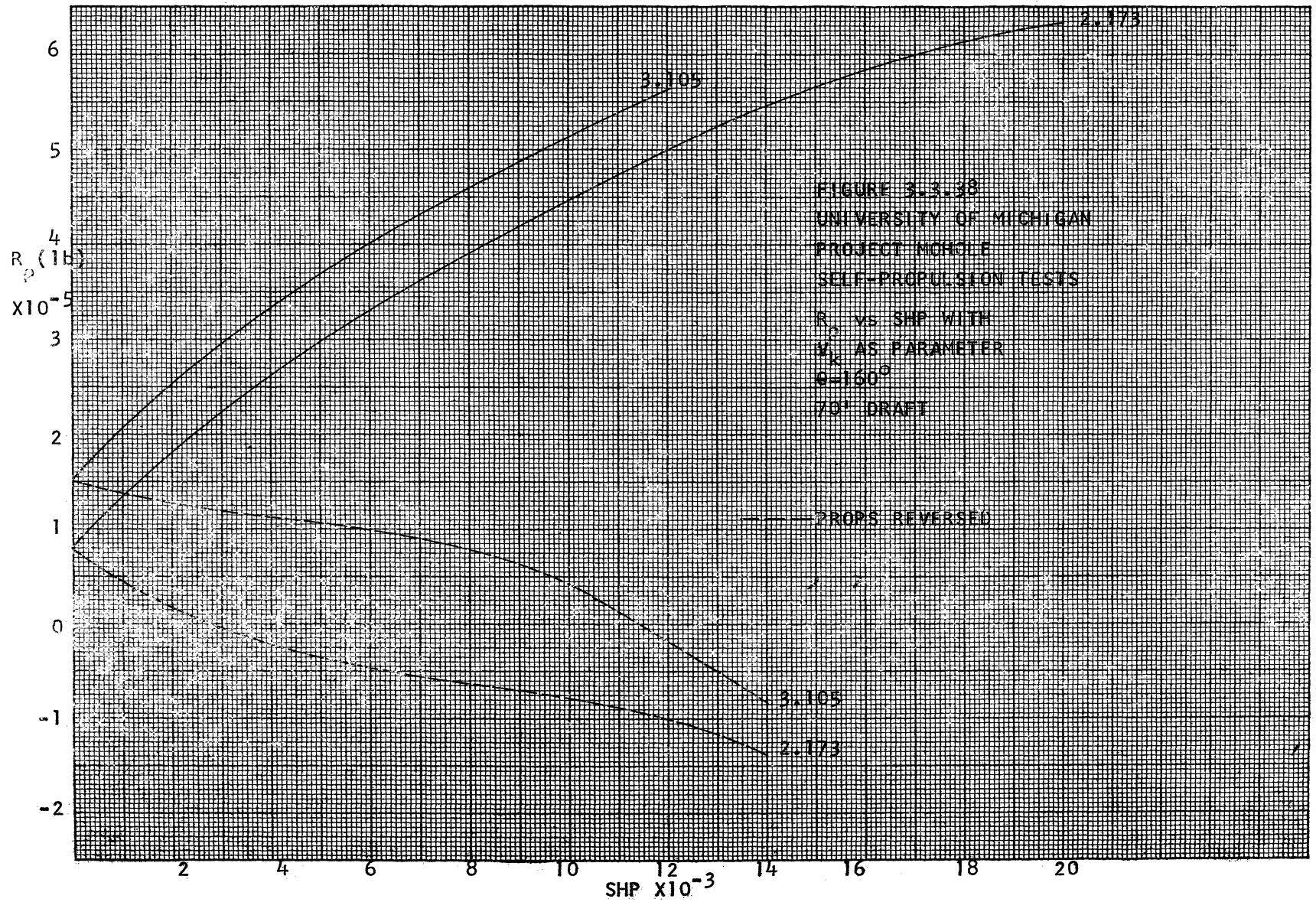
FIGURE 5.3.38
UNIVERSITY OF MICHIGAN
PROJECT MOHOLE
SELF-PROPULSION TESTS
R_o vs SHP WITH
V_k AS PARAMETER
θ=160°
70' DRAFT
PROPS REVERSED
2.173
3.105
3.105
2.173
R_o (lb)
X10^{-5}
SHP X10^{-3}
6
5
4
3
2
1
0
-1
-2
2
4
6
8
10
12
14
16
18
20

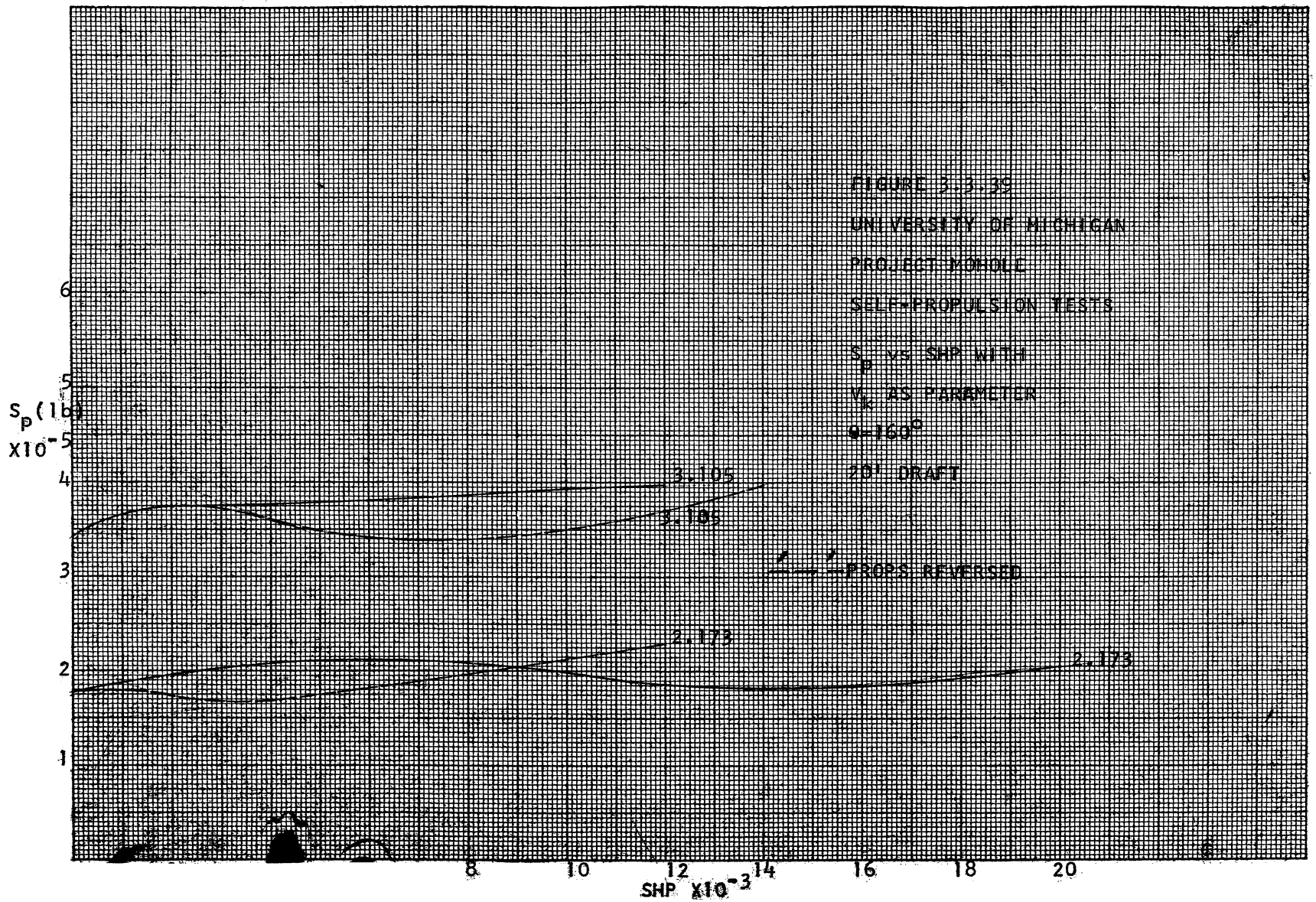
FIGURE 3.3.35
UNIVERSITY OF MICHIGAN
PROJECT MARIOLE
SELF-PROPULSION TESTS
S_p VS SHP WITH
V_K AS PARAMETER
ϕ=160°
20' DRAFT
PROPS REVERSED
S_p (lb)
X10^{-5}
SHP X10^{-3}
3.105
3.105
2.173
2.173
1
2
3
4
5
6
8
10
12
14
16
18
20

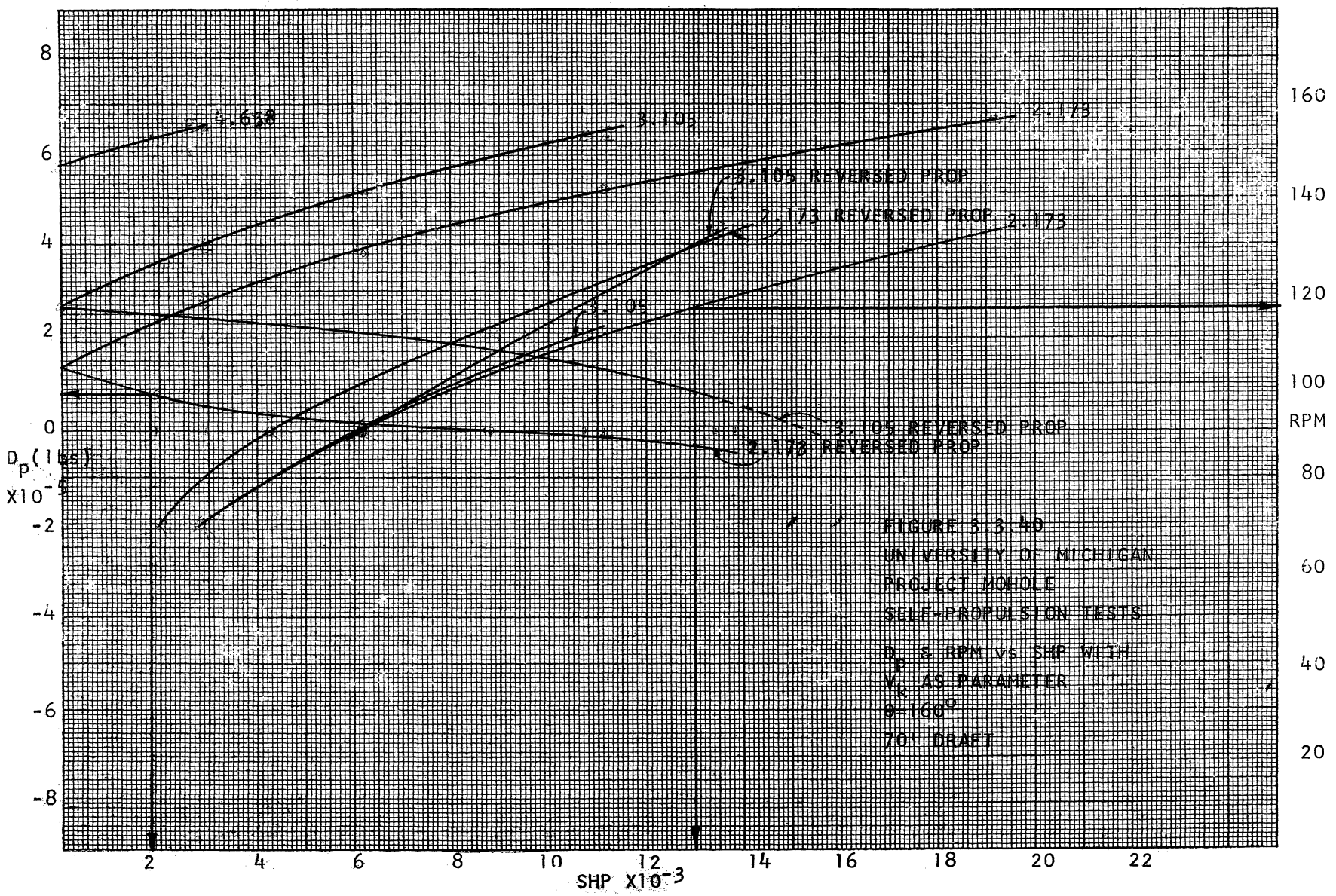

FIGURE 3.3.40
UNIVERSITY OF MICHIGAN
PROJECT MOHOLE
SELF-PROPULSION TESTS
D_p & RPM vs SHP WITH
V_k AS PARAMETER
θ=160°
70' DRAFT

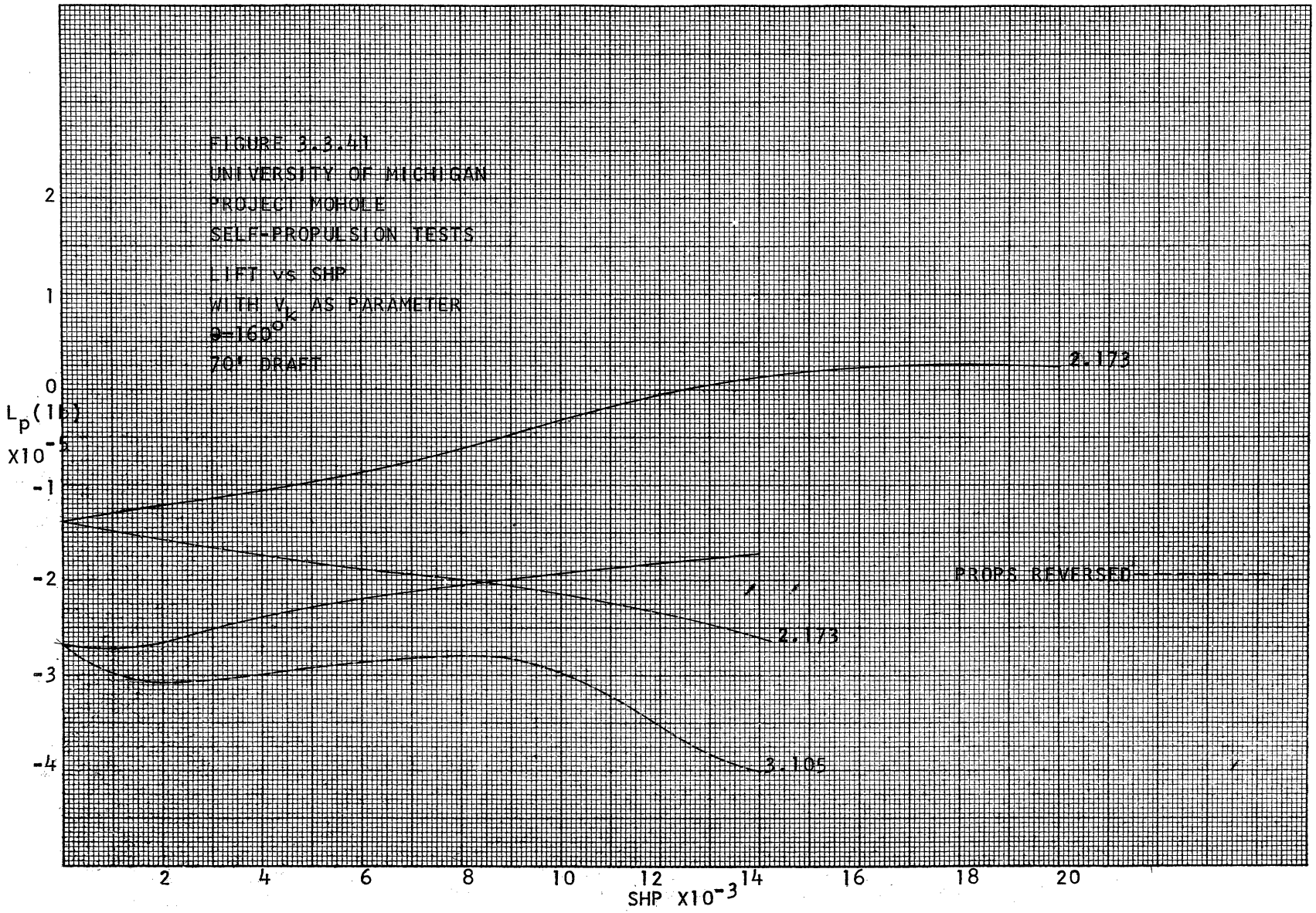
FIGURE 3.3.41
UNIVERSITY OF MICHIGAN
PROJECT MOHOLE
SELF-PROPULSION TESTS
LIFT vs SHP
WITH V_k AS PARAMETER
θ=160°
70' DRAFT
L_p(LB)
X10^{-3}
2
1
0
-1
-2
-3
-4
2.173
PROPS REVERSED
2.173
3.105
2
4
6
8
10
12
14
16
18
20
SHP X10^{-3}

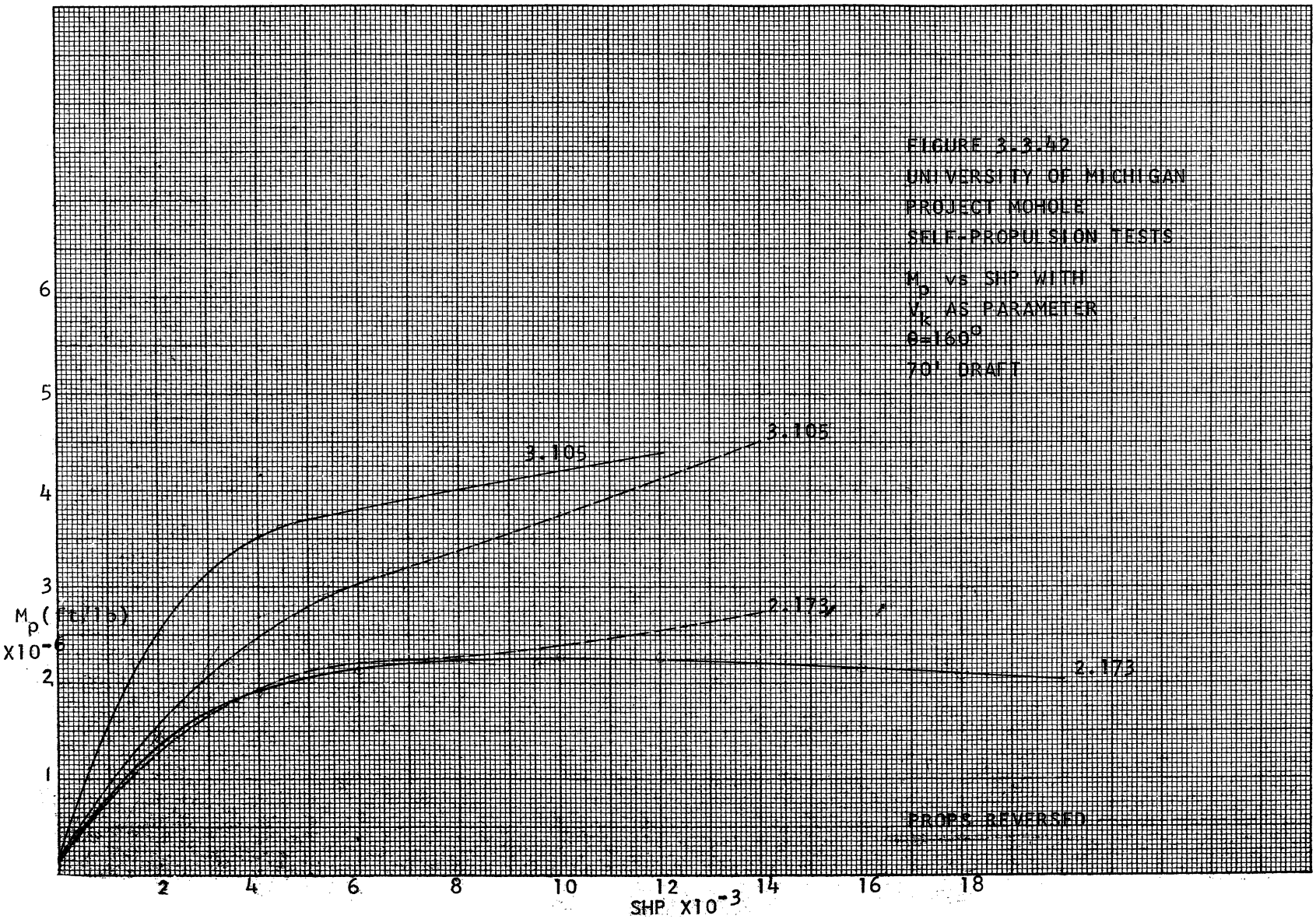
FIGURE 3.3.42
UNIVERSITY OF MICHIGAN
PROJECT MOHOLE
SELF-PROPULSION TESTS
M_p vs SHP WITH
V_k AS PARAMETER
θ=160°
70' DRAFT
3.105
3.105
2.173
2.173
PROPS REVERSED
M_p (ft.lb) X10^{-6}
SHP X10^{-3}
1
2
3
4
5
6
2
4
6
8
10
12
14
16
18

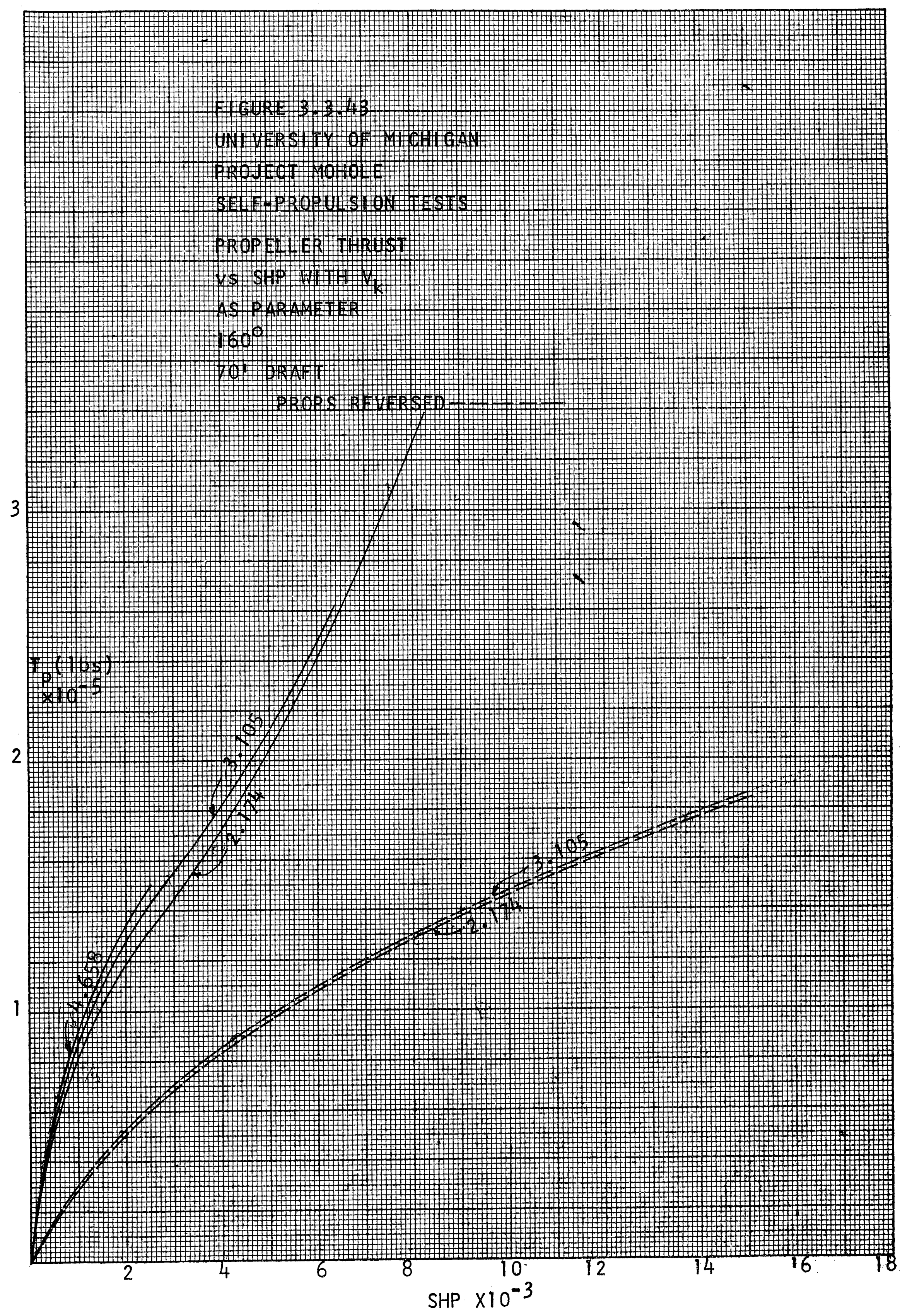
FIGURE 3.3.43
UNIVERSITY OF MICHIGAN
PROJECT MOHOLE
SELF-PROPULSION TESTS
PROPELLER THRUST
vs SHP WITH V_k
AS PARAMETER
160°
70' DRAFT
PROPS REVERSED
T_p (lbs)
x10^{-5}
3
2
1
3.105
2.174
4.658
3.105
2.174
2
4
6
8
10
12
14
16
18
SHP X10^{-3}

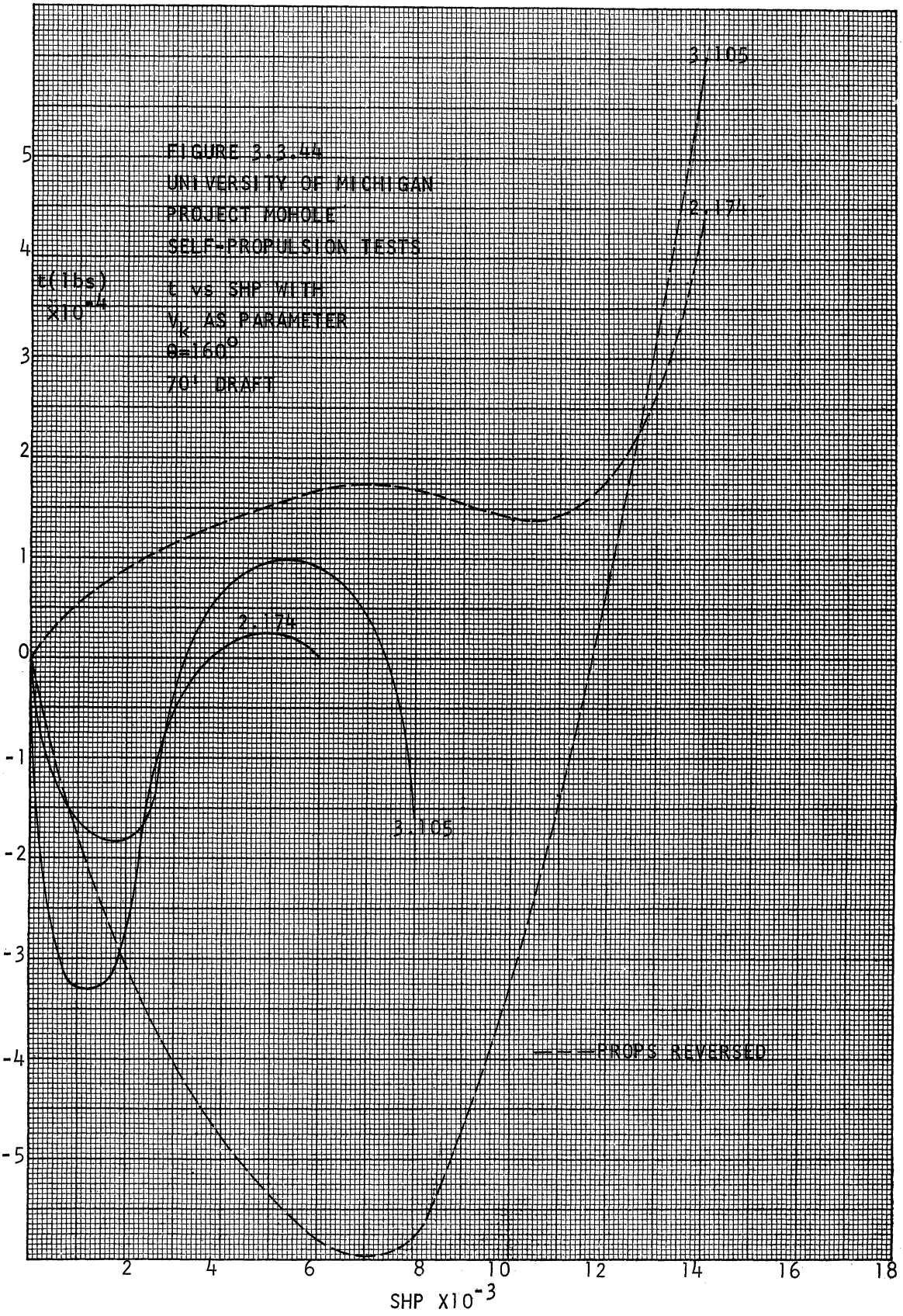
FIGURE 3.3.44
UNIVERSITY OF MICHIGAN
PROJECT MOHOLE
SELF-PROPULSION TESTS
t vs SHP WITH
V_k AS PARAMETER
θ=160°
70' DRAFT
t(lbs) X10**4
SHP X10**-3
3,105
2,174
2,174
3,105
———PROPS REVERSED
5
4
3
2
1
0
-1
-2
-3
-4
-5
2
4
6
8
10
12
14
16
18

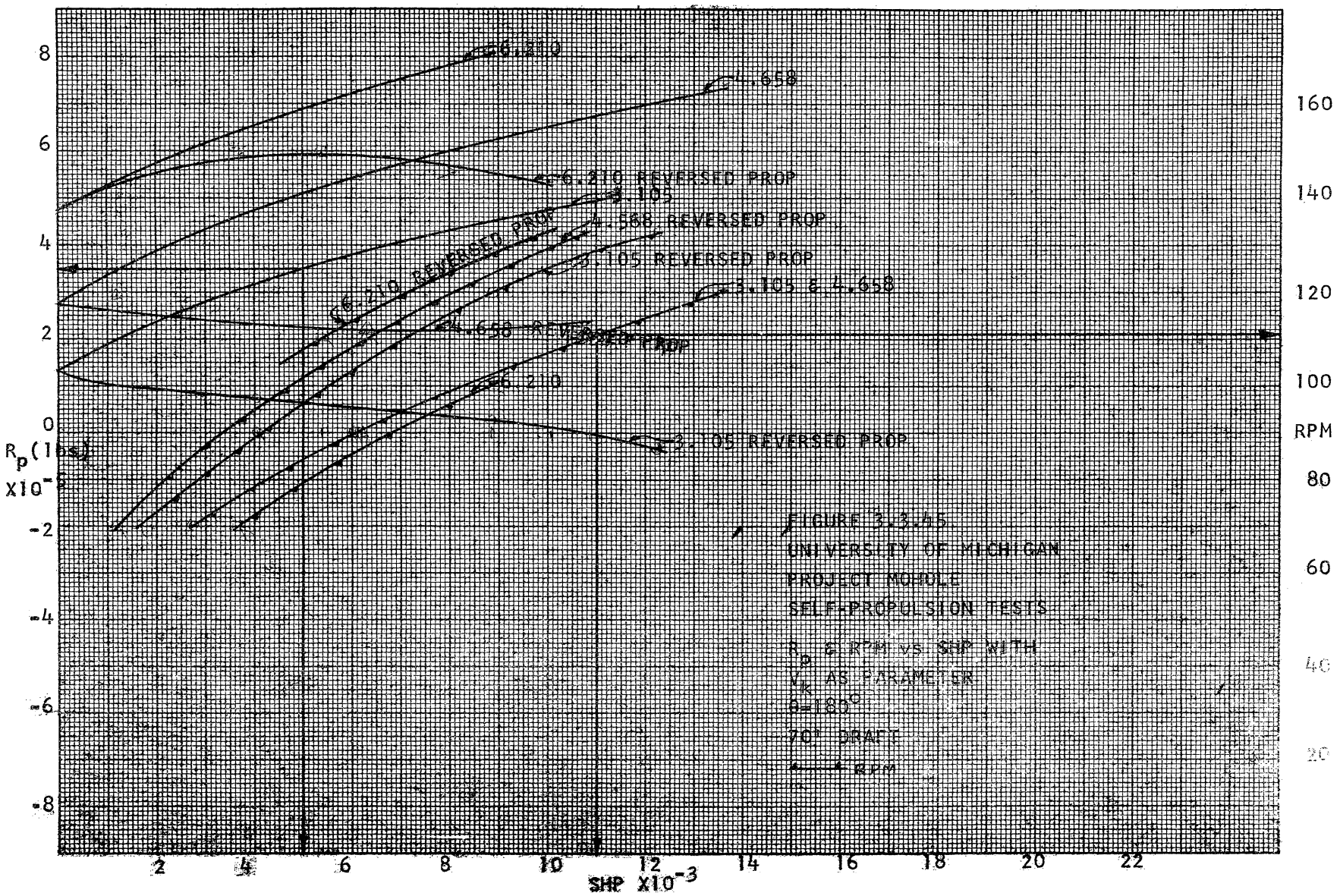
6.210
4.658
6.210 REVERSED PROP
3.105
4.658 REVERSED PROP
3.105 REVERSED PROP
3.105 & 4.658
6.210
3.105 REVERSED PROP
8
6
4
2
0
-2
-4
-6
-8
R_p (lbs) X10^{-3}
2
4
6
8
10
12
14
16
18
20
22
SHP X10^{-3}
160
140
120
100
RPM
80
60
40
20
FIGURE 3.3.45
UNIVERSITY OF MICHIGAN
PROJECT MARIOLE
SELF-PROPULSION TESTS
R_p & RPM vs SHP WITH
V_K AS PARAMETER
θ=180°
70' DRAFT
RPM

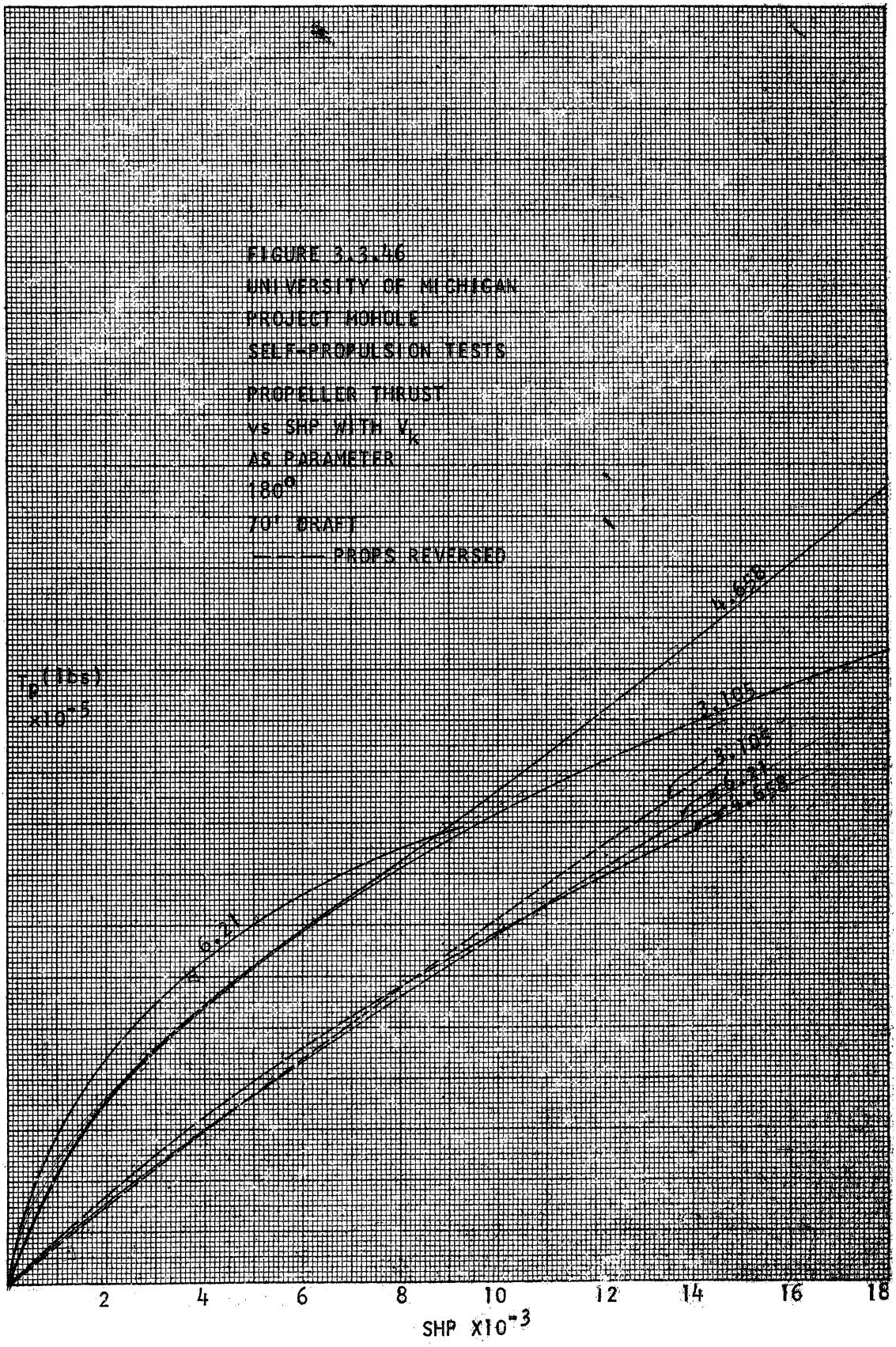
FIGURE 3.3.26
UNIVERSITY OF MICHIGAN
PROJECT NOHOLE
SELF-PROPULSION TESTS
PROPELLER THRUST
VS SHP WITH V_K
AS PARAMETER
180°
70' DRAFT
PROPS REVERSED
T_P (lbs)
$\times 10^{-5}$
SHP $\times 10^{-3}$
1
2
3
2
4
6
8
10
12
14
16
18

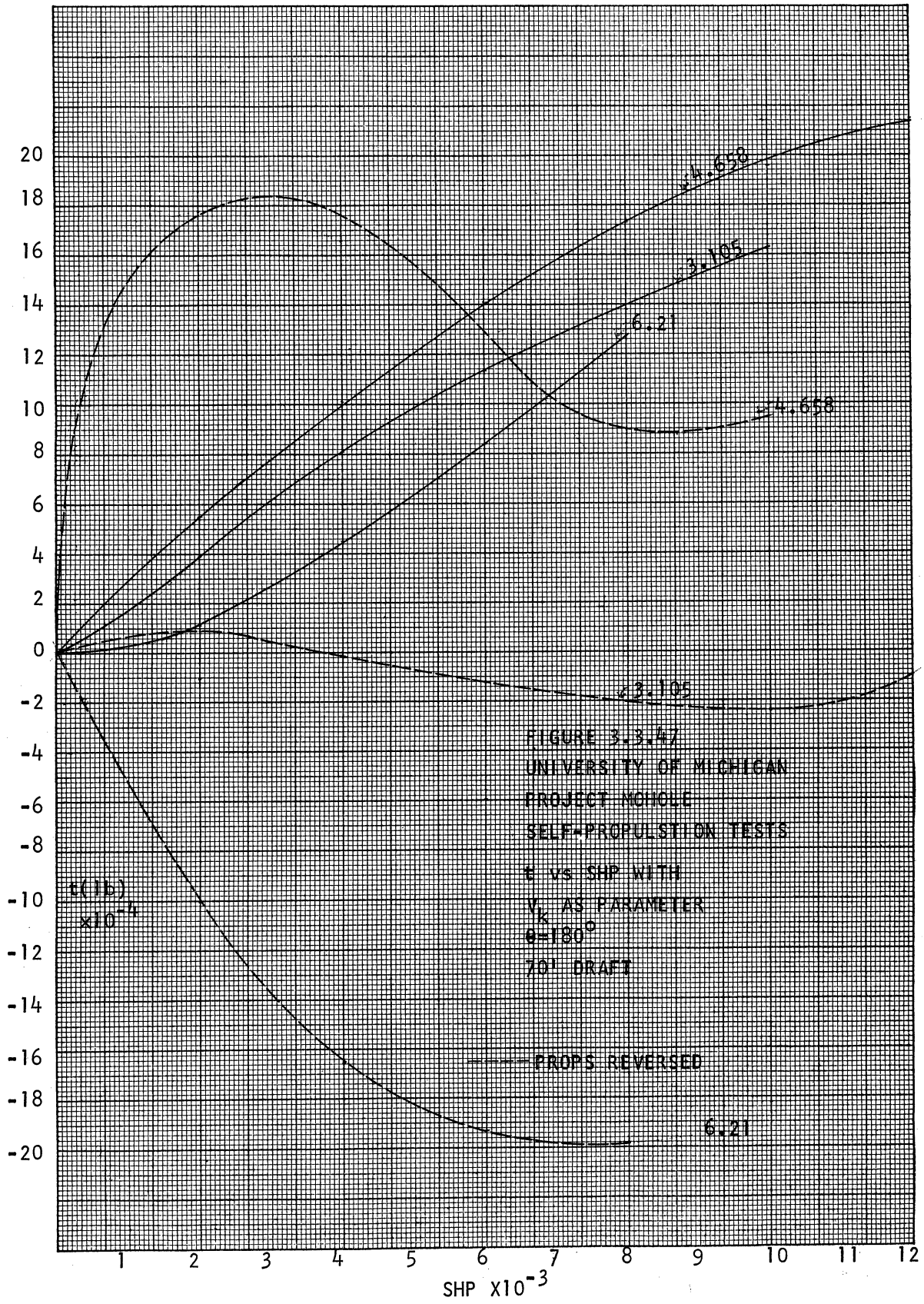
20
18
16
14
12
10
8
6
4
2
0
-2
-4
-6
-8
-10
-12
-14
-16
-18
-20
t(lb)
x10⁻⁴
1
2
3
4
5
6
7
8
9
10
11
12
SHP X10⁻³
4.658
3.105
6.21
4.658
3.105
6.21
FIGURE 3.3.47
UNIVERSITY OF MICHIGAN
PROJECT NOHOLE
SELF-PROPULSTION TESTS
t vs SHP WITH
Vk AS PARAMETER
θ=180°
70' DRAFT
---PROPS REVERSED

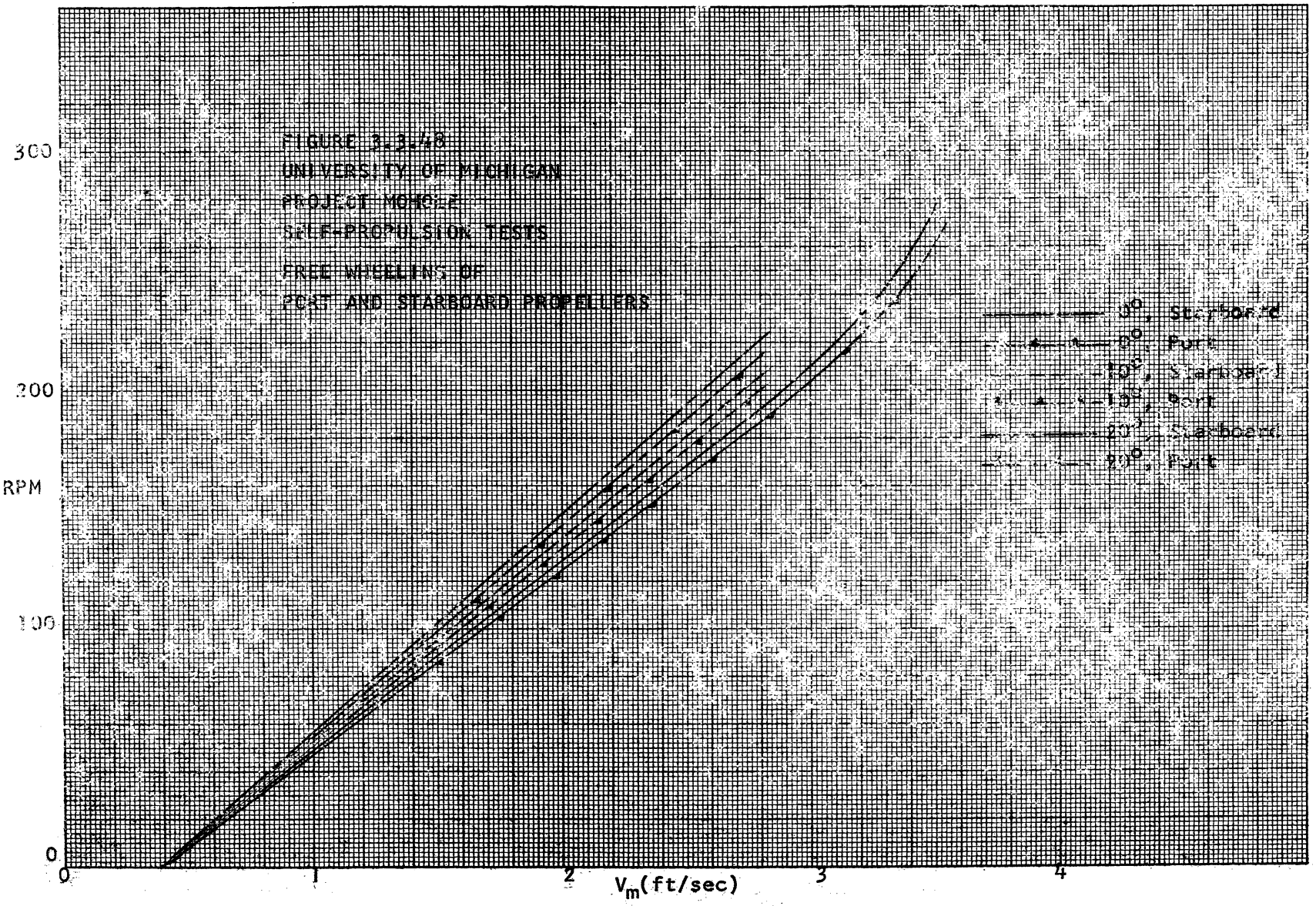
FIGURE 3.3.48
UNIVERSITY OF MICHIGAN
PROJECT MONOCLE
SELF-PROPULSION TESTS
FREE WHEELING OF
PORT AND STARBOARD PROPELLERS
0°, Starboard
0°, Port
10°, Starboard
10°, Port
20°, Starboard
20°, Port
300
200
100
0
RPM
0
1
2
3
4
V_m(ft/sec)

RESULTS OF BOLLARD PULL TESTS

V_k = 1.0 knots

28' Draft

Angle; °	RPM	SHPx10^{-3}	D_px10^{-5}	L_px10^{-5}	R_px10^{-5}	S_px10^{-5}	M_px10^{-6}
0	131.35	16.874	-5.095	0	-5.095	0	0
20	127.19	16.616	----	----	----	----	----
45	131.00	16.462	-3.348	3.868	-5.103	.368	1.716
135	127.38	16.696	4.305	2.912	2.460	.468	12.582
160	127.00	15.926	5.075	- .562	4.577	2.263	- 2.574
180	129.75	16.684	5.407	0	5.407	0	0

70' Draft

Angle; °	RPM	SHPx10^{-3}	D_px10^{-5}	L_px10^{-5}	R_px10^{-5}	S_px10^{-5}	M_px10^{-6}
0	132.72	18.116	-5.165	0	-5.165	0	0
20	132.72	18.201	-4.640	1.851	-4.991	.153	3.717
45	132.72	18.901	-2.912	4.388	-5.162	1.044	5.433
135	132.72	18.620	4.534	3.182	5.456	.956	7.721
135 Rev.	132.72	15.623	- .312	-2.724	-2.147	1.706	23.735
160	132.72	18.543	5.511	.957	5.506	.986	7.435
160 Rev.	132.72	14.676	-1.456	-1.270	-1.788	.655	8.865
180	128.26	16.414	5.345	0	5.345	0	0
180 Rev.	127.57	12.523	-1.581	0	-1.581	0	0

Fig. 3.3.49

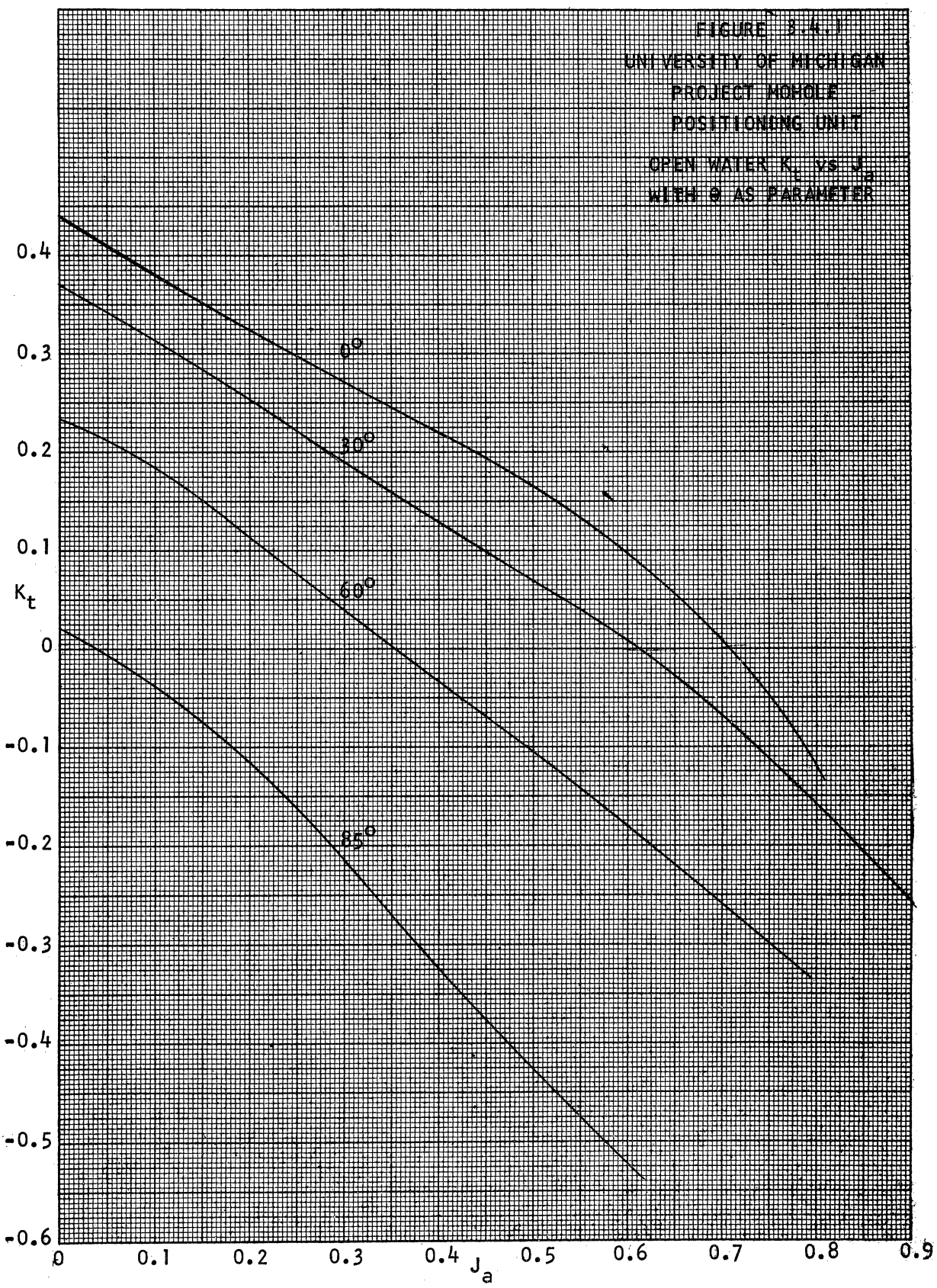
FIGURE 3.4.7
UNIVERSITY OF MICHIGAN
PROJECT MOHOLE
POSITIONING UNIT
OPEN WATER K_t vs J_a
WITH θ AS PARAMETER
0.4
0.3
0.2
0.1
K_t
0
-0.1
-0.2
-0.3
-0.4
-0.5
-0.6
0°
30°
60°
85°
0
0.1
0.2
0.3
0.4
J_a
0.5
0.6
0.7
0.8
0.9

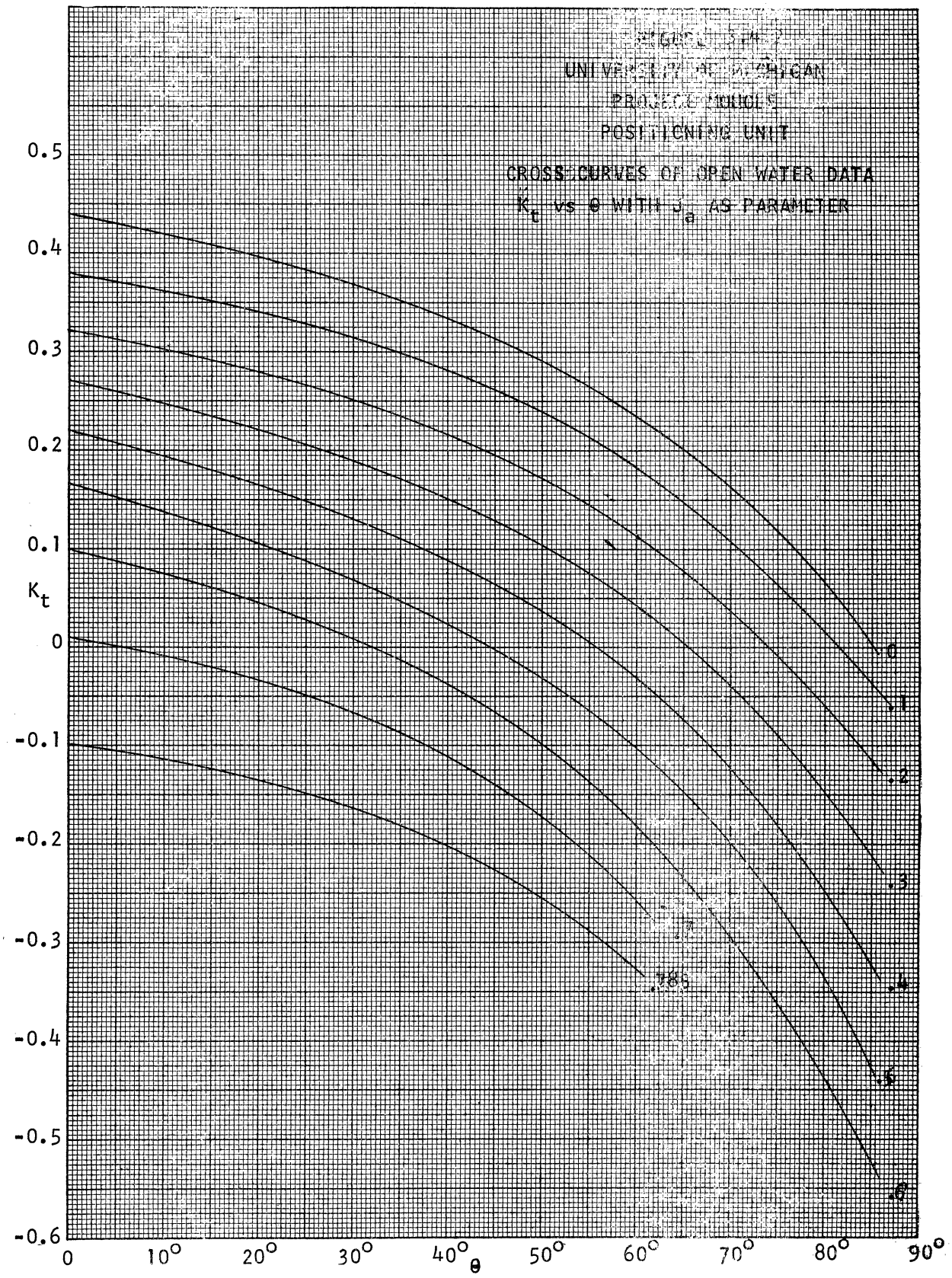
UNIVERSITY OF MICHIGAN
PROJECT TORQUE
POSITIONING UNIT
CROSS CURVES OF OPEN WATER DATA
K_t vs θ WITH J_a AS PARAMETER
0.5
0.4
0.3
0.2
0.1
K_t
0
-0.1
-0.2
-0.3
-0.4
-0.5
-0.6
0
10°
20°
30°
40°
θ
50°
60°
70°
80°
90°
.0
.1
.2
.3
.4
.5
.6

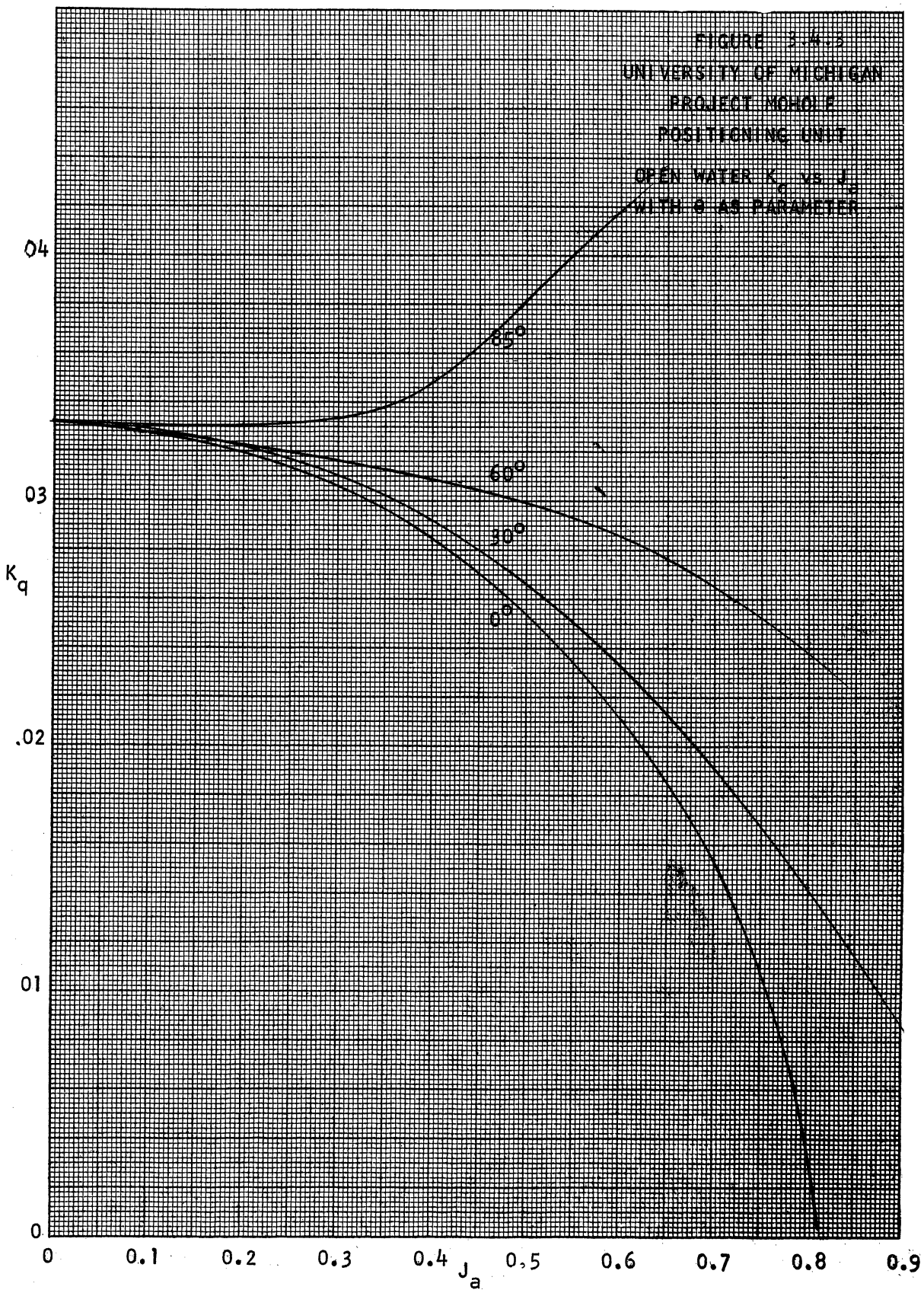
FIGURE 3.4.3
UNIVERSITY OF MICHIGAN
PROJECT MOHOLE
POSITIONING UNIT
OPEN WATER K_q vs J_a
WITH θ AS PARAMETER
.04
.03
.02
.01
0
K_q
85°
60°
30°
0°
0
0.1
0.2
0.3
0.4
J_a
0.5
0.6
0.7
0.8
0.9

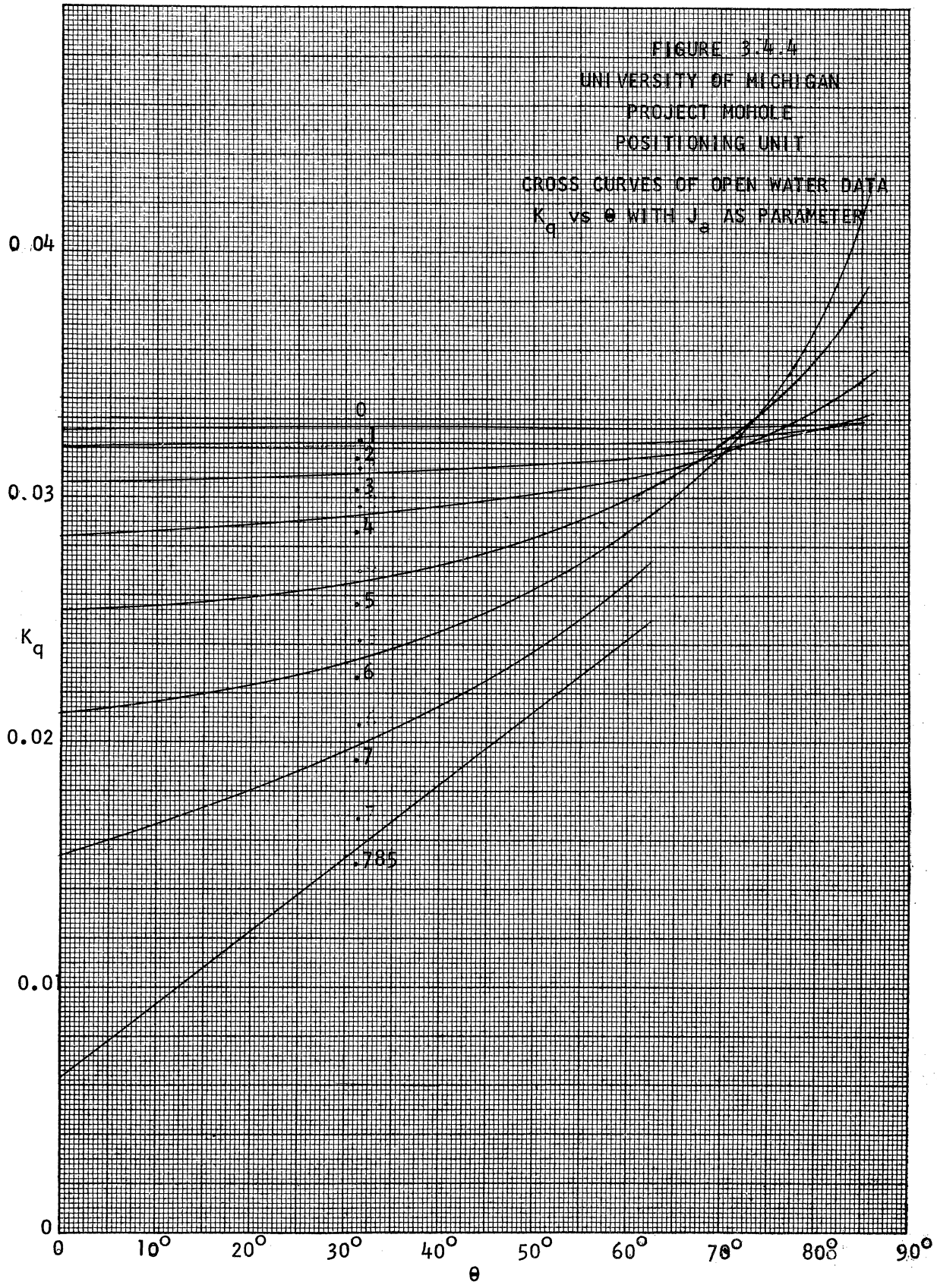
FIGURE 3.4.4
UNIVERSITY OF MICHIGAN
PROJECT MOHOLE
POSITIONING UNIT
CROSS CURVES OF OPEN WATER DATA
K_q vs θ WITH J_a AS PARAMETER
0.04
0.03
0.02
0.01
0
K_q
0
.1
.2
.3
.4
.5
.6
.7
.785
0
10°
20°
30°
40°
50°
60°
70°
80°
90°
θ

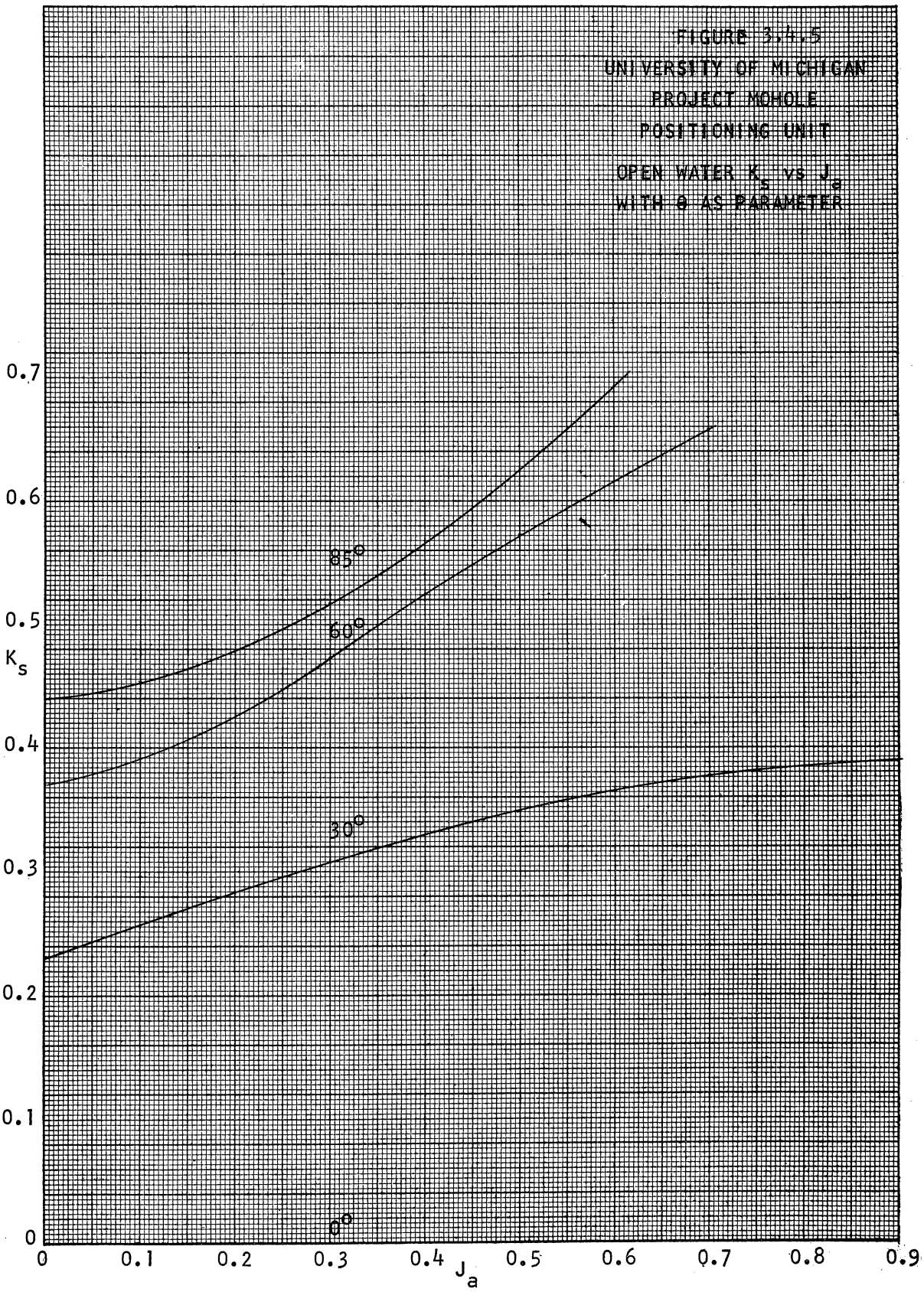
FIGURE 3.4.5
UNIVERSITY OF MICHIGAN
PROJECT MOHOLE
POSITIONING UNIT
OPEN WATER K_s vs J_a
WITH θ AS PARAMETER
0.7
0.6
0.5
K_s
0.4
0.3
0.2
0.1
0
85°
60°
30°
0°
0
0.1
0.2
0.3
0.4
J_a
0.5
0.6
0.7
0.8
0.9

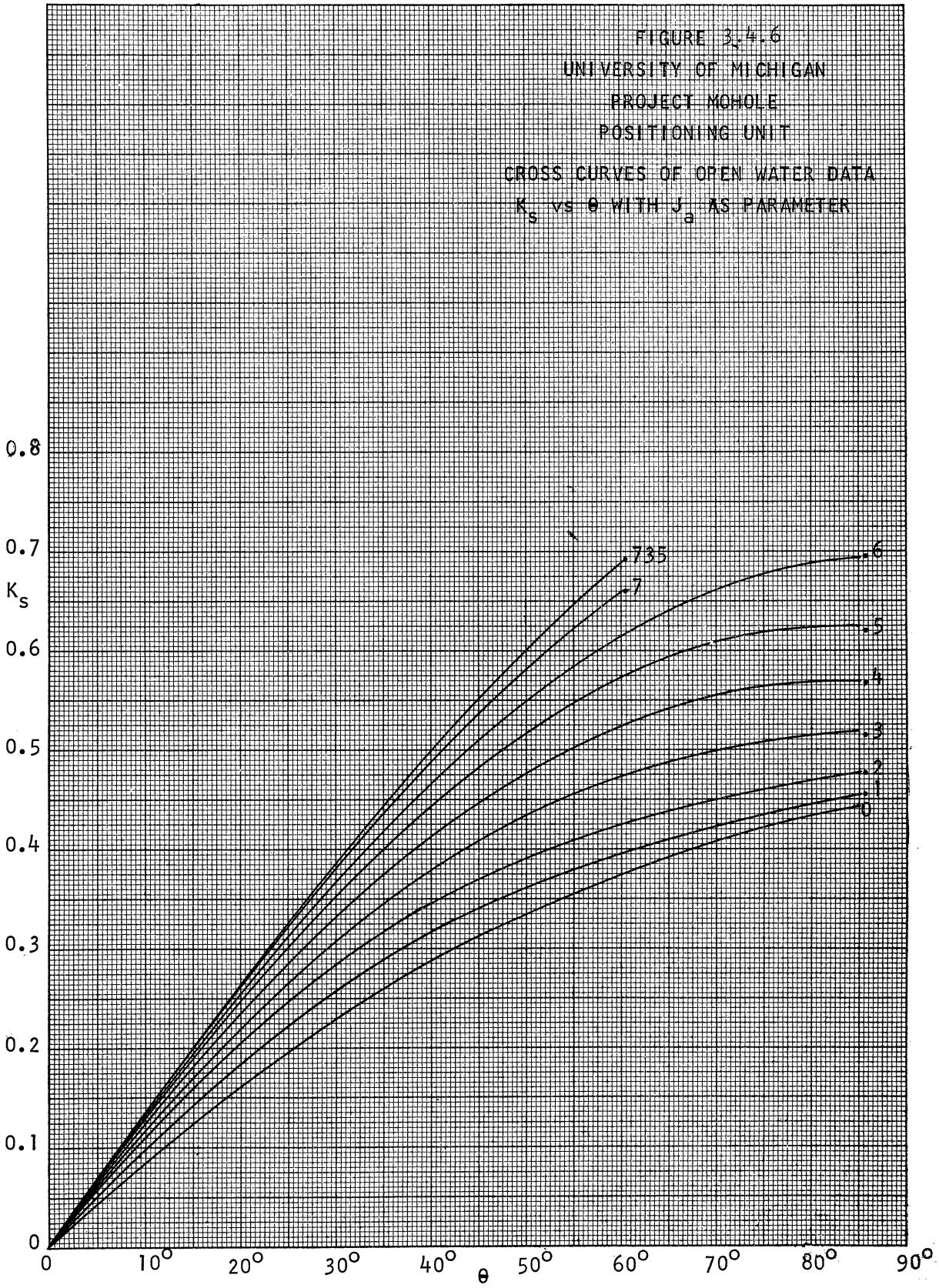
FIGURE 3.4.6
UNIVERSITY OF MICHIGAN
PROJECT MOHOLE
POSITIONING UNIT
CROSS CURVES OF OPEN WATER DATA
K_s vs θ WITH J_a AS PARAMETER
0.8
0.7
K_s
0.6
0.5
0.4
0.3
0.2
0.1
0
0
10°
20°
30°
40°
θ
50°
60°
70°
80°
90°
.735
.7
.6
.5
.4
.3
.2
.1
.0

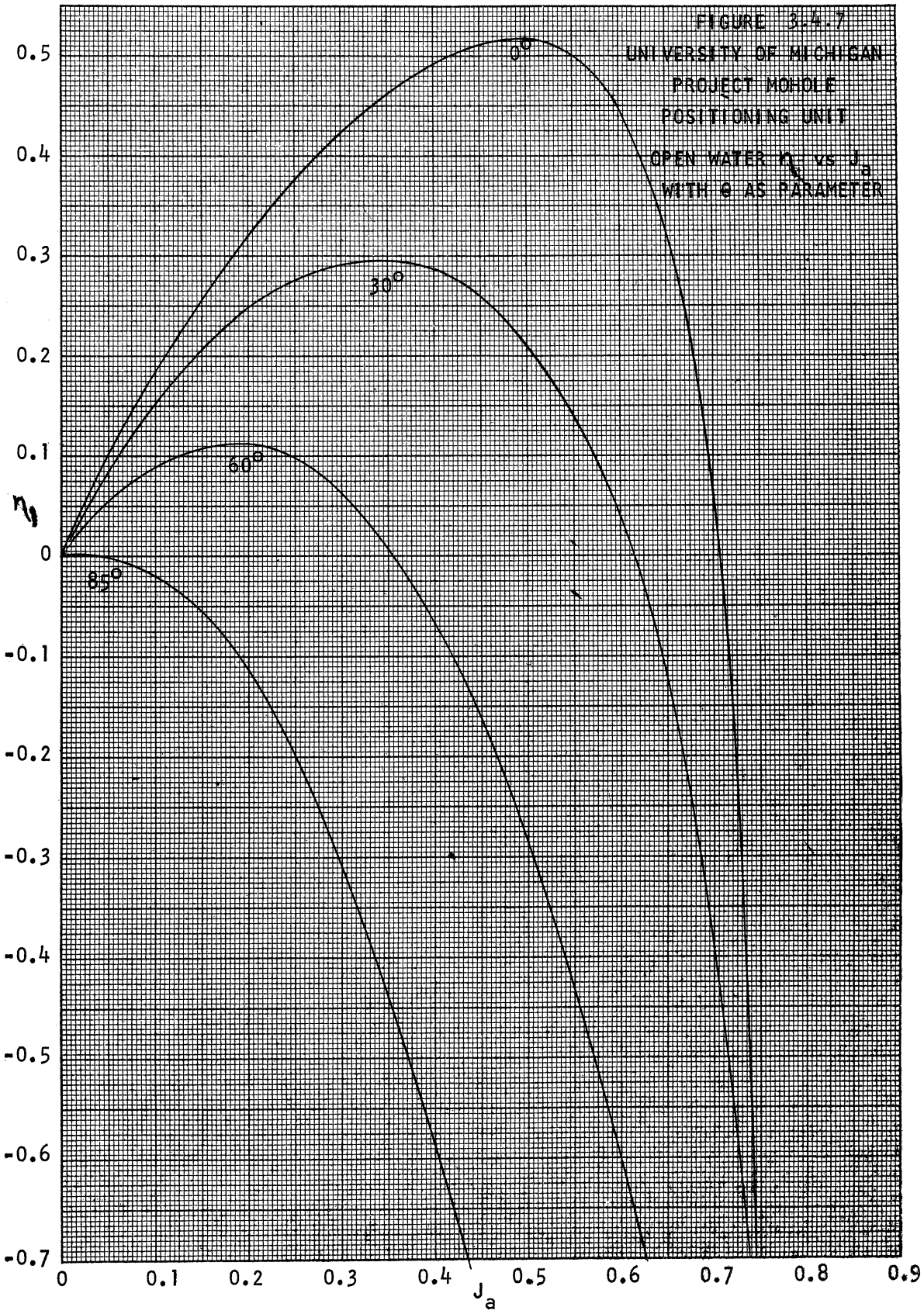
FIGURE 3.4.7
UNIVERSITY OF MICHIGAN
PROJECT MOHOLE
POSITIONING UNIT
OPEN WATER η_0 vs J_a
WITH θ AS PARAMETER
0°
30°
60°
85°
η_0
J_a
0.5
0.4
0.3
0.2
0.1
0
-0.1
-0.2
-0.3
-0.4
-0.5
-0.6
-0.7
0
0.1
0.2
0.3
0.4
0.5
0.6
0.7
0.8
0.9

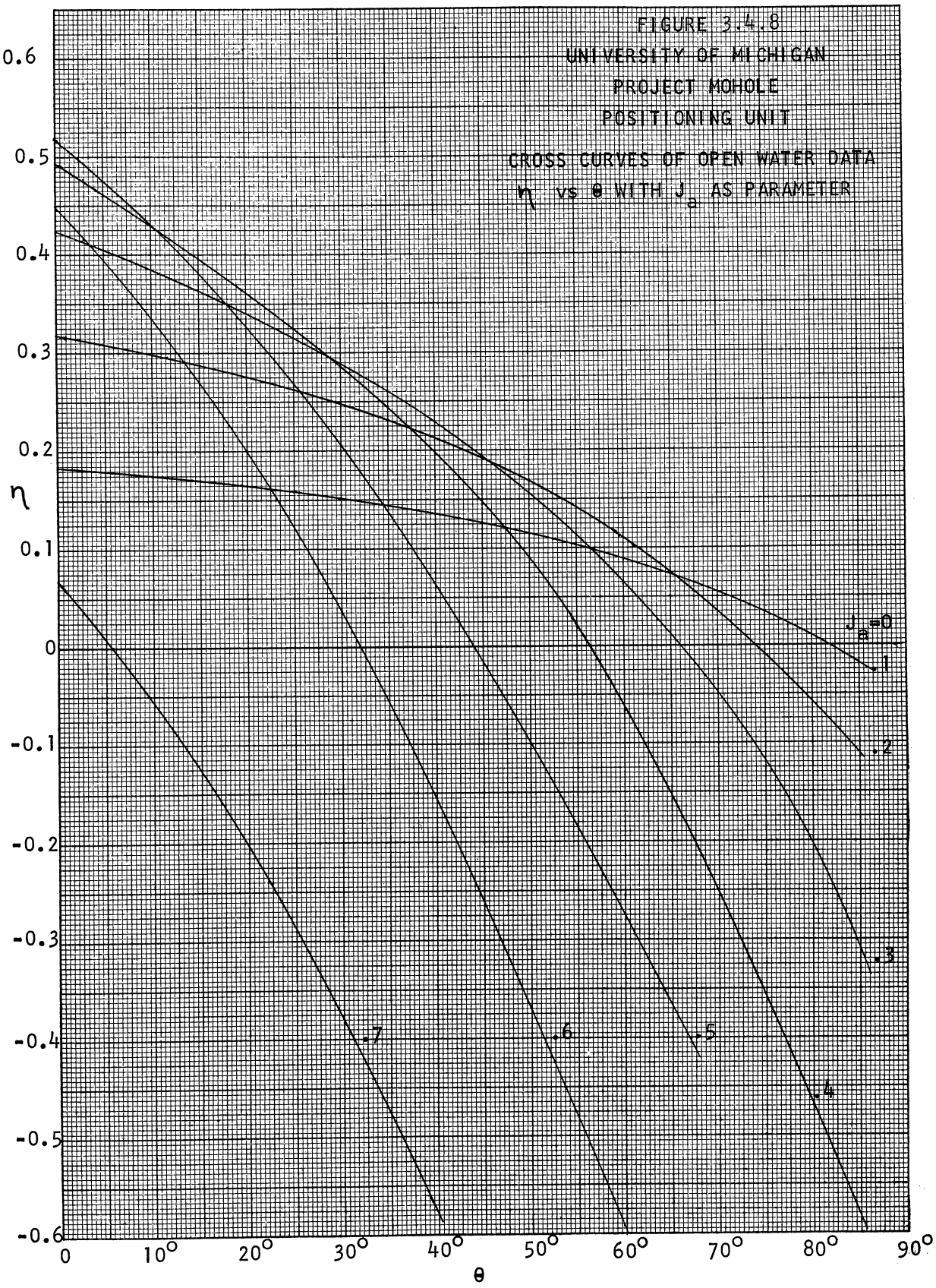
FIGURE 3.4.8
UNIVERSITY OF MICHIGAN
PROJECT MOHOLE
POSITIONING UNIT
CROSS CURVES OF OPEN WATER DATA
η vs θ WITH Ja AS PARAMETER
0.6
0.5
0.4
0.3
0.2
η
0.1
0
-0.1
-0.2
-0.3
-0.4
-0.5
-0.6
0
10°
20°
30°
40°
50°
60°
70°
80°
90°
θ
Ja=0
.1
.2
.3
.4
.5
.6
.7

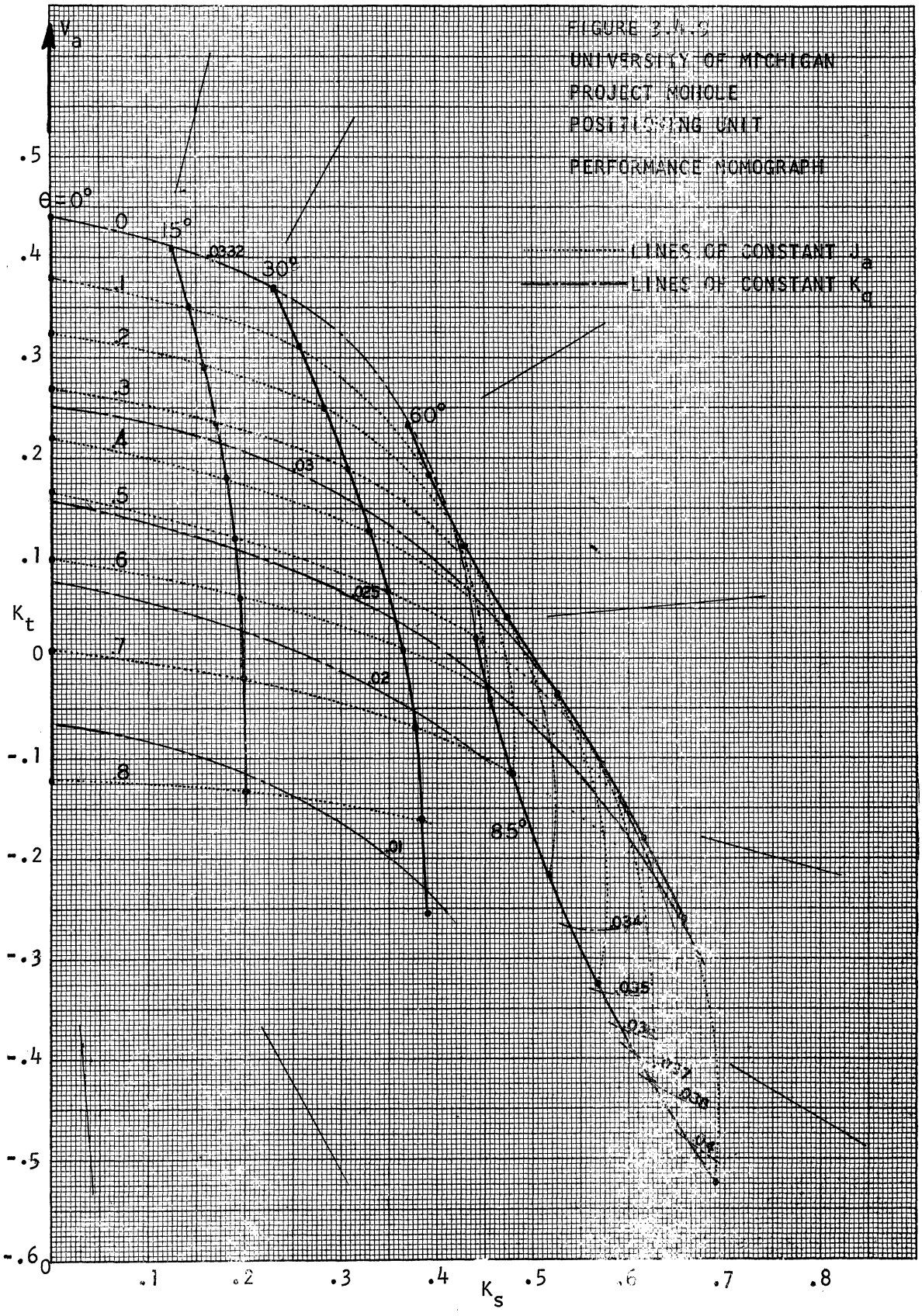
FIGURE 2.4.3
UNIVERSITY OF MICHIGAN
PROJECT MOHOLE
POSITIONING UNIT
PERFORMANCE NOMOGRAPH
LINES OF CONSTANT J_a
LINES OF CONSTANT K_q
V_a
K_t
K_s
θ=0°
15°
30°
60°
85°
.5
.4
.3
.2
.1
0
-.1
-.2
-.3
-.4
-.5
-.6
.1
.2
.3
.4
.5
.6
.7
.8
0
1
2
3
4
5
6
7
8
.0332
.03
.025
.02
.01
.034
.035

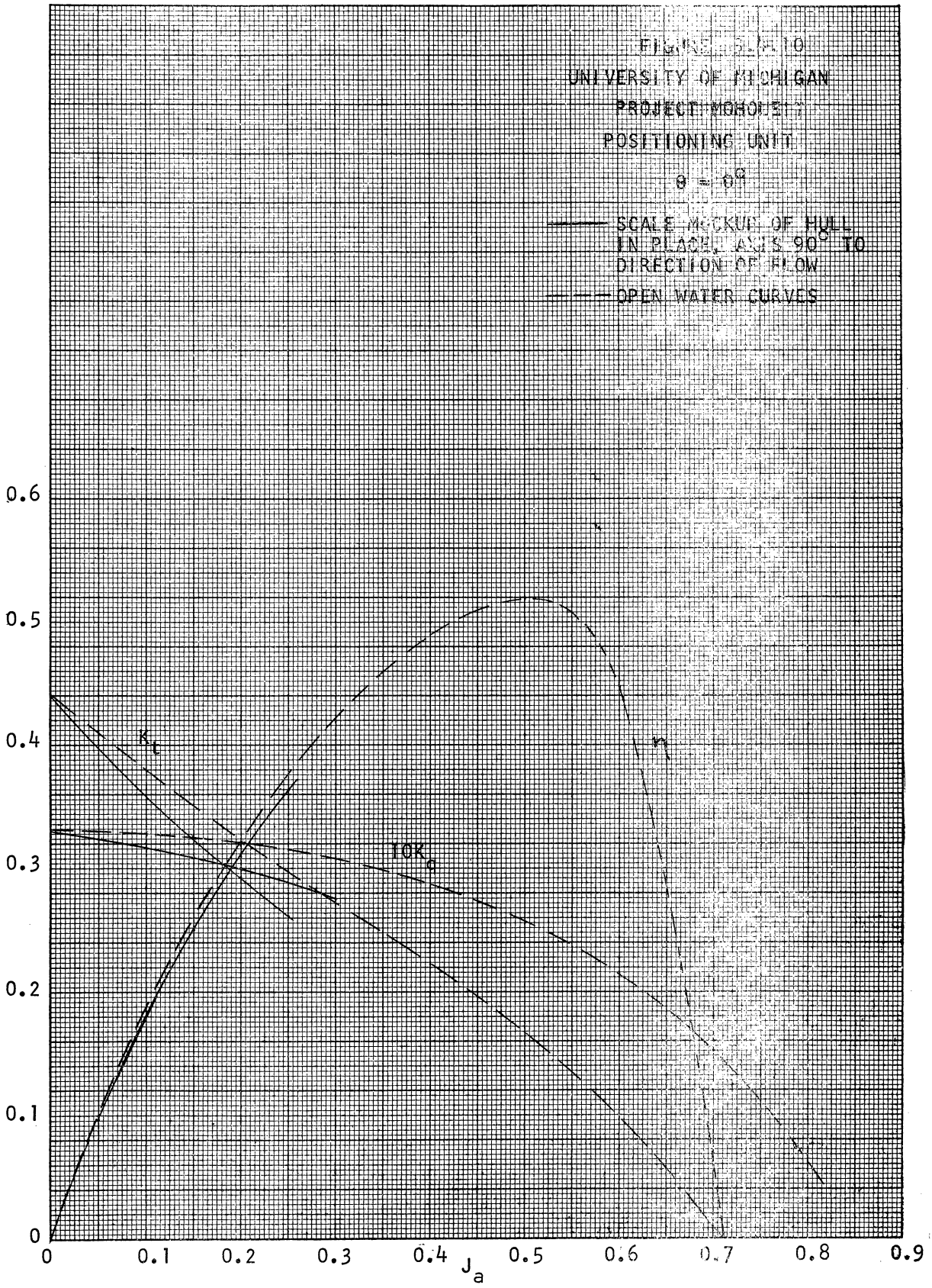
FIGURE B.4.10
UNIVERSITY OF MICHIGAN
PROJECT MOHOLE
POSITIONING UNIT
θ = 0°
SCALE MOCKUP OF HULL IN PLACE, AXIS 90° TO DIRECTION OF FLOW
OPEN WATER CURVES
K_t
$10K_q$
η
0.6
0.5
0.4
0.3
0.2
0.1
0
0
0.1
0.2
0.3
0.4
J_a
0.5
0.6
0.7
0.8
0.9

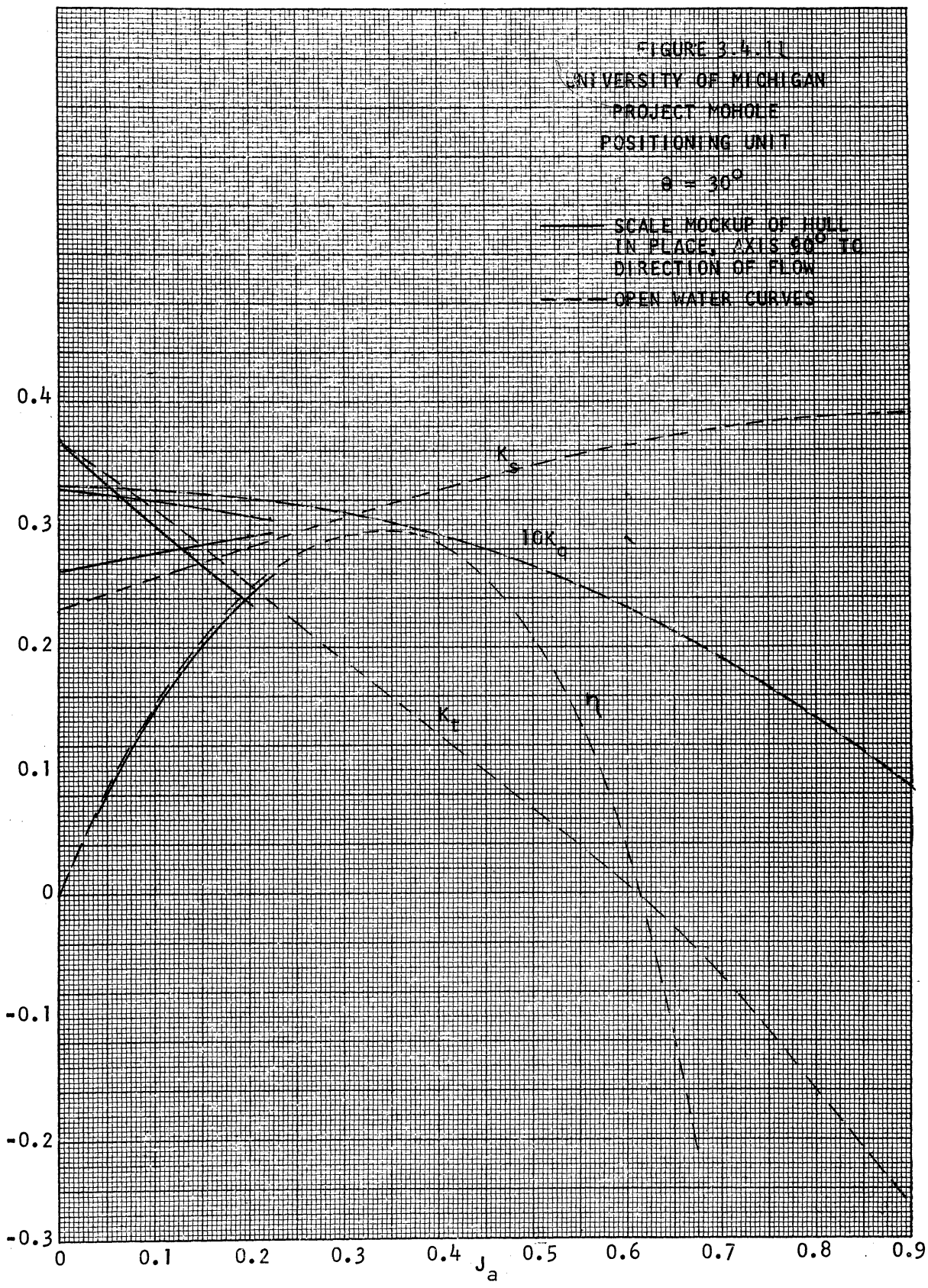
FIGURE 3.4.11
UNIVERSITY OF MICHIGAN
PROJECT MOHOLE
POSITIONING UNIT
θ = 30°
SCALE MOCKUP OF HULL IN PLACE, AXIS 90° TO DIRECTION OF FLOW
OPEN WATER CURVES
0.4
0.3
0.2
0.1
0
-0.1
-0.2
-0.3
0
0.1
0.2
0.3
0.4
0.5
0.6
0.7
0.8
0.9
J_a
K_s
$10K_q$
K_t
η

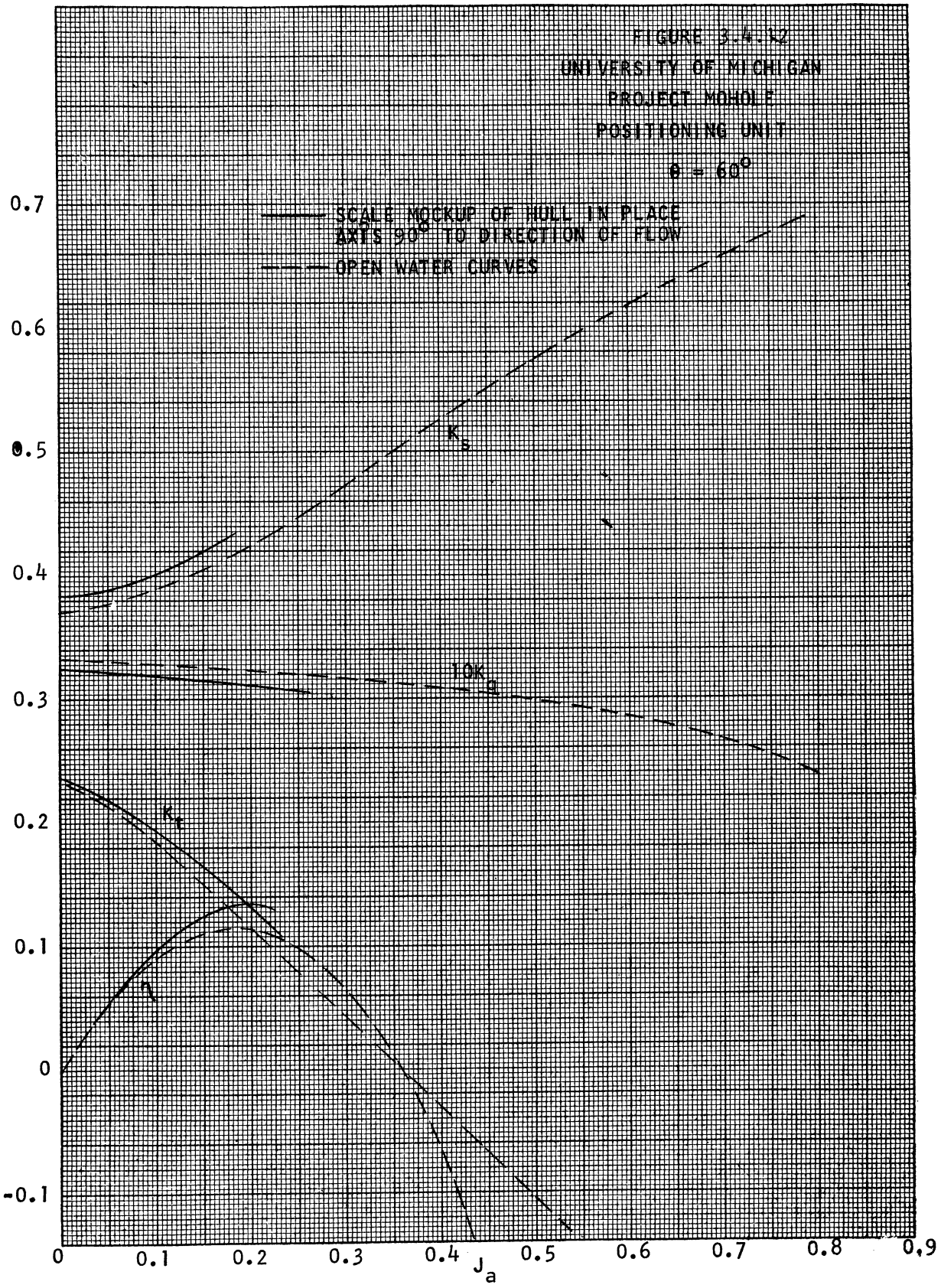
FIGURE 3.4.42
UNIVERSITY OF MICHIGAN
PROJECT MOHOLE
POSITIONING UNIT
θ = 60°
SCALE MOCKUP OF HULL IN PLACE
AXIS 90° TO DIRECTION OF FLOW
OPEN WATER CURVES
K_s
$10K_q$
K_t
η
0.7
0.6
0.5
0.4
0.3
0.2
0.1
0
-0.1
0
0.1
0.2
0.3
0.4
0.5
0.6
0.7
0.8
0.9
J_a

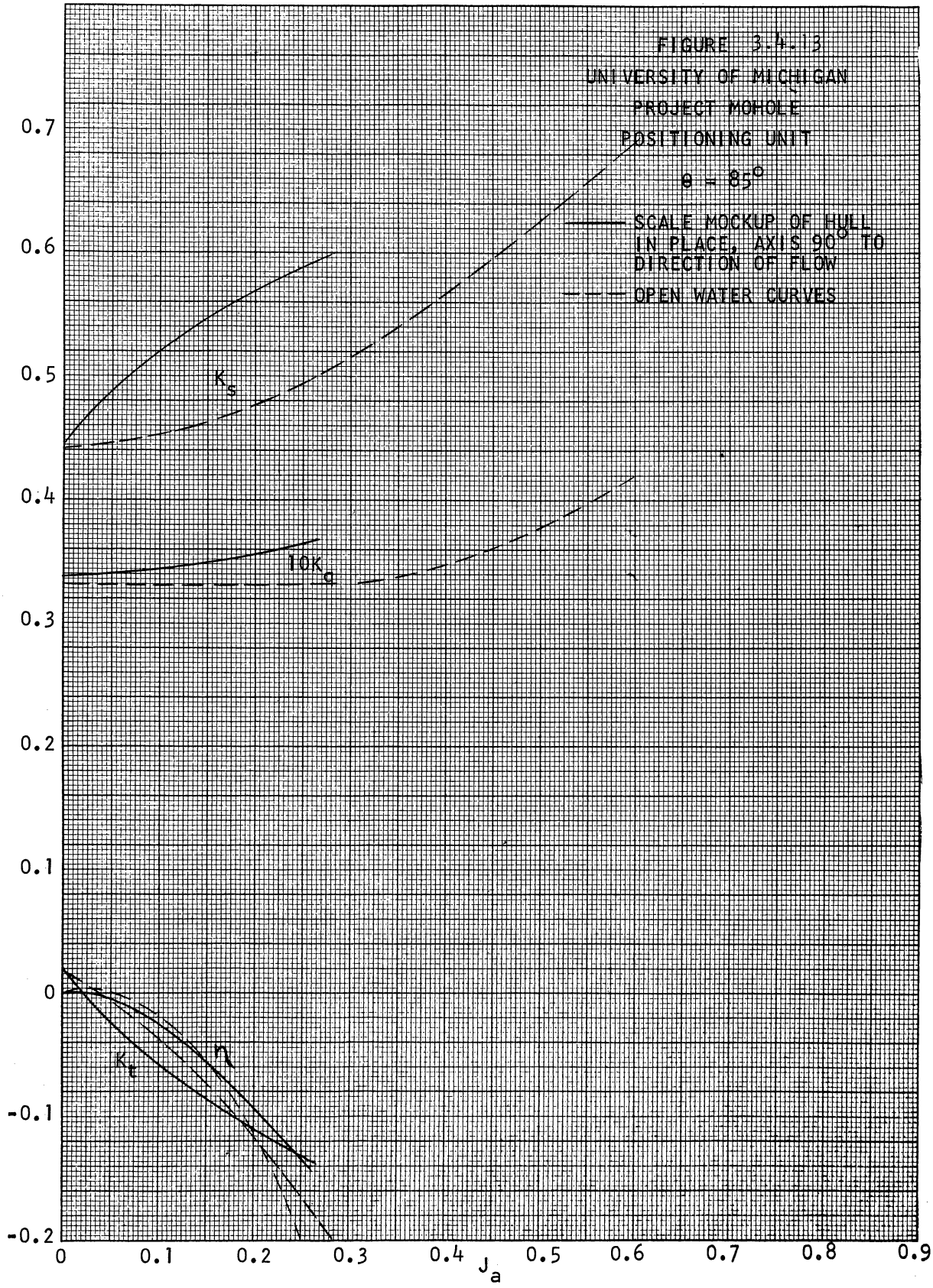
FIGURE 3.4.13
UNIVERSITY OF MICHIGAN
PROJECT MOHOLE
POSITIONING UNIT
θ = 85°
SCALE MOCKUP OF HULL IN PLACE, AXIS 90° TO DIRECTION OF FLOW
OPEN WATER CURVES
K_s
$10K_q$
K_t
η
0.7
0.6
0.5
0.4
0.3
0.2
0.1
0
-0.1
-0.2
0
0.1
0.2
0.3
0.4
0.5
0.6
0.7
0.8
0.9
J_a

FIGURE 3.4.14
UNIVERSITY OF MICHIGAN
PROJECT MOHOLE
POSITIONING UNIT
OPEN WATER TESTS

K_m vs J_a with θ as parameter

$K_m = \frac{\text{Moment about P}}{\rho n^2 d^4}$

a = Distance from propeller plane to point of application of moment

$J_a = \frac{V_a}{nd}$

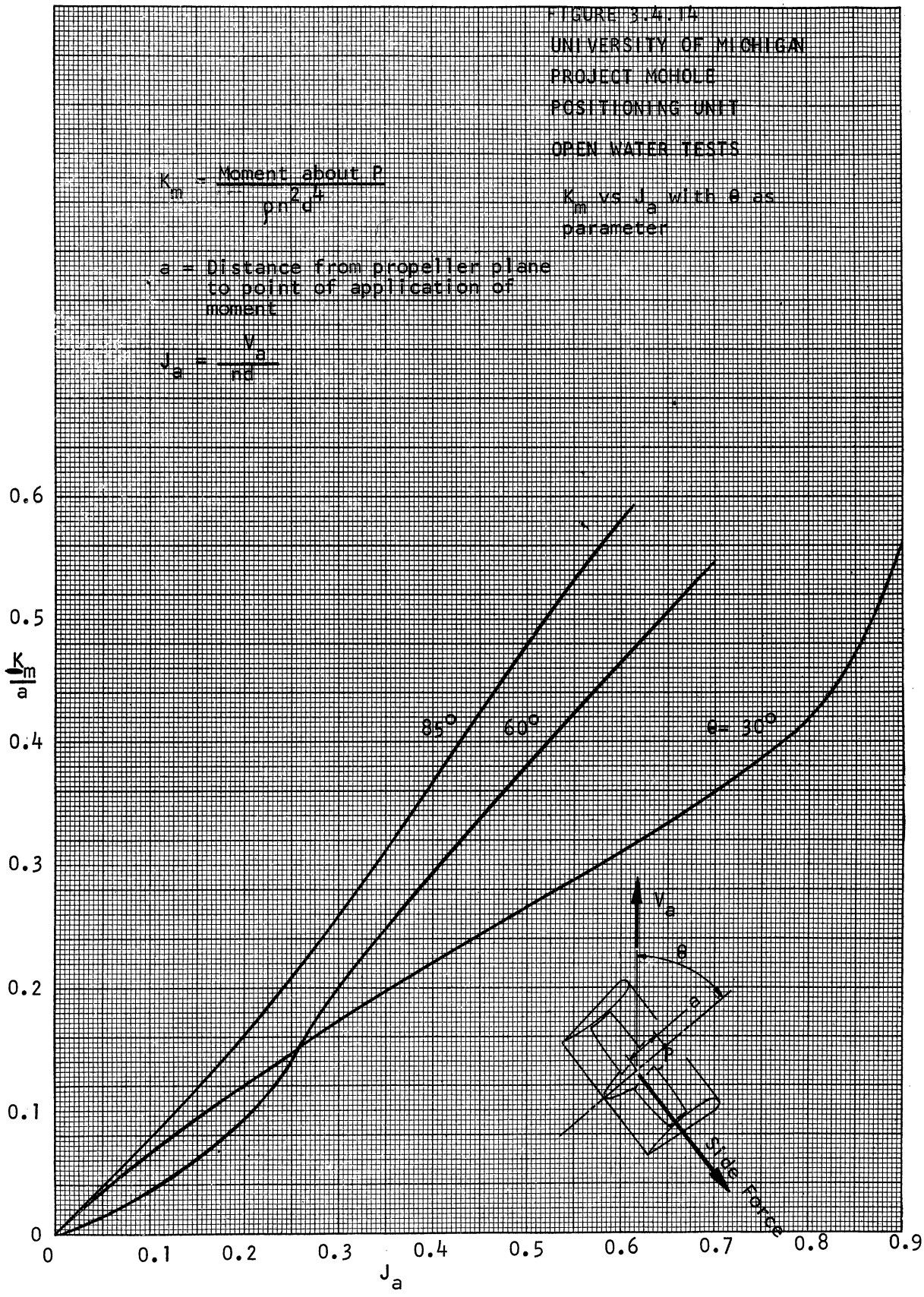

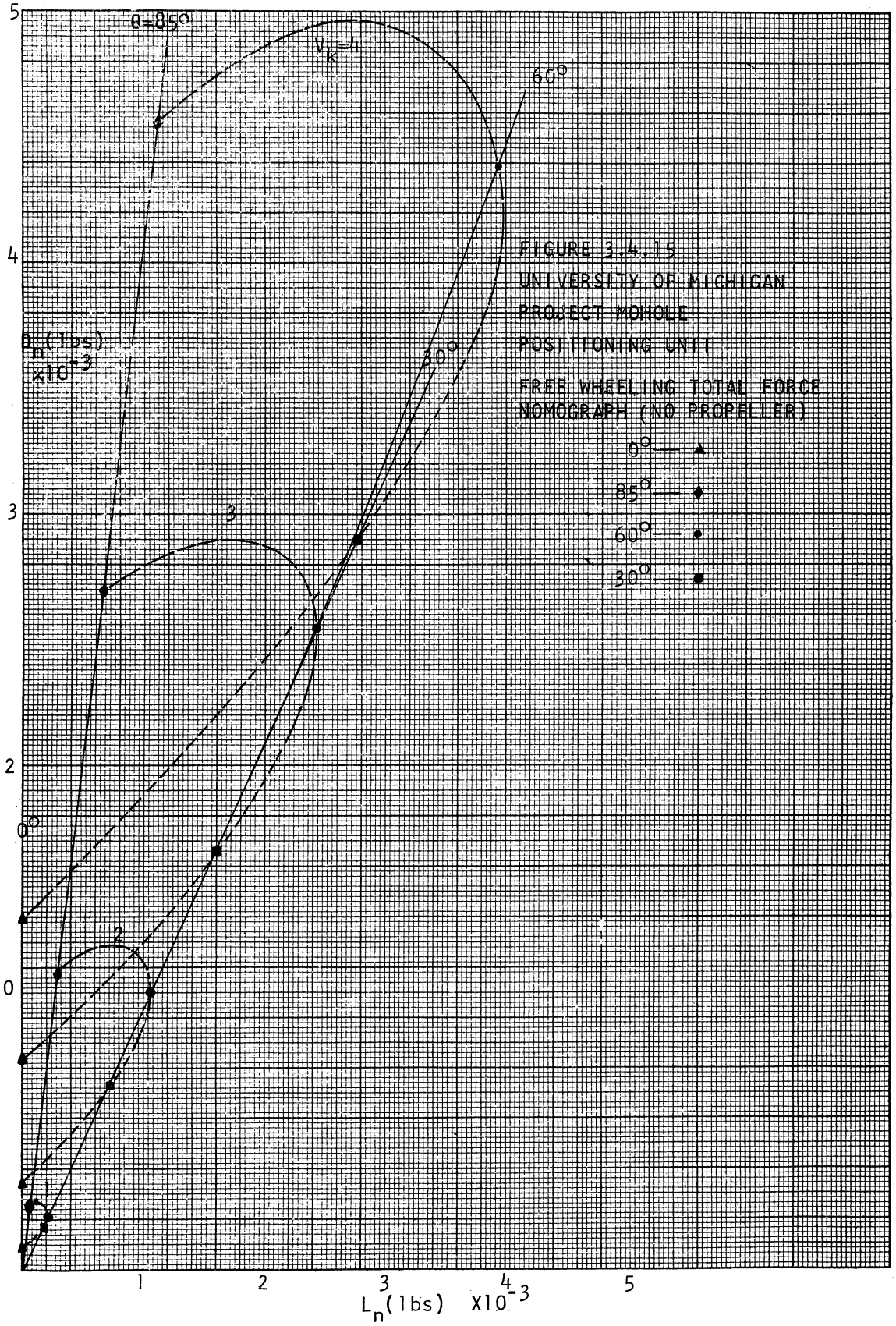

FIGURE 3.4.15
UNIVERSITY OF MICHIGAN
PROJECT MOHOLE
POSITIONING UNIT
FREE WHEELING TOTAL FORCE
NOMOGRAPH (NO PROPELLER)
0° — ▲
85° — ♦
60° — •
30° — •

ADDENDUM

STEERING UNIT PROPELLER

.5R	Pitch =	7.850"
.7R	=	7.856"
.9R	=	7.905"

For a $\frac{P}{D}$ = .875 and DIA. = 9.2" the required pitch is

$$P_R = .875 \times 9.2 = 8.05"$$

Using an average actual pitch of 7.87" the propeller is underpitched by

$$\left(\frac{8.05}{7.87} - 1\right) 100 = 2.3\%$$

To convert the given torque coefficient to the correct geometry propeller it is necessary to multiply values given in the graph by $(1.023)^2 = 1.0465$. However, the new K_Q should be plotted at an advance coefficient which is 2.3% greater than the value read from the figures.

A much easier procedure is to simply calculate the torque and thrust from the graphs and apply these to the correct propeller rotating at a 2.3% slower speed than the model propeller.